

The Distributional Consequences of Climate Change: The Role of Housing Wealth, Expectations, and Uncertainty

[[Click here for latest version](#)]

Jeffrey E. Sun

November 8, 2023

Abstract

In the United States, the majority of the median household's wealth is in the form of a single climate-exposed asset: their home. I study how this shapes household heterogeneity in the welfare impacts of climate change. In reality, house prices are location-specific, forward-looking, and determined in equilibrium by households uncertain about the future. I build a dynamic spatial equilibrium model of the U.S. with 1713 locations, incorporating heterogeneous and forward-looking households whose housing wealth depends on prices which they endogenously determine in spatially-segmented housing markets subject to climate news shocks and migration responses. I find the otherwise-intractable global solution under climate uncertainty using a simple and general deep learning method which I describe in a companion paper. I quantify the model using harmonized recent estimates of climate impacts on local productivity, amenities, maintenance costs, and disaster risk. I discipline uncertainty using climate projections and time series data on homeowners insurance premiums. Inequality in climate damages is large, though initially progressive by wealth. However, climate uncertainty causes ongoing regressive wealth transfers as higher housing asset risk is passed on to poorer households through higher rents. Incorporating homeownership reverses the ameliorative effects of migration adaptation for spatial inequality in welfare losses from climate change in the short-to-medium term. With housing wealth, a switch from widespread climate denial to widespread climate acceptance leads to an effective transfer of almost \$1tn of housing wealth from households in more-harmed to less-harmed regions.

1 Introduction

In the United States, housing wealth accounts for approximately one third of household wealth¹, or \$51.9 trillion (Zillow, 2023). The value of every individual home within this stock depends on current expectations about the economic future of its location: a future that will be shaped by climate change.

I study how homeownership—ownership by households of these climate-sensitive housing assets—shapes household inequality in the welfare impacts climate change. Complexity arises from the fact that the effects of climate change on housing wealth are mediated by forward-looking equilibrium housing prices. Climate change, climate news, and climate uncertainty all affect housing demand which nonlinearly determines housing prices and rents in spatial and intertemporal equilibrium. Even the first order effects of physical

¹Q2 2023 household net worth (FRB), \$154.3tn.

climate change on welfare and housing demand are complex, as the impacts of global climate change are heterogeneous across space and affect multiple factors of housing and location choice, even within locations. A final consideration is that housing ownership is endogenous, so that current expectations shape not only current housing prices, but also who is exposed to future price changes.

To quantify the role of housing wealth in shaping household heterogeneity in the welfare impacts of climate change, I split the problem into three parts. First, I build a heterogeneous-agent dynamic spatial equilibrium model of the U.S. with disaggregated housing wealth at the household level, 1713 locations, and climate change which impacts locations heterogeneously. Second, I quantify climate damages to economic fundamentals—how global climate conditions affect local economic fundamentals driving housing and location choice—and quantify expectations and uncertainty over future global climate conditions. Third, I solve the model under conditions of aggregate climate uncertainty. The global solution is made possible by a simple but general deep learning method which I introduce in a companion paper.

Model

I add disaggregated housing ownership at the household level to a dynamic spatial equilibrium model of the contiguous U.S. with 1713 locations. The primary challenges are (1) modeling the location and housing decisions of heterogeneous households, (2) modeling the determination of local housing prices in equilibrium and their response to climate change, climate news, and climate uncertainty, and (3) numerically solving the model under aggregate uncertainty. These challenges likely motivate some abstractions common in related models, such as the focus on between-location (spatial) inequality in climate impacts rather than within-location (household) heterogeneity, and the relatively standard assumption in the spatial literature generally that all housing is rented from absentee landlords.

I explicitly model heterogeneous households who make forward-looking migration, consumption-savings, and housing rent and ownership decisions. These decisions determine location-level housing demand which interacts with location-specific housing supply to determine housing prices in spatial and intertemporal equilibrium.² In the dynamic equilibrium, changes in climate conditions, climate expectations, or climate uncertainty, shape households' willingness to hold housing assets, which shapes housing prices, which impacts household wealth in the present.

The model is essentially a heterogeneous-agent dynamic small-open-economy model to which multiple locations have been added. The household block is modeled after Kaplan et al. (2020), although the household's housing choice is over continuous housing quality as in Favilukis et al. (2017). This is then embedded in a spatial equilibrium model with frictional migration and heterogeneous bilateral migration costs, similar

²Housing supply is in the form of location-specific durable housing stocks which depreciate over time but are added to by construction along the spatially-heterogeneous housing supply curves estimated by Saiz (2010).

to Borusyak et al. (2022). I calibrate the model to the 1713 locations³ covering the contiguous U.S. reported in the Public Use Microdata Sample (PUMS) of the 1990 U.S. Census. I calibrate location-specific amenity values, housing supply cost shifters, and productivity shifters for each location, exactly matching empirical populations, housing prices, and mean wages. I simultaneously calibrate the stationary steady state of the model to match key moments of the 1990-1992 U.S. economy computed from the PUMS microdata and the Survey of Consumer Finances (SCF). I choose this relatively early year to allow for the role of anticipatory adjustment to climate expectations in shaping 2020 populations, housing stocks, and asset holdings.

Quantification

I quantify expectations over climate impacts on economic fundamentals in two parts. First, the spatially-heterogeneous effects of global climate conditions on local economic fundamentals: productivity, amenities, energy costs, and disaster damages. Second, expectations and uncertainty over future global climate conditions.

Climate Damages to Economic Fundamentals—I combine and harmonize estimates from climate and environmental economics literatures to quantify the impact of global climate conditions on four specific local economic fundamentals: labor productivity, amenities,⁴ residential energy costs, and disaster damages. The overall strategy is to combine projections from climate models—on the impact of global climate conditions on local climate conditions—with estimates from environmental economics on the impacts of local climate conditions on local economic fundamentals. The primary challenge is avoiding double-counting: for each damage estimate I import, it is essential that the methodology used to generate it controls for the effects picked up by the other estimates. Additionally, estimates are reported in terms of different local climate variables. I show that, in the global temperature range of interest, both the climate science and environmental economics estimates are well-approximated⁵ by linear (or log-linear) functional forms taking (1) global temperatures to local annual heating- and cooling-degree-days⁶ and (2) local annual heating- and cooling-degree-days to economic fundamentals. This allows the modeled sensitivities of local economic fundamentals to global climate conditions to be fully-flexibly location-specific while remaining functionally simple due to local (log-)linearization.⁷

Expectations and Uncertainty—I combine climate and emissions projections with time series data on historical homeowners insurance premiums to quantify key parameters of climate expectations and uncer-

³Public Use Microdata Areas (PUMAs)

⁴A location-specific quality-of-life shifter.

⁵For disaster damages, data limitations preclude this check.

⁶Heating- and cooling-degree-days are a measure of how cold and hot a location is, respectively, relative to 18.3°C (65°F). See Section 3.2 for a formal definition. Disaster damages are modeled as location-specific functions of a global “disaster intensity” state and do not go through local temperatures.

⁷Although I linearize or log-linearize the impact of global climate conditions on local climate conditions, I do not generally linearize the model. I thus sacrifice the analytical tractability of fully log-linearized models such as Caliendo et al. (2019) and Kleinman et al. (2023).

tainty. That is, I parameterize and calibrate the market-relevant distribution of possible future climate paths. Quantifying overall uncertainty is challenging because multiple sources of climate uncertainty contribute to overall uncertainty in qualitatively different ways. The Intergovernmental Panel on Climate Change (IPCC) defines three major sources of global climate uncertainty: internal variability (natural fluctuations in climate conditions), scenario uncertainty (uncertainty over the path of future emissions), and model uncertainty (uncertainty over the climate impacts of emissions).⁸

I therefore employ an auxiliary model to aid in calibrating overall climate uncertainty. This auxiliary model consists of a richer stochastic climate process and a representative Bayesian household who observes realized climate outcomes but has imperfect information about the parameters of the generating process. This auxiliary model is rich enough to allow data on the multiple sources of climate uncertainty to be mapped to it in an interpretable way. The auxiliary model is calibrated to match key empirical moments relating to each source of uncertainty separately; the simpler climate process used in the main model is then calibrated to match key simulated moments of the auxiliary model representing overall climate uncertainty.⁹

In the auxiliary model, I quantify internal variability—natural climate variation from year to year—using historical data on annual temperatures from the National Centers for Environmental Information (NCEI) and historical data on disaster damages from the Spatial Hazard Events and Losses Database for the United States (SHELDUS). I quantify scenario uncertainty in the future path of emissions by setting the quartiles of 2020–2100 emissions to the values given by IPCC emissions scenarios RCP2.6, RCP4.5, and RCP6.0. I quantify two sources of model uncertainty: model uncertainty over the contribution of emissions to temperatures, using the variance of the estimates in the Coupled Model Intercomparison Project 5 (CMIP5) ensemble (Rasmussen & Kopp, 2017); and model uncertainty in the contribution of emissions to disaster damages, using historical data on the responsiveness of homeowners insurance premiums to disaster realizations and emissions. For the latter I first verify that, in reduced form, homeowners insurance premiums appear to rise in response to costly disasters, suggesting that markets’ beliefs about disaster frequencies are uncertain enough to be affected by such realizations. I then estimate this uncertainty using a form of “nested” Kalman filter.¹⁰

Numerical Solution

With aggregate climate uncertainty, the model has a very large state space. The household’s policy function in principle depends on the entire distribution of household states. A global solution is infeasible with conventional methods but a deterministic climate transition would fail to capture the equilibrium effect of the

⁸We might also expect considerable uncertainty over the economic model governing housing markets and equilibrium responses. This is beyond the scope of this study.

⁹Specifically, the quartiles of 2100 global temperatures and disaster damages given 2020 information and global climate state.

¹⁰Essentially, I assume that the insurer is applying a Kalman filter then use a Kalman filter of my own whose unobserved state embeds the insurer’s learning process and whose observables include the insurance premiums resulting from that process.

existence and slow resolution of aggregate climate uncertainty on housing prices and rents. Because climate scenarios differ substantially and impact housing prices in complex, nonlinear ways, I compute the global solution rather than use local approximations. To do so, I develop a simple but general deep learning method for solving dynamic spatial models with forward-looking heterogeneous agents facing complex frictions and aggregate uncertainty.

In particular, I exploit the fact that if a model is solvable in steady state then it is generally the case that, within each period, the household’s optimal decision can be derived from current prices and the conditional-on-choice continuation values¹¹ faced by the household. Whereas existing deep learning techniques typically use a neural network to approximate both the household policy and value functions, the training of the policy function approximator imposes both some practical difficulties in training the network and theoretical restrictions on the policy function.¹² Aided by optimized algorithms I develop for quickly solving for optimal household migration, consumption-savings, and housing ownership decisions given conditional continuation values, I show that solving for the optimal policy “live” during training is a viable—and more flexible and arguably simpler—alternative to training a policy function approximator.¹³ The method I use builds on recent advancements in the use of neural networks for solving discrete-time heterogeneous-agent models introduced in Azinovic et al. (2022) and Han et al. (2021).

Related Literature

First, an active recent dynamic spatial environmental economics literature seeks to understand heterogeneity in the welfare impacts of climate change, typically focusing on between-location spatial heterogeneity as opposed to within-location household heterogeneity. A key theme in this emerging literature is understanding how spatial climate damages are shaped by (1) different climate impacts and (2) different adaptation mechanisms. A seminal paper without dynamics, Hsiang et al. (2017) consider spatial climate impacts on disasters, mortality, productivity, energy costs, and crime, but do not incorporate economic or migration adaptation. Desmet et al. (2021) study the impact of land loss due to coastal flooding and find that adaptation through the dynamic responses of investment and migration largely ameliorate losses to global GDP. Krusell and Smith (2022) consider productivity impacts due to temperature and adjustment via capital mobility but not migration, finding that capital mobility does not significantly change results. Bilal and Rossi-Hansberg (2023) study the impact of disasters on capital depreciation. They introduce forward-looking migration in anticipation of climate change, finding that migration substantially reduces spatial inequality in climate

¹¹i.e. Conditional continuation value $\tilde{V}(x; \Gamma) \equiv \mathbb{E}[V(x'; \Gamma') | x, \Gamma]$, for some end-of-period individual state x and aggregate state Γ , start-of-next-period states x' and Γ' , and start-of-period value function V .

¹²For instance, that the continuation value be quasiconvex and differentiable in the policy variable.

¹³A relatively inexpensive restriction is that prices are pinned down by intratemporal market clearing conditions given household conditional continuation values. In principle, prices can also be solved for “online,” but in practice I use an auxiliary neural network to approximate prices, as in Azinovic et al. (2022).

damages.

In this tradition, I consider spatial climate impacts on location-level labor productivity, amenities, residential energy costs, and disaster damages. I incorporate migration and anticipation and introduce individual housing wealth and the endogenous response of housing prices to climate change, news, and uncertainty. With housing wealth, migration exacerbates spatial inequality in the welfare impacts of climate news, as the prospect of future out-migration from negatively-affected areas exacerbates the housing price impacts in those areas. I also introduce within-location household heterogeneity. In the calibrated model, within-location dispersion—by wealth, income, housing wealth, and age—in the immediate welfare impacts of climate news are approximately twice as large as between-location heterogeneity. In the global solution, household heterogeneity, housing wealth, and uncertainty interact to exacerbate wealth inequality, in expectation, along the stochastic climate transition. Climate uncertainty adds undiversifiable climate risk to housing assets, reducing demand for owning rental housing, thus reducing the supply of rental housing available to renters. This increases equilibrium rent, effectively shifting the costs of climate risk from households who own housing to households who rent.¹⁴ Wealthier households with endogenously lower absolute risk aversion benefit from this climate uncertainty through increased risk premia on housing assets. For them, this more than counteract the welfare costs of climate risk in housing prices.

Second, a literature on flood policy studies the role of government in subsidizing flood insurance and investing in flooding mitigation. These include Balboni (2021), Hsiao (2023), and Pang and Sun (2023). Fried (2022) incorporates household homeownership in a dynamic model with two locations.

Third, a new dynamic spatial literature seeks to understand how forward-looking agents make frictional decisions and/or respond to shocks in spatial equilibrium. These include Crews (2023), Komissarova (2022), and Kleinman et al. (2023). A subset of these papers specifically incorporate housing wealth, such as Giannone et al. (2023), Greaney (2021), and Fried (2022).

I draw from this literature methodologically and introduce fully local real estate and rental markets, uncertainty in the form of a stochastic transition, and a solution method for finding the global solution under aggregate uncertainty.

Fourth, an emerging literature develops deep learning tools to solve dynamic models with aggregate uncertainty, which in turn can be connected to the literature spawned by Krusell and Smith (1998) on the solution of dynamic models with aggregate uncertainty through state space reduction. This literature includes Azinovic et al. (2022), Han et al. (2021), Maliar et al. (2021), and Fernandez-Villaverde et al. (2020).

Fifth, I draw from a housing literature which provides the foundation for understanding and modeling the household's housing and homeownership choice, either alone or in equilibrium. These include Sinai and Souleles (2005), Kaplan et al. (2020), and Favilukis et al. (2017). Yao and Zhang (2005) specifically study

¹⁴These are ex-ante identical households who choose to rent or own based on their wealth and other individual state variables.

the relationship between wealth, portfolio choice, and asset returns.

Outline

The paper is structured as follows. In Section 2, I describe a dynamic spatial equilibrium model with forward-looking heterogeneous households and housing wealth. In Sections 3, 4, and 5, I quantify the model. In Section 3, I quantify the impact of global climate conditions on local economic fundamentals (labor productivity, amenities, residential, energy costs, and disaster risk) by combining and harmonizing estimates from the climate science and environmental economics literatures. In Section 4, I quantify expectations and uncertainty over the future course of climate change using CMIP5 projection ensembles and time series data on historical homeowners insurance premiums. In Section 5, I calibrate the economic model to match spatial and aggregate data on the contiguous U.S. from the 1990 PUMS and 1992 SCF. In Section 6, I explore how household heterogeneity, housing wealth, and uncertainty shape spatial and household heterogeneity in the welfare impacts of climate change in the calibrated model. Section 7 concludes.

2 A Dynamic Spatial Equilibrium Model

2.1 Overview

I describe a heterogeneous-agent dynamic spatial model with housing wealth traded in spatially-segmented housing markets. The 1713 locations in the model exist within a small open economy representing the contiguous United States. Locations have systematically heterogeneous exposure to a stochastic global climate process.

Time is discrete. The economy is populated by overlapping generations of heterogeneous households who differ, within generations, in their bondholdings, income type, real estate holdings, location, and age, and make forward-looking location, saving, and real estate investment decisions subject to a number of spatial and financial frictions. Each period, each household selects a single location to live and work in, paying monetary and utility migration costs if they change locations. Bilateral utility migration costs vary by origin-destination location pair.

Households may save through a risk-free foreign-issued bond with fixed and exogenous interest rate or by purchasing residential real estate. When buying real estate, households may obtain a mortgage in the form of negative bondholdings subject to a collateral constraint and a higher interest rate than is paid on savings. When selling real estate, households pay an adjustment cost. Housing assets are priced in equilibrium by households and are thereby exposed to location-specific climate risk which is neither insurable nor diversifiable across locations. Households may only own housing in the location in which they live and, conversely, all housing in each location is owned by households who live there.

In equilibrium, due to this illiquidity, risk, and borrowing constraint, residential real estate offers a higher expected return than the safe bond.

A household may let out some of its owned housing to other households in the same location, generating a stochastic cash flow. Conversely, households may rent housing from other households in the same location instead of owning. Homeowners pay lower maintenance costs, with the maintenance differential representing any administrative, moral hazard, and utility costs of renting.

Housing is durable and the housing stock depreciates over time. New housing is constructed by a competitive construction sector which is static, building new houses instantaneously and immediately selling them at the prevailing market price until it is unprofitable to do so. In effect, the quantity of housing in each location is given by the cost curve of construction if prices are sufficiently high or by the depreciated stock of existing housing if prices are sufficiently low.

Housing rent and real estate prices are determined in equilibrium in each location and period in spatial and intertemporal equilibrium. By contrast, the labor and goods markets are stylized. Production functions are linear, though productivity differs by location. Households supply labor inelastically and are paid their marginal product in the form of the consumption good, a numeraire costlessly tradable with the rest of the world. There is no capital.

Climate change introduces aggregate uncertainty. Global climate conditions affect local productivity, amenities, energy costs, and disaster risk heterogeneously across locations. These climate damages affect forward-looking household location and real estate investment choices, which collectively determine equilibrium housing prices.

Households are ex ante identical with constant relative risk aversion. However, absolute risk aversion varies endogenously, decreasing in consumption. Climate uncertainty thus affects households heterogeneously by wealth and age. In equilibrium, climate uncertainty reduces demand for owning housing, reducing the supply of rental housing and increasing housing rents relative to prices.

The full set of frictions that households in the model are subject to are: migration costs, real estate transaction costs, borrowing limits, borrowing costs, uninsurable income risk, and location-specific climate-driven uninsurable risk in fundamentals ¹⁵ and housing prices.

2.1.1 Timing

Time is discrete. At the beginning of each period, housing prices and rents are observed. Immediately afterward, the housing stock in each location depreciates and a construction sector builds new housing until the marginal cost of new construction in each location is equal to the housing price. Households then draw location preference shocks and choose locations, housing assets, consumption and, if they do not own a

¹⁵Productivity, amenities, energy costs, and disaster risk.

home, rental housing services. At the end of each period, households receive income, pay expenses, realize stochastic income shocks, and age. Then the global climate state evolves and a global climate news shock is drawn which affects the future trajectory of the global climate. The climate news shock does not immediately affect the physical state of the climate in the subsequent period, which is determined before the news shock is drawn.

That is, each period t :

- Housing prices $q_{\ell t}$ and rents $\rho_{\ell t}$ are observed in each location ℓ .
- Housing quantities $H_{\ell t}$ are determined in each location ℓ by depreciation and construction.
- Each household i inherits state $x_{it} = (b_{it}, z_{it}, h_{it-1}^{\text{live}}, h_{it-1}^{\text{let}}, \ell_{it-1}, a_{it})$.
- The household draws location preference shocks $\{\varepsilon_{\ell it}\}_{\ell}$.
- The household chooses location ℓ_{it} , real estate assets h_{it}^{live} and h_{it}^{let} , goods consumption g_{it} , and rental housing h_{it}^{rent} .
- The household receives income—earnings, interest, and rent—and pays expenses—goods consumption, interest, rent, and maintenance.
- The household realizes next-period human capital z_{it+1} .
- Global mean temperature SST_t and disaster intensity $\delta_t^{\text{disaster}}$ evolve.
- A global climate news shock ε_t^m is drawn.

2.2 Households

Households live for a_{max} periods, each representing one decade. There are six non-overlapping age groups representing adult households with the youngest aged 21-30 and the oldest aged 71-80.

Individual households, indexed by $i \in I$, are atomistic, with beginning-of-period state

$$x_{it} = (b_{it}, z_{it}, h_{it-1}^{\text{live}}, h_{it-1}^{\text{let}}, \ell_{it-1}, a_{it}),$$

consisting of bondholdings b_{it} , human capital z_{it} , owner-occupied real estate h_{it-1}^{live} , owned rental real estate¹⁶ h_{it-1}^{let} , location ℓ_{it-1} , and age a_{it} . Beginning-of-period owner-occupied real estate h_{it-1}^{live} , possibly zero, is housing which was owned and occupied by the household in the previous period. Beginning-of-period rental real estate h_{it-1}^{let} , possibly zero, is housing which was owned by the household and let out to other households

¹⁶Which the household lets out to other households in the same location.

in the same location in the previous period. Housing is perfectly divisible so that h_{it-1}^{live} and h_{it-1}^{let} will be chosen from a continuum as in Fabilukis et al. (2017).

2.2.1 Household Choices

Location

Within each period, a household must live, work, and own real estate in the same location. At the beginning of each period, a household realizes preference shocks over moving to each location, chooses a location, then pays migration costs if they move across locations.

At the beginning of each period t , a household i in location ℓ_{it-1} draws an additive preference shock $\varepsilon_{\ell it}$ for each location ℓ ,¹⁷

$$\varepsilon_{\ell it} \sim \text{Gumbel}(0, \psi^{-1}) \quad \text{i.i.d.}$$

The preference shock $\varepsilon_{\ell it}$ is added to the household's overall period- t utility, where ℓ_{it} is the chosen location. The preference shock does not persist into future periods.

Housing Investment, Housing Consumption, Goods Consumption, and Savings

The household then chooses owned housing h_{it}^{live} and h_{it}^{let} , location ℓ_{it} , goods consumption g_{it} , and rental housing h_{it}^{rent} :

$$\text{choice}_{it} = \{h_{it}^{\text{live}}, h_{it}^{\text{let}}, \ell_{it}, g_{it}, h_{it}^{\text{rent}}\}.$$

In contrast to a model of hand-to-mouth households, they need not spend all of their wealth each period. Any wealth not spent is saved in the form of a risk-free bond.

The household cannot occupy both a rented home and an owned one, so

$$h_{it}^{\text{live}} h_{it}^{\text{rent}} = 0.$$

2.2.2 Spatial and Financial Frictions

Households are subject to migration costs, an owned housing adjustment cost, borrowing costs, and a borrowing constraint.¹⁸

¹⁷Technically, this means that the household's action depends on both its state and its draw of ε (as well as the aggregate state Γ_t):

$$\ell_{it}(x_{it}, \{\varepsilon_{\ell it}\}_\ell; \Gamma_t).$$

In effect, however, the properties of the Gumbel distribution imply that, conditional on x_{it} and Γ_t , the probability that a household chooses a location is proportional to the (exponentiated) continuation value resulting from choosing that location. Furthermore, as the location preference shocks are additive and i.i.d., households effectively receive the mean preference-shock-contingent continuation value with certainty before the preference shock is drawn. This is made precise in Appendix E.

¹⁸Households are also subject to uninsurable idiosyncratic income risk and aggregate climate risk to which they differ in their exposure. I defer the exposition of these risks to their respective sections.

Migration Costs

If a household's new location, ℓ_{it} , differs from its previous location, ℓ_{it-1} , they pay a fixed monetary¹⁹ cost F^m and a utility cost proportional to the distance $d(\ell_{it-1}, \ell_{it})$ between the two locations:

$$F^u(\ell_{it-1}, \ell_{it}) = \tau d(\ell_{it-1}, \ell_{it}).$$

Housing Transaction Cost

If the household adjusts owned housing assets, either occupied, h_{it-1}^{live} , or let out, h_{it-1}^{let} , they pay a percentage of the sale price, $q_{\ell_{it-1}t} h_{it-1}^s$, as a realtor's fee:²⁰

$$\text{realtor's fee} = \phi q_{\ell_{it-1}t} h_{it-1}^s.$$

Borrowing Costs and Borrowing Constraint

After adjusting their location and housing assets (but before collecting income or paying other expenses), a household's new bondholdings are given by,

$$\tilde{b}_{it} = b_{it} - F^m \mathbb{1}_{it}^{\text{move}} + \sum_{s \in \{\text{live}, \text{let}\}} [(1 - \mathbb{1}^{\text{sell}}, s \phi) q_{\ell_{it-1}t} h_{it-1}^s - q_{\ell_{it}t} h_{it}^s],$$

$$\text{where } \mathbb{1}^{\text{move}} = \mathbb{1}[\ell_{it} \neq \ell_{it-1}]$$

Because households may only own housing in one location, they must sell all owned housing if they move across locations:

$$\mathbb{1}^{\text{sell}, s} = \mathbb{1}^{\text{move}} \vee \mathbb{1}[h_{it-1}^s \neq h_{it}^s] \quad \forall s \in \{\text{live}, \text{let}\}.$$

Bondholdings may be negative, representing borrowing. However, this borrowing must be collateralized by owned housing subject to a loan-to-value limit,

$$b_{it+1} \geq -\kappa q_{it\ell} (h_{it}^{\text{live}} + h_{it}^{\text{let}}),$$

and the interest rate which the household must pay when borrowing, r^m , is higher than the interest rate it receives when saving, r^f :

$$r^m > r^f.$$

¹⁹Technically this is not a monetary economy and F^m is in terms of the numeraire good.

²⁰The relevant housing price is the *current* price in the *old* location, $q_{\ell_{it-1}t}$.

2.2.3 Income

At the end of each period t , a household i living in location ℓ receives labor earnings equal to their marginal product under a linear production function with idiosyncratic component z_{it} and climate-impacted²¹ location-specific component $A_{\ell t}$. They receive interest income and rental income on post-adjustment liquid bond-holdings, \tilde{b}_{it} , and rental real estate, h_{it}^{let} , respectively.²²

Given location-level productivity $A_{\ell t}$ and rent $\rho_{\ell t}$, the household receives income,

$$\text{Income}_{it} = \underbrace{A_{\ell t} z_{it}}_{\text{earnings}} + \underbrace{r^f \tilde{b}_{it} \mathbb{1}[\tilde{b}_{it} \geq 0]}_{\text{interest income}} + \underbrace{\rho_{\ell t} h_{it}^{\text{let}}}_{\text{rental income}}.$$

2.2.4 Expenditures

If the household rents, they pay rent at rate $\rho_{\ell t}$. If they own housing, they pay maintenance at rate $\chi_{\ell t}^{\text{live}}$ or $\chi_{\ell t}^{\text{let}}$ for owner-occupied or rental housing, respectively. Maintenance consists of a fixed cost depending only on whether the home is owner-occupied and two location-specific climate-impacted variables: energy costs $y_{\ell t}$ and disaster intensity $\delta_{\ell t}^{\text{disaster}}$:

$$\begin{aligned}\chi_{\ell t}^{\text{live}} &= \chi^{\text{live}} + y_{\ell t} + \delta_{\ell t}^{\text{disaster}} \\ \chi_{\ell t}^{\text{let}} &= \chi^{\text{let}} + y_{\ell t} + \delta_{\ell t}^{\text{disaster}} \\ \text{where } \chi^{\text{live}} &< \chi^{\text{let}}.\end{aligned}$$

Given location-level energy costs $y_{\ell t}$, disaster intensity $\delta_{\ell t}^{\text{disaster}}$, and rent $\rho_{\ell t}$, total expenditures are,

$$\text{Expenditures}_{it} = \underbrace{g_{it}}_{\text{goods}} + \underbrace{\rho_{\ell t} h_{it}^{\text{rent}}}_{\text{rent}} + \underbrace{\chi_{\ell t}^{\text{live}} h_{it}^{\text{live}} + \chi_{\ell t}^{\text{let}} h_{it}^{\text{let}}}_{\text{maintenance}} + \underbrace{r^m \tilde{b}_{it} \mathbb{1}[\tilde{b}_{it} < 0]}_{\text{interest expenses}}.$$

The maintenance cost $\chi^{\text{let}} > \chi^{\text{live}}$ is higher for rental properties and summarizes a number of reasons why owner-occupied housing might provide a lower user cost of housing services than rental housing for an unconstrained household, in equilibrium, before frictions are taken into account. These include the higher utility value of owner-occupied housing, the maintenance and administrative requirements of maintaining a rental property, and income tax on rental income.

Without this wedge, households would have no reason to own their home as homeownership would

²¹Housing prices $q_{\ell t}$ and rents $\rho_{\ell t}$ are indirectly impacted by the climate state and expectations in equilibrium, but are not directly impacted by the climate state as productivity $A_{\ell t}$ is.

²²Note that this aspect of the model's timing is slightly unusual: households receive investment income within the same period that the investment is chosen. I choose this timing so that (1) renters, homeowners, and investors make housing decisions simultaneously (at the beginning of the period) and (2) rent paid by renters is received by landlords within (at the end of) the same period. To do otherwise imposes an unrealistic cost on landlords, who would otherwise have to wait ten years between the consumption foregone by purchasing a rental property and the consumption enjoyed out of rental income.

only impose borrowing constraints, illiquidity, and risk for no benefit. Without these frictions, however, households would have no reason to rent, as homeownership would provide unambiguously cheaper housing services. With these frictions, homeownership is more attractive in equilibrium for wealthier households who, needing to borrow less to buy housing, pay a lower effective user cost than less wealthy households for housing services from owned housing. Similarly, in equilibrium, rental housing investments provide higher expected returns than liquid assets at the cost of illiquidity and risk.

2.2.5 Idiosyncratic Shocks

At the end of the period, the household's income type evolves according to,

$$\begin{aligned}\log z_{it+1} &= p \log z_{it} + \zeta_{a_{it+1}} + \nu_{it} \\ \nu_{it} &\sim \mathcal{N}(0, \sigma_\nu) \quad \text{i.i.d.},\end{aligned}$$

where $p \in [0, 1]$ is mean reversion and ζ_a is an age-specific shifter.²³

2.2.6 Utility

Similarly to Kaplan et al., 2020, a household i in location ℓ derives utility from goods g_{it} , housing services h_{it} , and location-level amenities $\alpha_{\ell t}$, with constant elasticity of substitution $1/\sigma$ between goods and housing services and constant elasticity of intertemporal substitution $1/\eta$. Location-specific and climate-impacted amenities $\alpha_{\ell t}$ enter as an effective multiplier on consumption spending. Formally,

$$u(g, h, \alpha) = \frac{\left(\alpha (g^{1-\sigma} + \gamma h^{1-\sigma})^{\frac{1}{1-\sigma}}\right)^{1-\eta} - 1}{1 - \eta}.$$

Households i who have reached the maximum age $a_{it} = a_{\max}$ enjoy “warm-glow” bequest utility from the liquidation value of any assets which they own at end of the period.²⁴

$$\begin{aligned}V_{a_{\max}+1,t}(b, z, h^{\text{live}}, h^{\text{let}}, \ell) &= Q \frac{\tilde{b}^{1-\eta}}{1 - \eta} \\ \text{s.t. } \tilde{b} &= b + (1 - \phi) (q_{\ell t} h^{\text{live}} + q_{\ell t} h^{\text{let}}).\end{aligned}$$

The full household's problem is given in recursive form in Appendix D.

²³This is isomorphic to the idiosyncratic human capital process of Kaplan et al. (2020), except that I pull out the aggregate productivity shifter $A_{\ell t}$ into the income equation and make it location-specific.

²⁴This model does not consider the general equilibrium implications of these bequests (or indeed of any goods consumption). In particular, there is no explicit intergenerational wealth transmission and a reduction in end-of-life saving would not feed back into lower initial wealth for new households.

2.2.7 Household Entry

Each period, a new cohort, representing age 20-29, enters. Each household i in the new cohort draws individual state

$$x_{it} = (b_{it}, z_{it}, 0, 0, \ell_{it-1}, 1),$$

where $h_{it-1}^{\text{live}} = h_{it-1}^{\text{let}} = 0$ and $a_{it} = 1$. Bondholdings b_{it} and human capital z_{it} are drawn from an initial distribution

$$(b_{it}, z_{it} \mid a_{it} = 1) \sim \Lambda^{\text{init}}.$$

Initial location ℓ_{it-1} is equal to the population distribution of households in the fourth age group, representing age 50:

$$\Pr_t(\ell_{it} \mid a_{it} = 1) \sim \int_{x \in \mathbf{X}} \mathbb{1}[\ell(x; \Gamma_t) = \ell \wedge a(x; \Gamma_t) = 4] d\lambda_t(x),$$

where $\lambda_t : \mathcal{P}(\mathbf{X}) \rightarrow \mathbb{R}$ is the measure over individual states $x \in \mathbf{X}$ in period t , and Γ_t is the aggregate state in period t .

2.3 Housing

At each time t , the stock of housing $H_{\ell t} \in \mathbb{R}^+$ in each location ℓ is a state variable. Housing assets are traded in local residential real estate markets and rented in local housing rental markets. Markets are spatially segmented and all housing must be owned by households in the same location. A household may only own or rent housing in the location in which they live.

Housing depreciates over time and new housing is constructed by a static, competitive construction sector which produces using a location-specific housing production function.

2.3.1 Residential Real Estate Market

Let $\lambda_t : \mathcal{P}(\mathbf{X}) \rightarrow \mathbb{R}$ be the measure over individual states $x \in \mathbf{X}$, and Γ_t the aggregate state, in period t .

Demand In any location ℓ and time t , the stock of housing $H_{\ell t}$ is entirely owned by households who live in that location. Denote demand for residential real estate by²⁵

$$H_{\ell t}^D(q) \equiv \int_{x^{\text{choice}} \in \mathbf{X}^{\text{choice}}} (h^{\text{live}}(x; q, \Gamma_t) + h^{\text{let}}(x; q, \Gamma_t)) \mathbb{1}[\ell(x; q, \Gamma_t) = \ell] d\lambda_t(x).$$

²⁵I omit the dependence of choice variables on housing rent $\rho_{\ell t}$ in this subsection to focus on the dependence on housing price $q_{\ell t}$. In a sense, $\rho_{\ell t}$ is a function of Γ_t anyway.

Supply Before real estate is traded, a competitive construction sector constructs a quantity $(H_{\ell t} - \tilde{H}_{\ell t})$ of new housing, where $\tilde{H}_{\ell t} \equiv (1 - \delta^h)H_{\ell t-1}$ is the quantity of housing carried over from the previous period, and then sells it onto the market. The construction sector observes prices then builds instantaneously and immediately sells at those prices, making its decision static. The marginal cost of housing construction is a location-specific convex function of the (new) housing stock $H_{\ell t}$, as in Greaney (2021) and Saiz (2010).

$$c_\ell(H) = \Pi_\ell H^{\beta_\ell}.$$

I assume that the construction sector is competitive, so that if $H_{\ell t} > \tilde{H}_{\ell t}$, then $q_{\ell t} = c_\ell(H_{\ell t})$. Housing supply is thus given by

$$H_{\ell t}^S(q) = \begin{cases} c_\ell^{-1}(q) & q \geq c_\ell(\tilde{H}_{\ell t}) \\ \tilde{H}_{\ell t} & q < c_\ell(\tilde{H}_{\ell t}) \end{cases} \quad (1)$$

where $H_{\ell t}^D(q)$ denotes housing demand given housing price q .

The equilibrium condition for each residential real estate market is

$$H_{\ell t}^S(q) = H_{\ell t}^D(q). \quad (2)$$

2.3.2 Housing Rental Market

In each location ℓ , demand for rental housing is given by²⁶

$$H_{\ell t}^{\text{rent}}(\rho) = \int_{x \in \mathbf{X}} (h^{\text{rent}}(x; \rho, \Gamma_t)) \mathbb{1}[\ell(x; \rho, \Gamma_t) = \ell] d\lambda_t(x)$$

and demand for rental real estate is given by

$$H_{\ell t}^{\text{let}}(\rho) = \int_{x \in \mathbf{X}} (h^{\text{let}}(x; \rho, \Gamma_t)) \mathbb{1}[\ell(x; \rho, \Gamma_t) = \ell] d\lambda_t(x).$$

Rental housing markets are also segmented by location. The equilibrium condition for each rental housing market is

$$H_{\ell t}^{\text{rent}}(\rho) = H_{\ell t}^{\text{let}}(\rho). \quad (3)$$

2.4 Climate

Locations are heterogeneously exposed to global climate conditions, affecting local productivity $A_{\ell t}$, amenities $\alpha_{\ell t}$, residential energy costs $y_{\ell t}$, and disaster damages $\delta_{\ell t}$. Global climate conditions evolve according

²⁶I omit the dependence of choice variables on housing price $q_{\ell t}$ in this subsection to focus on the dependence on housing rent $\rho_{\ell t}$. In a sense, $q_{\ell t}$ is a function of Γ_t anyway.

to a stylized process whose purpose is to match key moments of climate uncertainty and to allow for a news shock affecting the future global climate trajectory without affecting the current physical climate state.²⁷

2.4.1 Productivity, Amenities, and Energy Costs

Productivity $A_{\ell t}$, amenities $\alpha_{\ell t}$, and residential energy costs $y_{\ell t}$ are fully flexible by location both in their level and in their response to global mean temperature SST_t . I linearize (or log-linearize) this relationship:

$$\begin{aligned}\log A_{\ell t} &= \log \bar{A}_{\ell} + A_{\ell}^g SST_t \\ \log \alpha_{\ell t} &= \log \bar{\alpha}_{\ell} + \alpha_{\ell}^g SST_t \\ y_{\ell t} &= \bar{y}_{\ell} + y_{\ell}^g SST_t\end{aligned}$$

I argue in Section 3 that this linearization is reasonable around the $\sim 4^{\circ}\text{C}$ range of global temperatures of interest, for both the sensitivity of local temperatures to global temperatures and the sensitivity of these economic fundamentals to local temperatures.²⁸

In each location ℓ and period t , local disaster intensity (damages per unit of housing) $\delta_{\ell t}^{\text{disaster}}$ is a (temporally-constant, spatially-varying) multiple of the aggregate disaster intensity $\delta_t^{\text{disaster}}$ for that period:

$$\delta_{\ell t}^{\text{disaster}} = \delta_{\ell}^g \delta_t^{\text{disaster}}.$$

2.4.2 Global Climate State

The global climate state evolves according to the following stylized process. This is an approximant to the richer climate process which I take to the data, described in Section 4.

Each period t , the global climate state is given by

$$\mathbf{D}_t = \{w_t, m_t, \underbrace{SST_t}_{\text{Global Temperature}}, \underbrace{\delta_t^{\text{disaster}}}_{\text{Global Disaster Intensity}}\},$$

where w_t and m_t are state variables loosely corresponding to global energy generation and emissions intensity, respectively, though in their calibration they will be effectively adjusted to account for scenario uncertainty and model uncertainty.

An annual index of global anthropogenic climate forcing rates (loosely representing annual emissions) e_t is constructed as the product of a factor w_t that grows at constant rate and a stochastic factor m_t that shrinks in expectation faster than m_t grows, so that e_t starts near zero, grows once w_t becomes sufficiently

²⁷This stylized process will be calibrated to match moments generated by a richer, quantified model of climate change and Bayesian climate expectations in Section 4.

²⁸When local temperatures are measured in heating- and cooling-degree-days.

large, then almost surely eventually converges to zero as m_t extinguishes w_t . I am interested in the region of the process, away from the stationary distribution, where e_t is still positive. Formally,²⁹

$$\begin{aligned} e_t &= w_t m_t \\ \log w_{t+1} &= \log w_t + g^w \\ \log m_{t+1} &= \log m_t - \beta_m w_t + \varepsilon_t^m \\ \varepsilon_t^m &\sim \mathcal{N}(0, \sigma_m^2). \end{aligned} \tag{4}$$

Global temperature SST_t and disaster intensity δ_t (expressed as the deviation from pre-industrial levels³⁰) follow an autoregressive process impacted by forcings e_t :

$$\begin{aligned} \text{SST}_{t+1} &= \rho_c \text{SST}_t + \beta_{\text{SST}} e_t \\ \log \delta_{t+1} &= \rho_\delta \log \delta_t + \beta_\delta e_t. \end{aligned}$$

The evolution of m_t is stochastic and summarizes all uncertainty about the future trajectory of the global climate. Note that ε_t^m represents a persistent shock to the growth rate of temperatures and disaster damages and impacts the future trajectory of the global climate state but not its current physical state.

2.5 Recursive Stochastic Equilibrium

2.5.1 State Space

I now drop time t subscripts and define the evolution of the aggregate state in recursive form.

The beginning-of-period aggregate state Γ is,

$$\Gamma = (\lambda, \mathbf{H}, \mathbf{D}),$$

where $\lambda : \mathcal{P}(\mathbf{X}) \rightarrow \mathbb{R}$ is the measure over individual states $x \in \mathbf{X}$, $\mathbf{H} = \{\tilde{H}_\ell\}_\ell$ is the set of beginning-of-period location-level housing stocks, and \mathbf{D} is the aggregate climate state.

2.5.2 Equilibrium

A recursive stochastic equilibrium is

²⁹Note that this particular process does not admit simulation from the infinitely distant past because m_t is nonstationary. This is easily solved by substituting $\log m_{t+1} = \log m_t - (\rho_m + \varepsilon_t^m)w_t$, but this is unnecessary for the purposes of this study.

³⁰Disaster damages at the pre-industrial baseline level can be considered a form of maintenance, whose spatial variation can be approximately soaked up by $\Pi_{\ell t}$.

- A set of household policy and value functions solving Equation (10),
- The aggregate transition function

$$\Omega(\Gamma' | \Gamma),$$

over

$$\Gamma = \{\lambda, \mathbf{H}, \mathbf{D}\}$$

composed of the transition functions over λ , \mathbf{H} , and \mathbf{D} (formally defined by Equation (11) in Appendix D, and Equations (1) and (4), respectively), and

- Prices $q_\ell(\Gamma)$, $\rho_\ell(\Gamma)$ satisfying the market clearing conditions in Equations (2) and (3), respectively.

2.6 Shock Concept

I consider an economy subject to two types of shock: (1) a shock to an initial stationary steady state corresponding to the unexpected onset of a stochastic climate transition and (2) subsequent per-period news shocks from an anticipated distribution about the future trajectory of the global climate.

First, I consider an economy in an initial stationary steady state which unexpectedly begins to experience climate change. Second, as soon as the stochastic climate process begins, households correctly anticipate that it will continue according to the stochastic climate process described in Section 2.4.2.

Note that climate change is highly persistent but not permanent. Climate forcings e_t almost surely eventually converge to zero, as do, consequently, all temperature and disaster intensity deviations-from-baseline,

$$\begin{aligned} \lim_{t \rightarrow \infty} e_t &= 0 \\ \lim_{t \rightarrow \infty} \text{SST}_t &= 0 \\ \lim_{t \rightarrow \infty} \delta_t &= 0, \end{aligned}$$

returning the economy to the stationary steady state.

I use this stationary steady state as the initial aggregate state which experiences an unexpected climate transition. Specifically, I consider an initial stationary steady state in which $m_t = m = 0$. (The value of $w_t \in \mathbb{R}$ affects nothing.) After the shock, the values (m, w) are then unexpectedly set to (m_0, w_0) , which I calibrate in Section 4.

3 Climate Damages

I spend the next three sections quantifying the model. In this section, Section 3, I combine and harmonize estimates from the climate science and environmental economics literatures to quantify the impact of global climate conditions on local economic fundamentals: productivity, amenities, energy costs, and disaster risks.

In Section 4, I calibrate the global climate process. I do this by constructing and quantifying a richer model of stochastic global climate change and Bayesian climate expectations, then calibrating the simpler climate process in the economic model to match key moments of the richer, quantified model.

In Section 5, I calibrate the remaining parameters of my economic model using data from the Survey of Consumer Finances and the Public Use Microdata Sample of the U.S. Census.

3.1 Global Climate Conditions → Local Economic Fundamentals

To calibrate the impact of global climate conditions on local economic fundamentals, I combine estimates of the impact of global climate conditions on local climate conditions with estimates of the impact of local climate conditions on local economic fundamentals:

Global Climate Conditions → Local Climate Conditions → Local Economic Fundamentals.

As my spatial unit, I use the Public Use Microdata Areas (PUMAs), which are the smallest spatial unit available in publicly available U.S. Census microdata.³¹

Available in the literature are estimates of local climate conditions under specific climate scenarios and estimates of the effects of local temperature metrics on local economic fundamentals. Furthermore, estimates of different local economic impacts taken from different studies may overlap in terms of the effects they pick up.

To generalize estimates of local temperature responses to global climate conditions, I linearize between estimates for 2000 and 2080 under RCP4.5.

To combine and generalize estimates of the response of local economic fundamentals to local temperature metrics, I compile a set of studies whose methodologies, where applicable, each control for the effects measured by the other studies. Where available, I use nonparametric or overparameterized estimates and show that the effects measured are approximately linear in the temperature metric I choose. I therefore argue that I am able to linearize all the way through, obtaining reasonably linearized estimates of the responses of local economic fundamentals to global climate conditions.³²

Explicitly, I allow local labor productivity $A_{\ell t}$, amenities $\alpha_{\ell t}$, residential energy costs $y_{\ell t}$, and disaster

³¹In particular, I use the 1990 PUMA boundaries used in the 1990 U.S. Census Public Use Microdata Sample.

³²For impacts on disaster damages, data limitations preclude this check.

damages to housing $\delta_{\ell t}$, to depend on global climate conditions. I allow these variables to be fully-flexibly location-specific in their levels and sensitivity to global climate conditions:³³

$$\begin{aligned}\log A_{\ell t} &= \log \bar{A}_{\ell} + A_{\ell}^g \text{SST}_t \\ \log \alpha_{\ell t} &= \log \bar{\alpha}_{\ell} + \alpha_{\ell}^g \text{SST}_t \\ y_{\ell t} &= \bar{y}_{\ell} + y_{\ell}^g \text{SST}_t \\ \delta_{\ell t} &= \delta_{\ell}^g \bar{\delta}_t.\end{aligned}$$

I define $A_{\ell t}$ as a multiplier on the effective quantity of labor supplied by each household in a location. I define $\alpha_{\ell t}$ as a multiplier on the effective quantity of consumption enjoyed by each household in a location. I define $y_{\ell t}$ as the overall cost of energy required to heat and cool a typical owner-occupied two-bedroom in location ℓ over the course of period t . I define $\delta_{\ell t}$ as the excess disaster damages due to climate change suffered by a typical owner-occupied two-bedroom housing unit in location ℓ in period t .

In Section 3.4, I report the general magnitudes and economic and spatial heterogeneity of these estimated climate damages, by naively dollarizing and summing them for each household in the 2020 American Community Survey (ACS). By far the most severely affected individual locations are those exposed to severe flooding, primarily along the East Coast and in Central Appalachia. However, a far larger area is exposed to temperature changes, such that overall damages due to temperature are likely much larger than those due to flooding.³⁴

3.2 Global Climate Conditions → Local Climate Conditions

I use climate projections from the Coupled Model Intercomparison Project 5 (CMIP5) to estimate the impacts of global climate conditions on local climate conditions. The relevant measure of local climate conditions that I use are heating degree days (HDD) and cooling degree days (CDD).

The number of annual heating (cooling) degree-days in a location is sum over the days in a year of the number of degrees by which daily temperatures are below (above) 18.3°C (65°F). For location i , year t , days d ,

$$\begin{aligned}\text{HDD}_{it} &= \sum_{d \in D_i} \max(18.3 - T_{idt}, 0) \\ \text{CDD}_{it} &= \sum_{d \in D_i} \max(T_{idt} - 18.3, 0).\end{aligned}$$

³³The intercept for $\delta_{\ell t}$ is zero because $\delta_{\ell t}$ and $\bar{\delta}_t$ are defined as the deviation from the same pre-industrial baseline.

³⁴The comparison of overall magnitudes at the end of this section is only meant to be descriptive and does not take into account the behavioral and price responses whose quantification is the purpose of the full model.

For each location, I linearize between CMIP5 ensemble model median projections of 2000 HDDs and 2080 HDDs under RCP8.5 to obtain the projected change in HDD and CDD per °C global warming. I do the same for CDD. Figure 1 displays the results.

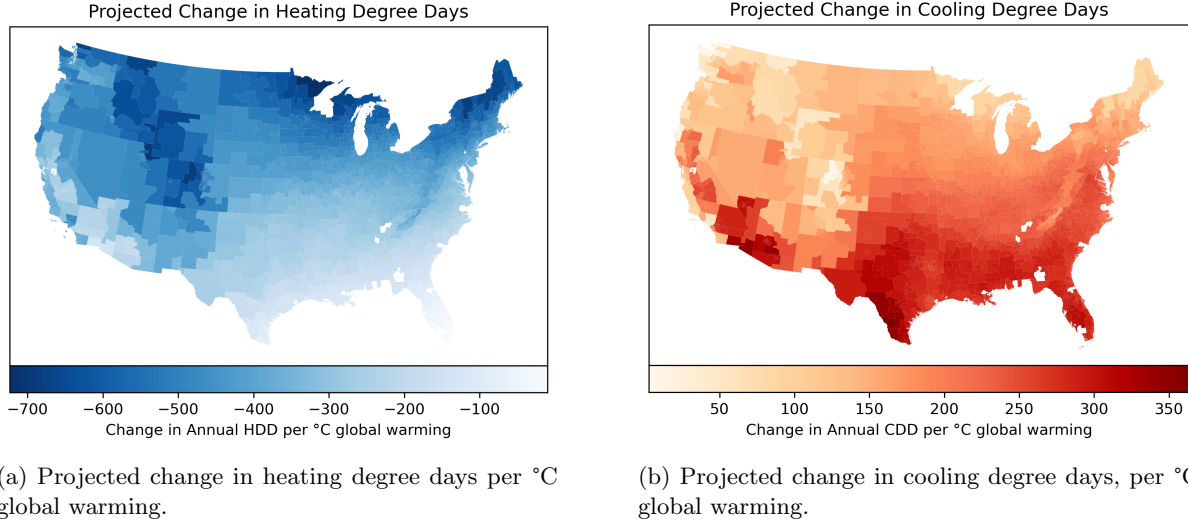


Figure 1

Projected change in heating and cooling degree days (HDD and CDD) per °C global warming. I use CMIP5 ensemble median estimates of projected HDD and CDD under RCP8.5 for 2000 and 2080 (Gassert et al., 2021). I average over each location for each scenario. For each location, I divide the projected 2020-2080 increase in HDD (CDD) by the corresponding CMIP5 ensemble median projected change in global sea surface temperatures (SST) under RCP8.5 (Hsiang et al., 2017). Locations are Public Use Microdata Areas, 1990 boundaries.

3.3 Local Climate Conditions → Local Economic Fundamentals

I compile and harmonize estimates from the environmental economics literature on the impact of local climate conditions on local economic fundamentals: productivity, amenities, energy costs, and disaster risks. For each impact, I use estimates from a study which, where applicable, controls in its methodology for effects picked up by each other study. This is necessary to prevent double-counting.

3.3.1 Labor Productivity

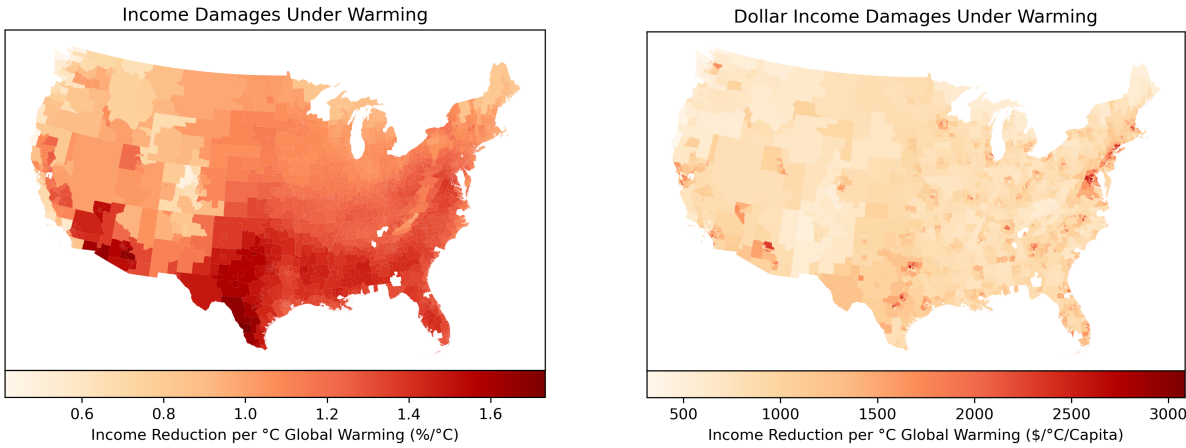
I take estimates of the effect of temperature on income from Deryugina and Hsiang (2017). They use spatial panel data on weather variation and income for U.S. counties in the period 1969-2014 to estimate the effect of temperature on income.³⁵

³⁵See Appendix Section A.1 for details.

Parameter	Productivity Effect per DD (% of Annual Income)	Productivity Effect per 365 DD (% of Annual Income)
HDD	6.57×10^{-6}	0.240
CDD	4.50×10^{-5}	1.66

Table 1: Productivity Damages per Heating and Cooling-Degree Day

Productivity damages per single ($^{\circ}\text{C}$) degree-day, and per 365 degree-days, relative to the 18.3°C (65°F) baseline, as a percentage of annual income. The second column, representing the effect of 365 additional CDDs (HDDs), is the implied marginal damage (benefit) of a one-degree increase in temperature for each day of the year, in a location where every day is already above (below) 18.3°C .



(a) Percentage reduction in productivity per capita, per $^{\circ}\text{C}$ global warming. Estimates are from Deryugina and Hsiang (2017). I linearize and multiply their estimates by the estimated change in HDD and CDD per $^{\circ}\text{C}$ global warming described in Figure 1. Further details are in Appendix Section A.1.

(b) Naively dollarized reduction in productivity per capita, per $^{\circ}\text{C}$ warming. I merely multiply the percentage reduction in productivity reported in Figure 2a by observed annual wages for each household in the 2020 ACS and mean across households by location.

Figure 2: Productivity Damages per $^{\circ}\text{C}$ Global Warming

3.3.2 Heat and Cold Disamenities

I take estimates of heat and cold disamenities from Albouy et al. (2016). The authors estimate the largest percentage of one's income one would be willing to forego in order to avoid one marginal day at a certain temperature. I introduce this damage into my model as an effective multiplier on consumption spending in utility. As described in Appendix A.3, their estimates are close to log-linear in the *difference* between the daily temperature and 18.5°C (65°F), suggesting that they can be well-approximated by a linear function of HDD and CDD. I report these estimated coefficients on HDD and CDD in Table 2.

Figure 3 shows the implied change in heat and cold disamenities per $^{\circ}\text{C}$ global warming. Figure 4 shows the implied net change in location-level amenities per $^{\circ}\text{C}$ global warming.

Parameter	WTP per DD (% of Income)	WTP per 365 DD (% of Income)
HDD	3.05×10^{-3}	1.11
CDD	4.40×10^{-3}	1.61

Table 2

Amenity Damages per Heating- and Cooling-Degree Day. The first column represents the willingness-to-pay to avoid a single ($^{\circ}\text{C}$) degree-day, relative to the 65°F baseline, as a percentage of annual income. The second column, representing the willingness to pay to avoid 365 CDD (HDD), is the marginal damage (benefit) of a one-degree increase in temperature for each day of the year, in a location where every day is already above (below) 18.3°C .

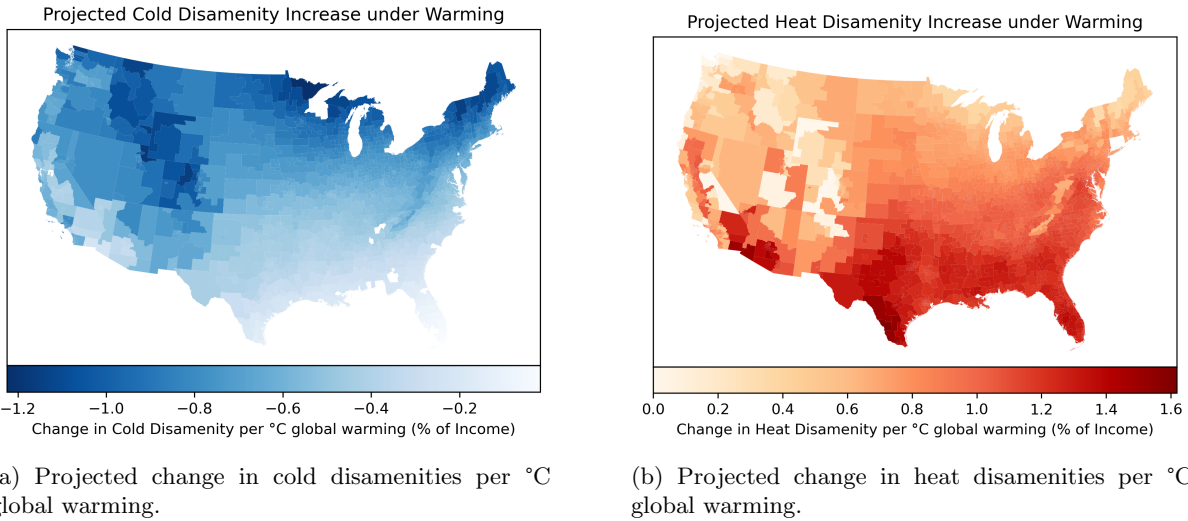


Figure 3

Heat and Cold Disamenities per $^{\circ}\text{C}$ Global Warming. Panel (3a) reports the estimated maximum percentage of income an average household in a location would be willing to forego in order to avoid the change in local amenities resulting from 1°C global warming. Estimates are obtained by, first, linearizing the estimates of Albouy et al., 2016 of the amenity impacts of one additional annual cooling-degree-day (the results of this linearization are reported in Table 2), then multiplying by the estimates of the change in local cooling-degree-days induced by 1°C global warming reported in Figure 1b. Panel (3b) reports the same, but for heating-degree-days.

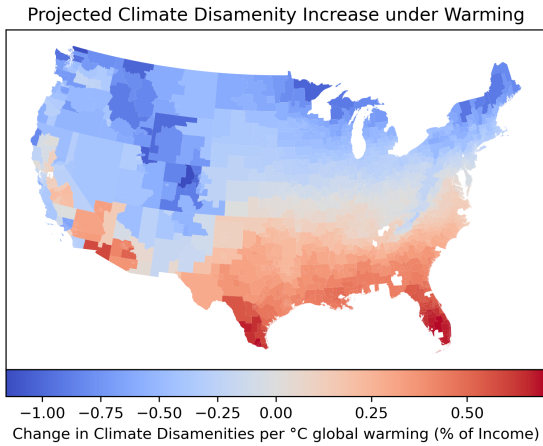


Figure 4: Net Climate Amenity Damages per °C Global Warming

Net projected change in cold and heat disamenities, as an equivalent percentage of annual income, per °C global warming. Estimates are obtained by adding the estimated local cold disamenity and heat disamenity impacts of 1°C global warming, reported in Figure 3.

3.3.3 Energy Costs

I take projections of the effect of warming on energy costs from Rode et al. (2021). Figure 5a describes the current levels of residential electricity consumption per capita in the ACS. Figure 5b describes the projected change in energy expenditure per capita per °C global warming.

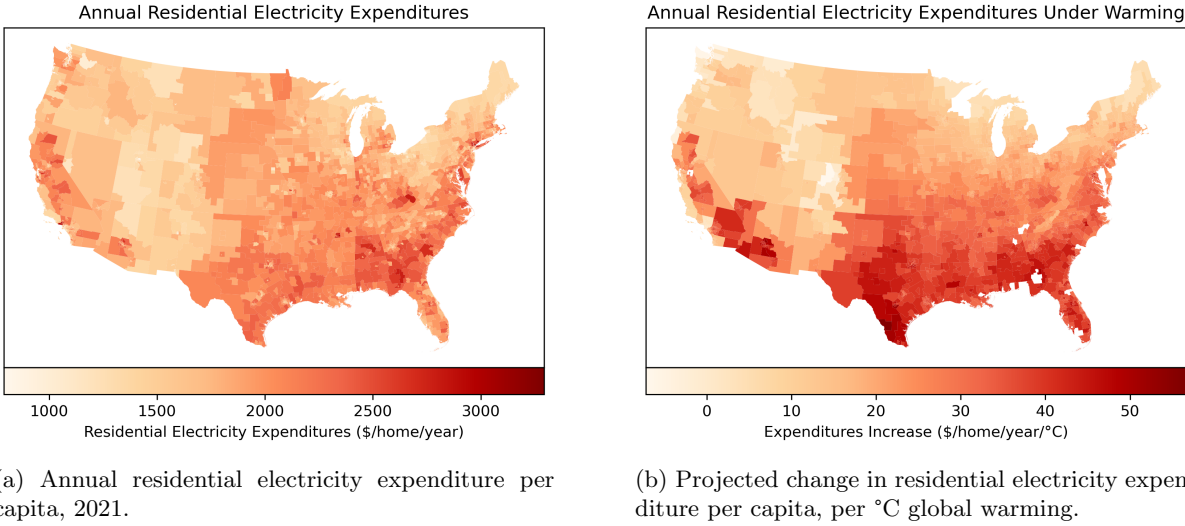


Figure 5

Residential energy expenditure damages per °C global warming. Estimates are obtained by dividing projected percentage electricity consumption growth between 2020 and 2100 under RCP8.5 for each county from Rode et al. (2021) by the ensemble median projected increase in mean global temperatures in that period and scenario from Rasmussen and Kopp (2017). I then apply a population-based crosswalk to PUMAs and multiplying by residential electricity expenditure per capita from the 2020 ACS.

3.3.4 Disaster Damages

I use projections of climate impacts on property damages due to flooding from Bates et al. (2021), as reported in Wing et al. (2022). The authors use a high-resolution inundation model to compute comprehensive coastal, fluvial, and pluvial flood risk. Theirs is the first large-scale inundation model to incorporate all three forms of flooding.

Flooding represents the large majority of projected climate damages through natural disasters. Figure 6 shows the relative property damages from flooding between 1975 and 2020 by FEMA hazard type from the Spatial Hazard Events and Losses Database for the United States (SHELDUS). Damages which involve both storms and flooding are split evenly between the relevant flooding-related category and storm-related category. This may thus represent a significant underestimate of total damages from flooding, as flooding damages often occur in conjunction with storms. This leaves wind-related damages and wildfires as quantitatively large, plausibly climate-impacted hazards. However, recent climate literature projects only small (on average) and highly uncertain impacts of climate change on wind-related damages. Wildfires remain unaccounted for, but I nevertheless conclude that the comprehensive flooding damage projections of Bates et al. (2021) likely capture a substantial share of overall excess disaster damages due to climate change.³⁶

Figure 7a displays their model-predicted Average Annual Losses (AAL), as a percentage of residential

³⁶See Appendix Section A.2 for details.

structure value, under 2020 climate conditions. Figure 7b shows projected flooding damage growth, as a percentage of current AAL, per °C global warming.

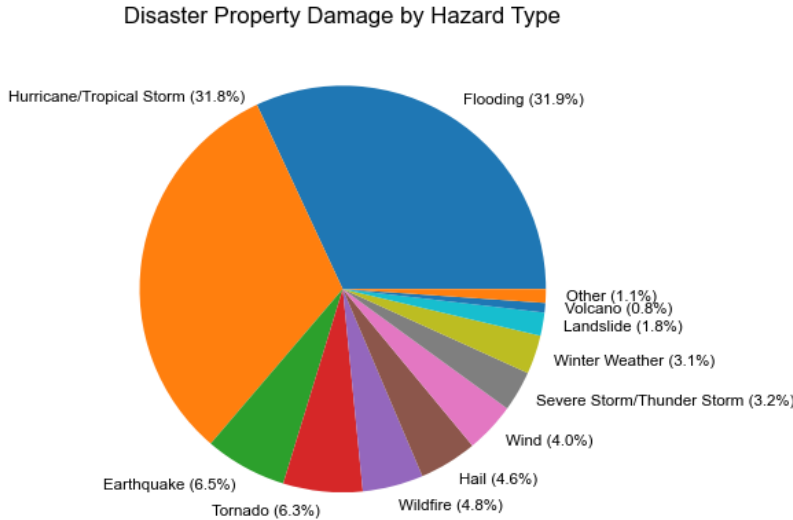
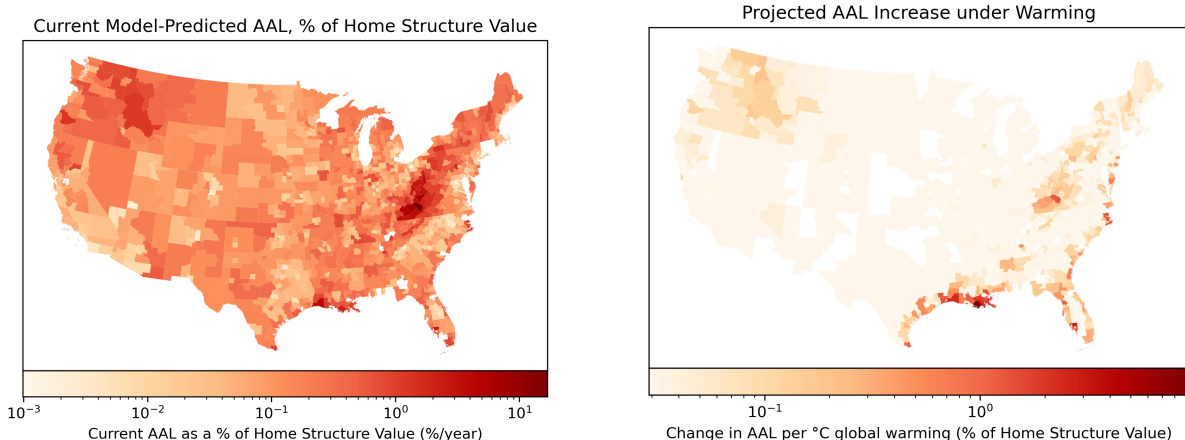


Figure 6: Total disaster property damage by FEMA hazard type, 1975-2020. From SHELDUS.



(a) Model-predicted 2020 Average Annual Losses (AAL), as a % of housing structure value, from the model of Bates et al. (2021) as reported by Wing et al. (2022).

(b) Projected flooding damage growth as a percentage of housing structure value in the model of Bates et al. (2021) as reported by Wing et al. (2022). I divide their projections, which are changes from 2020-2050 under RCP4.5, by the ensemble median of global temperature change in that period and scenario from Rasmussen and Kopp (2017). Units are percentage *points*, representing the expected percentage of total home structure value destroyed by flooding in each location following 1°C global warming. Log scale.

Figure 7

3.4 Damage Magnitudes and Variation

In order to roughly gauge the relative magnitudes and spatial distribution of these damages, I naively dollarize estimates of annual damages from each source, per 1°C global warming, for every household in the 2020 ACS. Specifically, I compute damages incurred by 1°C global warming, in the absence of behavioral or equilibrium responses, as a percentage of income. Damages are dollarized as follows. Productivity and amenity damages are both multiplied by current income. Residential energy expenditure damages are multiplied by current residential electricity expenditures. Disaster damages are multiplied by current home value, if the home is owned, or set to zero if the home is rented.

Figure 8 shows net damages from all sources combined. Figure 8a shows damages on a log scale to highlight the severity of damages in highly flooding-exposed counties. Figure 8b is on a linear scale to illustrate more widespread but less localized damages, mostly temperature-related.

Figure 9 compares damages as a percentage of income by income and by latitude. Damages are relatively flat by income, partly by construction: productivity and amenity damages are constructed as a percentage of income. Nevertheless, flooding and energy cost damages are proportionally larger for lower-income households, due to larger housing price exposure and energy expenditure for these households as a proportion of income.

Spatial inequality in damages is quite dramatic. Figure 9b shows damages by latitude. Households at lower latitudes experience significantly greater heat disamenities and productivity damages and smaller decreases in cold disamenities. Flooding damages are relatively small as a proportion of total damages, but are highly spatially concentrated.

Figure 10 displays mean damage estimates—in absolute dollar terms and as a percentage of income—per $^{\circ}\text{C}$ global warming in the absence of behavioral or equilibrium responses, along other spatial margins: distance to coast, latitude, and 2020 mean annual temperature. Damages are decreasing in distance from the coast. This is primarily driven by climate amenities and income impacts, which operate through temperature rather than flood risk, though flood risk is a contributor. Damages are strongly increasing in current mean annual temperature, due largely to climate impacts on amenities and income, though flood risk is a contributor in this case too. Overall damages are positive for most households, with households in the bottom decile of current mean annual temperature still experiencing positive damages (net harms) on average and households in the top decile of current mean annual temperature experiencing mean damages of almost 3% of income per $^{\circ}\text{C}$ global warming.

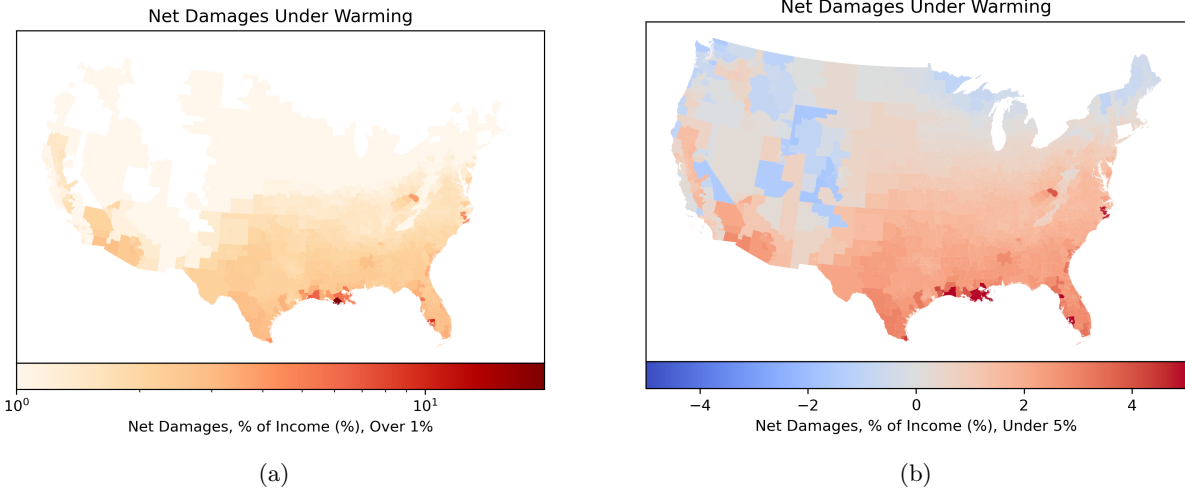


Figure 8

Mean damages per $^{\circ}\text{C}$ global warming, as an equivalent percentage of income, in the absence of behavioral or equilibrium responses. Estimates are obtained by summing over damages to labor income, location amenities, residential energy costs, and residential disaster damages, as computed in this section, for each household in the 2020 American Community Survey. Damages are then meaned within each PUMA. Panel (8a) is on a log scale and bottom coded at 1%. Panel (8b) is on a linear scale and top coded at 5%.

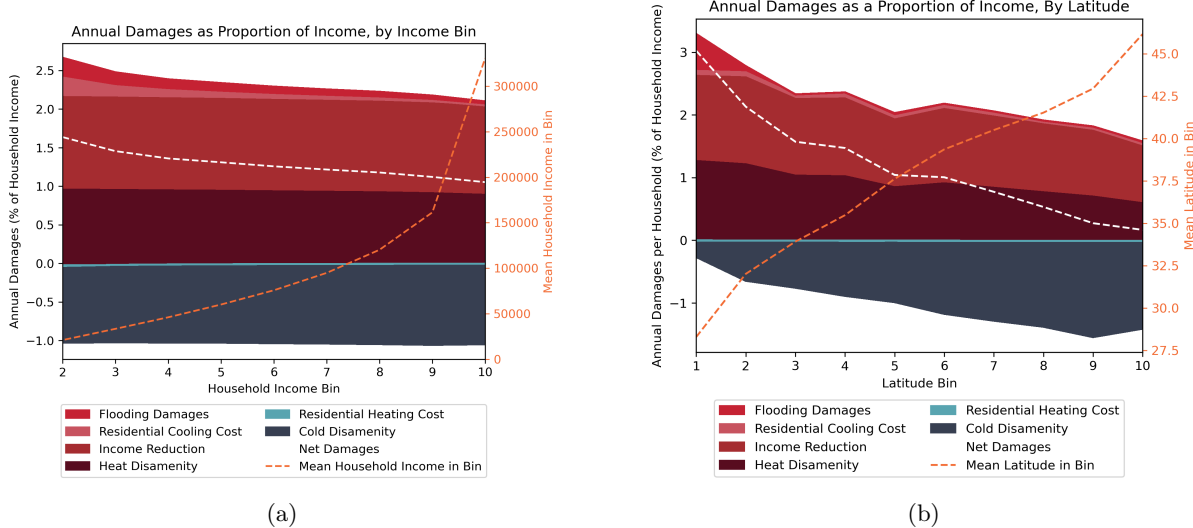


Figure 9

Mean damages per $^{\circ}\text{C}$ global warming, as an equivalent percentage of income, in the absence of behavioral or equilibrium responses. Estimates are obtained by summing over damages to labor income, location amenities, residential energy costs, and residential disaster damages, as computed in this section, for each household in the 2020 American Community Survey. Panel (9a) reports the mean for each income bin. Panel (9b) reports the mean for each latitude bin.

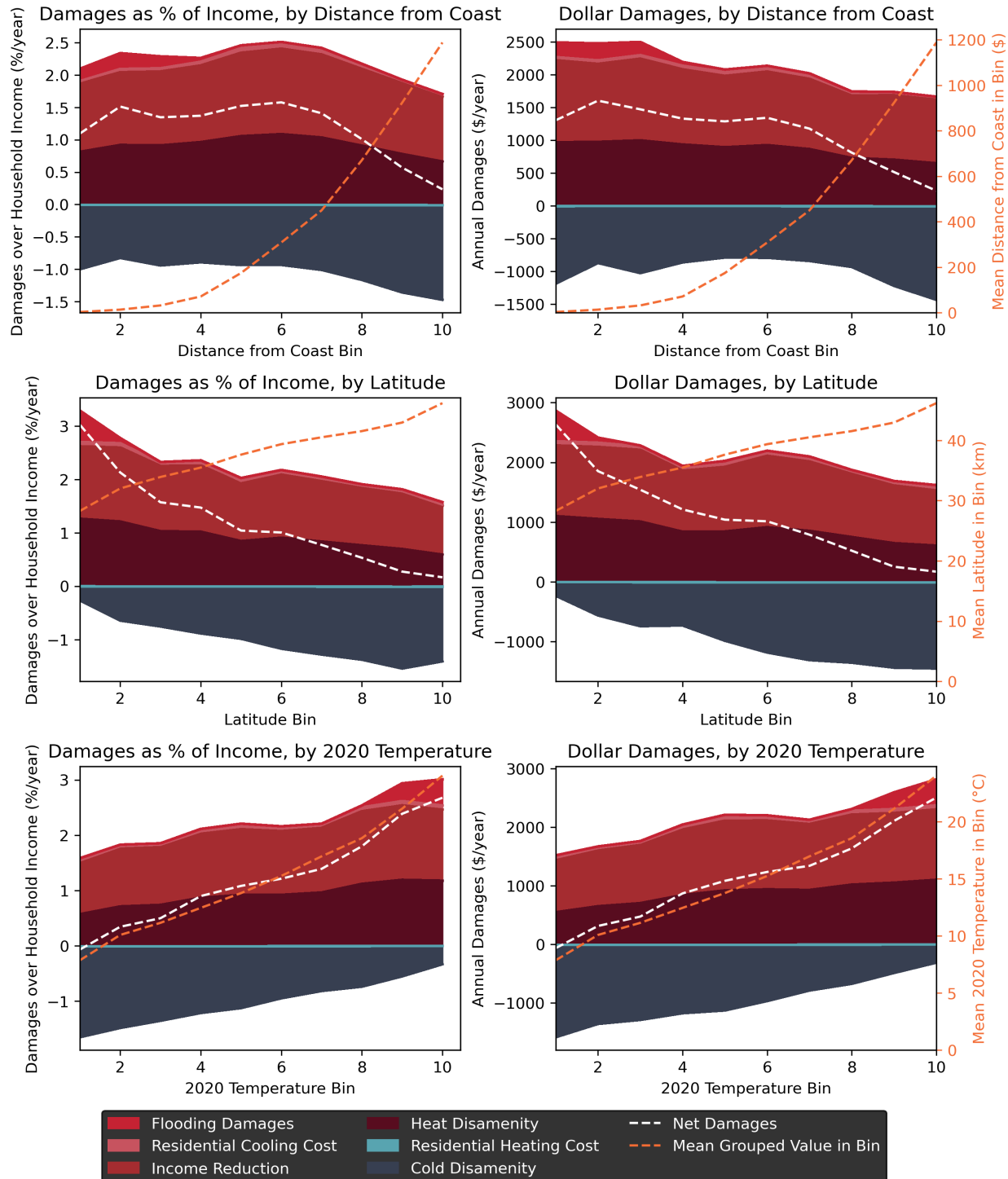


Figure 10

Mean damages by household income, distance from coast, and urban population share of household location (PUMA). Estimates are obtained by summing over damages to labor income, location amenities, residential energy costs, and residential disaster damages, as computed in this section, for each household in the 2020 American Community Survey.

4 Calibrating Climate Expectations

In this section I calibrate the climate process by mapping data on climate expectations and uncertainty to an enriched auxiliary model of global climate and climate expectations. The auxiliary model explicitly incorporates multiple climate variables and sources of climate uncertainty and can exactly match moments from the data and existing climate projections on the expected evolution of the global climate, as well as each source of uncertainty. I then calibrate the simplified climate process in the main model to match key moments in the auxiliary model representing overall uncertainty: in particular, I match the model-predicted quartiles, given 2020 information, of 2100 global temperatures and disaster damages.

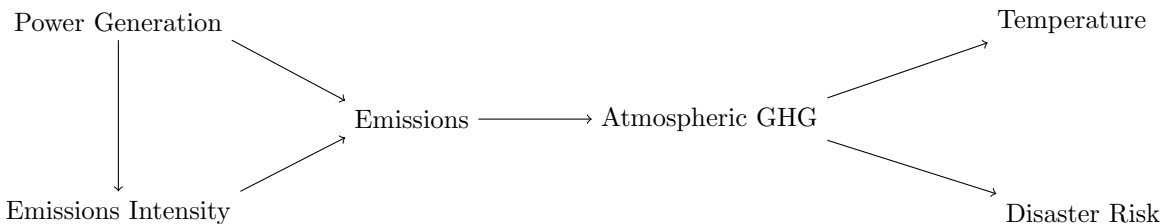
The auxiliary model consists of a richer stochastic global climate process and a representative Bayesian household who is uncertain about the sensitivities of global temperatures and disaster damages to emissions and learns about these over time by observing realized global temperatures and disaster damages.

The auxiliary model explicitly incorporates: internal variability, in that annual realized global temperatures and disaster damages have a random component; scenario uncertainty, in that the path of global emissions is stochastic; and climate model uncertainty, in that the household learns over time about the unobserved sensitivities of global temperatures and disaster damages to emissions.

4.1 Stochastic Global Climate Process

I describe a process in which the evolution of global climate conditions is influenced by greenhouse gas (GHG) emissions. The purpose of this model is not to be a realistic representation of the climate system but to parsimoniously encode, at any point in time, a plausible distribution of future climate paths, such that (1) the model can match key moments from data and climate projections on the evolution of, and uncertainty in the evolution of, the global climate; (2) news shocks affect the distribution of future paths in a straightforward and quantitatively plausible way, impacting the anticipated trajectory of the global climate without immediately impacting the physical climate state.

The enriched stochastic global climate process consists of a nonlinear process on the following variables, where arrows indicate dependence within each period:



Conceptually, global power generation grows at a constant rate. The annual level of GHG emissions is the product of global power generation and the emissions intensity of power generation. The emissions

intensity decreases over time, eventually overtaking power generation, so that emissions eventually vanish.³⁷ Emissions contribute to a stock of atmospheric GHGs which is gradually absorbed out of the atmosphere by natural processes. Annual mean temperatures and disaster damages are drawn each year from a distribution whose mean depends on the stock of atmospheric GHG.

Formally, time is discrete. Global power generation w_t grows deterministically at constant rate g^w :

$$\log w_{t+1} = \log w_t + g^w.$$

The log emissions intensity of power generation, m_t , decreases in proportion to current power generation:

$$\begin{aligned}\log m_{t+1} &= \log m_t - \beta_m w_t + \varepsilon_t^m \\ \varepsilon_t^m &\sim \mathcal{N}(0, \sigma_m).\end{aligned}$$

Annual emissions are simply the product of power generation and emissions intensity:

$$e_t = w_t m_t. \tag{5}$$

The stock of atmospheric greenhouse gases, GHG_t follows an autoregressive process. GHGs are added to by emissions and subtracted from by natural absorption at rate $(1 - \rho_{\text{GHG}})$:

$$\text{GHG}_{t+1} = c_{\text{GHG}} + \rho_{\text{GHG}} \text{GHG}_t + e_t. \tag{6}$$

Each year, realized temperatures and logged disaster damages are independently drawn from Normal distributions with means $\overline{\text{SST}}_t$ and $\bar{\delta}_t$ respectively,

$$\begin{aligned}\text{SST}_t &\sim \mathcal{N}(\overline{\text{SST}}_t, \sigma^d) \\ \log \delta_t &\sim \mathcal{N}(\log \bar{\delta}_t, \sigma^d).\end{aligned}$$

The mean of the temperature distribution $\overline{\text{SST}}_t$ is linear in the stock of atmospheric GHG:

$$\overline{\text{SST}}_t = \tilde{c}_{\text{SST}} + \tilde{\beta}_{\text{SST}} \text{GHG}_t.$$

³⁷This process remains agnostic on the extent to which these emissions intensity reductions are due to policy responses or “natural” technological progress.

Substituting in Equations 5 and 6 and simplifying,

$$\overline{\text{SST}}_{t+1} = c_{\text{SST}} + \rho_c \overline{\text{SST}}_t + \beta_{\text{SST}} w_t m_t. \quad (7)$$

Without loss of generality, I define $\overline{\text{SST}}_t$ as the deviation from the stationary steady state baseline, so that,

$$\overline{\text{SST}}_{t+1} = \rho_c \overline{\text{SST}}_t + \beta_{\text{SST}} w_t m_t.$$

Similarly, the mean of the annual disaster damage distribution $\bar{\delta}_t$ is log-linear in the stock of atmospheric GHG,

$$\log \bar{\delta}_t = \tilde{c}_\delta + \tilde{\beta}_\delta \text{GHG}_t.$$

Simplifying similarly to Equation (7),

$$\log \bar{\delta}_{t+1} = \rho_\delta \log \bar{\delta}_t + \beta_\delta w_t m_t.$$

Altogether, the global climate process of the auxiliary model is as follows:

$\log w_{t+1} = \log w_t + g^w$	Global Energy Generation
$\log m_{t+1} = \log m_t - \beta_m w_t + \varepsilon_t^m$	Emissions Intensity
$\overline{\text{SST}}_{t+1} = \rho_{\text{SST}} \overline{\text{SST}}_t + \beta_{\text{SST}} w_t m_t$	Global Temperature
$\log \bar{\delta}_{t+1} = \rho_\delta \log \bar{\delta}_t + \beta_\delta w_t m_t$	Global Disaster Risk
$\varepsilon_t^m \sim \mathcal{N}(0, \sigma_m^2)$	Scenario Uncertainty
$\text{SST}_t \sim \mathcal{N}(\overline{\text{SST}}_t, \sigma_{\text{SST}}^2)$	Internal Temperature Variability
$\log \delta_t \sim \mathcal{N}(\log \bar{\delta}_t, \sigma_\delta^2)$	Internal Disaster Variability

Two sources of uncertainty are already present: internal variability, in the variability of annual temperature and disaster realizations given global climate conditions; and scenario uncertainty, in that emissions intensity evolves stochastically. The following section adds climate model uncertainty, in which households do not directly observe the coefficients β_{SST} and β_δ , but instead must learn about them over time.

4.2 Bayesian Updating of Climate Expectations

In order to incorporate model uncertainty over the coefficients β_{SST} and β_δ , consider a representative rational Bayesian household who observes the climate process defined in Section 4.1. The household does not directly observe the coefficients β_{SST} and β_δ or the true means $\bar{\delta}_t$ and $\overline{\text{SST}}_t$. Instead, they observe the noisy

realizations δ_t and SST_t . Assume that all households have common priors and common signals so that it suffices to consider the beliefs of the representative household. Assume also that the household observes all other time- t states $(w_t, m_t, \varepsilon_t^m)$ and parameters $(g^w, \beta_m, \rho_{SST}, \beta_{SST}, \rho_\delta, \beta_\delta, \sigma_m^2, \sigma_{SST}^2, \sigma_\delta^2)$ of the model and has no uncertainty over the functional form of the model.

At the beginning of each period t , the household's information set

$$\mathcal{I}_t = \left\{ \hat{\mathbf{x}}_t^{SST}, \hat{\mathbf{P}}_t^{SST}, \hat{\mathbf{x}}_t^\delta, \hat{\mathbf{P}}_t^\delta \right\}$$

encodes a multivariate Normal prior on parameters β_{SST} and \overline{SST}_t governing the evolution of temperatures,

$$\mathcal{N}\left(\hat{\mathbf{x}}_t^{SST}, \hat{\mathbf{P}}_t^{SST}\right) \quad \text{over} \quad \begin{bmatrix} \overline{SST}_t \\ \beta^{SST} \end{bmatrix}$$

and a multivariate Normal prior on parameters β_δ and $\bar{\delta}_t$ governing the evolution of disaster damages,

$$\mathcal{N}\left(\hat{\mathbf{x}}_t^\delta, \hat{\mathbf{P}}_t^\delta\right) \quad \text{over} \quad \begin{bmatrix} \log \bar{\delta}_t \\ \beta^\delta \end{bmatrix}.$$

I assume that these two multivariate priors are initially independent, in which case they remain independent. The learning processes for β_{SST} and β_δ are identical. For brevity, I describe only the process for β_δ . Each period t , the expected value $\bar{\delta}_t$ of disaster damages evolves and disaster damages themselves, δ_t , are realized as described in Section 4.1. Households observe δ_t and a Normally distributed news shock n_t^δ ,

$$\begin{aligned} \log \delta_t &\sim \mathcal{N}(\log \bar{\delta}_t, \sigma_\delta^d) \\ n_t^\delta &\sim \mathcal{N}(\mu_\delta^\delta, \sigma_\delta^n). \end{aligned}$$

Though they do not know the values of β_δ or $\bar{\delta}_t$, they know that $\bar{\delta}_{t+1}$ evolves according to

$$\log \bar{\delta}_{t+1} = \rho_\delta \log \bar{\delta}_t + \beta_\delta w_t m_t$$

This is a linear Gaussian state space model. Assuming rational Bayesian learning, the posterior given emissions is linear in the shock realizations and given by the Kalman filter.

In matrix form, the unobserved state evolves according to:

$$\underbrace{\begin{bmatrix} \log \bar{\delta}_{t+1} \\ \beta_\delta \end{bmatrix}}_{\mathbf{x}_{t+1}} = \underbrace{\begin{bmatrix} \rho_\delta & w_t m_t \\ 0 & 1 \end{bmatrix}}_{\mathbf{F}_t} \underbrace{\begin{bmatrix} \log \bar{\delta}_t \\ \beta_\delta \end{bmatrix}}_{\mathbf{x}_t}.$$

and shock realizations are generated according to:

$$\underbrace{\begin{bmatrix} \log \bar{\delta}_t \\ n_t \end{bmatrix}}_{\mathbf{z}_t} = \underbrace{\begin{bmatrix} 1 & 0 \\ 1 & 0 \end{bmatrix}}_{\mathbf{H}_t} \underbrace{\begin{bmatrix} \log \bar{\delta}_t \\ \beta_\delta \end{bmatrix}}_{\mathbf{x}_t} + \mathbf{v}_t$$

$$\mathbf{v}_t \sim \mathcal{N}(0, \Sigma_v).$$

Given the prior $\mathcal{N}(\hat{\mathbf{x}}_t^\delta, \hat{\mathbf{P}}_t^\delta)$ for \mathbf{x}_t at the beginning of period t ,

$$\mathbf{x}_t | \mathcal{I}_t \sim \mathcal{N}(\hat{\mathbf{x}}_t^\delta, \hat{\mathbf{P}}_t^\delta),$$

the rational prior for \mathbf{x}_{t+1} at the beginning of period $t+1$ is given by the Kalman filter:

$$\hat{\mathbf{x}}_{t+1}^\delta = \mathbf{F}_t(\mathbf{I} - \mathbf{K}_t \mathbf{H}_t) \hat{\mathbf{x}}_t^\delta + \mathbf{F}_t \mathbf{K}_t \mathbf{z}_t$$

$$\hat{\mathbf{P}}_{t+1}^\delta = \mathbf{F}_t(\mathbf{I} - \mathbf{K}_t \mathbf{H}_t) \hat{\mathbf{P}}_t^\delta \mathbf{F}_t'$$

$$\mathbf{K}_t = \hat{\mathbf{P}}_t^\delta \mathbf{H}_t' (\mathbf{H}_t \hat{\mathbf{P}}_t^\delta \mathbf{H}_t' + \Sigma_v)^{-1},$$

where \mathbf{K}_t is the optimal Kalman gain.

$$\log \delta_t | \mathcal{I}_t \sim \mathcal{N}(\hat{\mu}_t, \sigma_d + \hat{o}_{\mu t}).$$

4.3 Calibration of Climate Process

The Intergovernmental Panel on Climate Change (IPCC) define greenhouse gas concentration scenarios which are labelled RCP x , where x is the level of radiative forcing (net energy transfer from space) per m^2 of the Earth's surface. Figure 11 shows median temperature projections for each pathway in the Coupled Model Intercomparison Project 5 (CMIP5) ensemble (Rasmussen & Kopp, 2017).

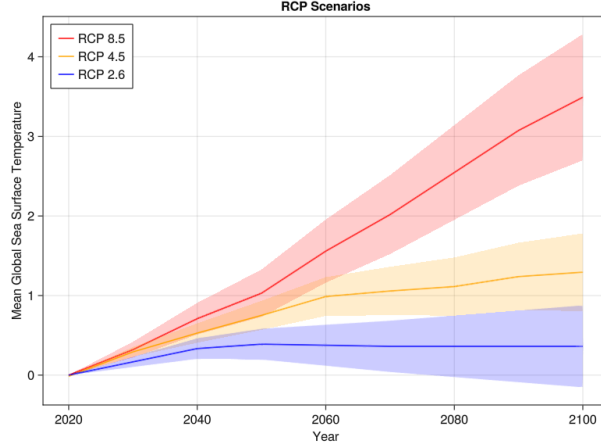


Figure 11

Representative Concentration Pathways (RCPs) from the IPCC Fifth Assessment Report (AR5). The RCPs are labelled by the level of radiative forcing (net energy transfer from space) per m^2 of the Earth's surface.

I calibrate the free variables of the climate process as follows. I set initial global energy generation, w_0 , to global energy generation in 1900. I set the growth rate of global energy generation, g^w , to the growth rate of global energy generation between 1900 and 2020. I set initial emissions intensity, m_0 , to match average global emissions intensity in 2020. I set the parameter controlling the decline in emissions intensity, β_m , to match model-predicted median annual emissions in 2100, $w_{2100}m_{2100}$, conditional on 2020 emissions, to 2100 emissions in the RCP4.5 scenario.

I jointly set the variance of the emissions intensity shock, σ_m^2 ; the contribution of emissions to global temperatures, β_{SST} ; and the natural rate of regression of temperatures to the pre-industrial baseline, ρ_{SST} . I set them to the model-predicted first, second, and third quartiles of global temperatures in 2100, conditional on 2020 emissions, to the RCP2.0, RCP4.5, and RCP6.0 scenarios.

I set the contribution of emissions to disaster damages, β_δ , to match the increase in disaster damages between 2020 and 2050 predicted by the model of Bates et al. (2021), as reported by Wing et al. (2022). I estimate the natural rate of regression of disaster damages to the pre-industrial baseline, ρ_δ , using data on historical homeowners insurance premiums in Appendix B.

4.4 Quantification: Model Uncertainty

I use historical data on homeowners insurance premiums and losses to estimate market-relevant internal variability and model uncertainty. Homeowners insurance contracts are one-year contracts, representing a plausibly static decision on the part of the insurer. Using aggregate accounting data, I back out anticipated annual losses from storm damage, given insurers' beliefs and information sets, in each year.

Table 3: Calibrated Parameters, Auxiliary Climate Process

Parameter	Interpretation	Value	Target or Source	Moment	Value
w_0	Initial global energy generation	107 PWh	Global energy generation, 1900	107 PWh	
g^w	Global energy generation growth rate	0.0155	Growth rate of global energy generation, 1900-2020	0.0155	
m_0	Initial emissions intensity	0.358 t/MWh	Global emissions intensity, 2020	0.273 t/MWh	
β_m	Decline in emissions intensity	0.016	RCP4.5 annual emissions, 2100 (as median)	12.3 Gt	
σ_m^2	Variance of emissions intensity shock	0.40	RCP2.0/4.5/6.0 SST, 2100 (as quartiles)		
β_{SST}	Contribution of emissions to global temperatures	0.00053	" "		
ρ_{SST}	Natural rate of temperature regression	0.93	" "		
β_δ	Contribution of emissions to disaster damages	0.051	Increase in disaster damages 2020-2050 (Bates et al., 2021)	26.4%	
ρ_δ	Natural rate of disaster damage regression	0.98	Homeowners insurance premiums		

All moments are either unitless or in units of decade⁻¹. Each parameter influences all moments; I merely report the most directly influenced moment for each parameter.

In order to calibrate uncertainty, I back out the responsiveness of homeowners insurance providers' anticipated losses (which I back out of premiums) to realized losses. Intuitively, the less certain insurers are in their climate beliefs, the more we would expect them to adjust their premiums in response to realized losses.

I model insurer's beliefs as arising from the Bayesian learning process described in Section 4.2. I then use data on premiums and losses to estimate the parameters of this process. Essentially, I am learning from the observed learning behavior of insurers. I show that the specific procedure I employ, which resembles a nested Kalman filter, can be constructed at a high level of generality.

As the procedure for estimating the Bayesian model is quite lengthy and complex and yields few qualitative insights into the climate welfare impact heterogeneity which is the primary focus of this study, I move it to Appendix B. Table 4 reports the result of the estimation.

Variable	Estimate
σ_δ^n	0.21306
σ_δ^d	0.28874
ρ	0.98
T_0	1965.87

Table 4: Results of state space estimation. Point estimates are by maximum likelihood.

5 Calibration

It remains to set the climate-unrelated parameters of the full model. Because the goal is to explore the implications of the model for the period 2020-2100, I calibrate the model's stationary steady state to be consistent with key features of the U.S. economy in the early 1990s. This is the initial steady state in which climate change unexpectedly begins, as described in Section 2.6.

I choose the early 1990s to achieve a balance between the contribution to the state of housing markets in 2020 of, on one hand, anticipatory adaptation to climate change and, on the other hand, factors which are not accounted for in the model. Calibrating the model to a more recent steady state allows for the initial conditions to be more similar to the current economy, but allows for less pre-2020 adjustment by households in anticipation of climate change.

I primarily calibrate the model using indirect inference. I match moments computed from the 5% Public Use Microdata Sample (PUMS) of the 1990 U.S. Census and the 1992 Survey of Consumer Finances (SCF).

The parameters of the model can be divided into four categories: location-level parameters, the parameters of the income process, the initial wealth distribution, and all other parameters.

Each location is calibrated to data on a single Public Use Microdata Area (PUMA), the smallest spatial unit available in the 1990 PUMS. I directly plug in PUMA-level estimates of housing price computed from the 1990 PUMS, solve for local rents and populations in spatial equilibrium, and calibrate location-specific amenities and labor productivity shifters to match empirical location populations and mean incomes from PUMS. These estimates are independent of local housing supply elasticities. I assign these externally using the spatially-heterogeneous estimates of Saiz (2010).

The labor income process is calibrated by quantifying an annual AR(1) process on labor, welfare, and pension income from the 1989 and 1990 Panel Study of Income Dynamics (PSID), then calibrating a decadal AR(1) income process to the moments of the annual process.

I parameterize the initial wealth distribution to be log-uniform within each income quartile, yielding the five quartile boundaries (including the minimum and maximum wealth) as the free parameters. I set the minimum to \$1 and the remaining four by indirect inference, matching the mean and inner three quartiles of overall net worth in the 1992 SCF.

To quantify non-spatially-varying parameters, I use a combination of indirect inference, external estimates, and standard values. Seven parameters are calibrated by indirect inference. Abstractly, I define seven moments and find values for these seven parameters such that the simulated moments equal the empirical moments.

Concretely, I assign to each parameter a corresponding moment which the model suggests should be particularly informative about that parameter. I do this for all parameters of the model calibrated by indirect

inference: the parameters of the wealth distribution, the non-spatially-varying parameters, as well as the location-specific amenities and productivity shifters.³⁸ I then simply guess all parameters at once, compute simulated moments, then update each parameter guess using only the difference between the simulated and empirical values of the moment associated with that parameter. I repeat until all simulated moments converge to their empirical counterparts within a tolerance of 10^{-6} .

That is, I essentially find the parameters by gradient descent, where I set the derivative of a moment with respect to a parameter to zero unless that parameter is the “relevant” parameter for that moment. The fact that this process converges demonstrates that the chosen moments are indeed informative about their corresponding parameters, at least within the context of the model.

For brevity, in the remainder of this section it is often stated that a parameter X is calibrated to match a moment Y . This is not intended to imply that parameter X affects *only* moment Y , but that the above procedure is applied in full and that parameter X is associated with moment Y therein. All parameters calibrated by indirect inference are calibrated jointly.

5.1 Spatial Parameters

I choose the 1990 Public Use Microdata Area (PUMA) as my spatial unit. These are the smallest spatial unit reported in the 1990 PUMS. I use the $N = 1713$ PUMAs which cover the contiguous U.S. completely. A PUMA is an area with 1990 population between 100,000 and 200,000, generally following the boundaries of Metropolitan Statistical Areas (MSAs) where applicable.

For each location ℓ , I set the housing price level³⁹ q_ℓ to the value of a typical owner-occupied two-bedroom home in the 1990 PUMS.⁴⁰ By indirect inference, I calibrate the amenity value of a location (which enters the model as an effective multiplier on consumption spending) $\bar{\alpha}_\ell$ to match the population of location ℓ in the 1990 PUMS. By indirect inference, I calibrate the local labor productivity shifter \bar{A}_ℓ to match the mean annual labor earnings among the working-age population in location ℓ in the 1990 PUMS.

In equilibrium, these imply a value in each location for the quantity of housing H_ℓ and the rent level⁴¹ ρ_ℓ , which are untargeted. Note that the house price level q_ℓ is also an equilibrium quantity and not a parameter. In theory, q_ℓ is a moment and Π_ℓ is calibrated to match that moment, solving,

$$q_\ell = \Pi_\ell H_\ell^{\beta_\ell}.$$

In practice, I assign q_ℓ before the indirect inference step and defer the calibration of Π_ℓ until after the indirect

³⁸As an optimization, I also treat steady-state location-level rent levels $\rho_{\ell t}$ as parameters, with the market clearing condition as the “associated moment.” This removes the need to solve for equilibrium rents for every parameter guess.

³⁹As I am calibrating a steady-state version of the model, I omit time t subscripts.

⁴⁰I regress all owner-occupied home values on a PUMA fixed effect and a “number of bedrooms” fixed effect, with “two bedrooms” as the reference group and no intercept, and use the PUMA fixed effect as my house price level estimate.

⁴¹In units which correspond to the typical owner-occupied two-bedroom home.

inference step, at which point I externally assign the estimates of Saiz (2010) to set β_ℓ for each location, then set,

$$\Pi_\ell = q_\ell / H_\ell^{\beta_\ell}.$$

The estimates of Saiz (2010) are at the level of MSAs, which generally nest PUMAs. Details of the imputation procedure are in Appendix F.

5.2 Initial Wealth Endowments

By indirect inference, I set the distribution of initial wealth endowment (at age 20) to match the mean and quartiles of net worth in the SCF. A household is equally likely to be born in each quartile. Conditional on quartile, initial wealth endowment is log-uniform. The minimum initial wealth endowment is \$1. I set the maximum initial wealth endowment to match the empirical mean of net worth.

5.3 Non-Spatial Parameters

The non-spatial parameters of the model determine preferences, the lifecycle income process, initial wealth endowments, housing investment and maintenance costs, and migration costs. In addition to Census data, I also use data from the 1992 Survey of Consumer Finances (SCF).

5.3.1 Lifecycle

One model period represents ten years. Households are born at age 20 and die at age 80.

5.3.2 Preferences

By indirect inference: I set the weight of housing in consumption, γ , to match the median rent-to-income ratio among renters in the 1990 Census; I set the strength of the bequest motive, Q , to match the ratio between overall mean wealth and mean wealth of households with a head between 70 and 80; and I set the elasticity of substitution between housing and goods consumption, $1/\sigma$, to match the reduced form relationship β_{RTI} , across locations, between the housing asset price level q_ℓ and median rent-to-income ratio:⁴²

$$RTI_\ell = \alpha_{RTI} + \beta_{RTI} \log q_\ell + \varepsilon_\ell.$$

where RTI_ℓ is the median rent-to-income ratio in location ℓ .

Externally, I set the elasticity of intertemporal substitution to $1/\eta = 2.0$ as in Kaplan et al. (2020).

⁴²Ideally, I would regress on the housing rent level, but I do not observe this in the data.

5.3.3 Housing

By indirect inference, I calibrate the interest rate on mortgage borrowing, r_m , to match the ratio between the mean wealth of homeowners to overall mean wealth. I calibrate the baseline cost of maintaining a rental property to match the homeownership rate. I calibrate the excess maintenance and administrative cost on rental properties, $\chi^{\text{let}} - \chi^{\text{live}}$, to match the homeownership rate.

Externally, I set the transaction cost for housing assets, ϕ , to 7% as in Kaplan et al. (2020). I set the maximum loan-to-value ratio of a mortgage, κ , to 80%. I set χ^{live} , the baseline cost of maintaining an owner-occupied home, to \$1,000 annually.

5.3.4 Migration

I parameterize the utility migration cost,⁴³ $F^u(\ell', \ell)$, as a multiple of the distance $d(\ell', \ell)$ between the source location ℓ and destination location ℓ' :

$$F^u(\ell', \ell) = \tau d(\ell', \ell).$$

I calibrate the “monetary” fixed cost of moving F^m to match the share of households who move across PUMAs each decade and the per-distance utility cost of moving τ to match the share of households who move across states each decade.

While it is not necessarily true in reality that fixed costs of moving are monetary and distance-dependent costs of moving are preferences, this setup is necessitated by a feature of the numerical solution method that does not allow for variable monetary moving costs. However, this is not a model whose goal is to measure monetary versus utility moving costs and I argue that this assumption is generally not too violent. Monetary costs of moving do exist and it is believable that households prefer to stay close to their current location even if they are moving.

5.4 Calibration Result

Table 5 lists the units that all quantities are expressed in. The model is just-identified and all targeted moments are matched exactly. Table 6 lists the non-spatially-varying parameters, their calibrated values, and their associated moments. To visualize spatially-varying moments, Figure 12 describes the estimated local amenity values across the U.S. Figure 13 describes the estimated local productivity shifters across the U.S. Figure 14 describes estimated local amenity values for six cities, and Figure 15 describes local productivity shifters around New York City at various scales.

⁴³No aspect of the model solution depends on any particular functional form for F^u , however. In a future version, I plan to flexibly calibrate migration costs for each pair of locations to match data on bilateral migration flows.

Table 5: Units

Quantity	Unit
Location	1990 Public Use Microdata Area (PUMA)
Time	10 years
Housing	Typical two-bedroom owner-occupied home
Numeraire Good	Thousand 2020 USD (\$1,000)
Distance	Kilometers (km)
Temperature	Degrees Celsius (°C)

Units used throughout the quantification, unless otherwise specified. “Monetary” values such as income and monetary moving costs are paid in the form of the numeraire good, which are expressed in units of one thousand 2020 USD.

5.5 Model Fit: Price-to-Rent Ratios

Local rent levels and housing stocks are not targeted in the calibration, but arise in the model equilibrium. Figure 16 shows that rent levels vary with housing prices, as both are driven by local amenity values, productivities, and housing supply elasticities. Furthermore, Figure 17 reveals that the model reproduces a key feature of the data: the price-to-rent ratio is higher in locations with higher housing prices. This is primarily driven by the fact that a greater concentration of wealth in more expensive locations creates greater demand for rental real estate assets, decreasing equilibrium rents. Second, a small proportion of this effect is due to a particular modeling choice: the wedge between the maintenance cost of rental housing and owner-occupied housing is a fixed cost per unit of housing, so it is relatively lower in locations with higher housing prices. However, in the calibrated model maintenance costs account for only between 5% and 25% of rent and cannot account for the large variation in price-to-rent ratios.

Table 6: Non-Spatially-Varying Parameters

Parameter	Interpretation	Value	Target or Source	Moment Value
Lifecycle:				
a_{\max}	Length of adult life	6		
Preferences:				
γ	Taste for housing	0.2	Median (renter) rent-to-income ratio	0.23
$1/\sigma$	Elasticity of Substitution (goods vs. housing)	0.87	Rent-to-income sens. to housing price	0.011
$1/\eta$	Elasticity of intertemporal substitution	0.5		
Q	Bequest motive	4.3	Mean wealth ratio oldest-to-overall	1.62
Housing:				
r_m	Mortgage interest rate	0.80	Mean wealth ratio homeowners-to-overall	1.52
ϕ	Transaction cost	0.07	Kaplan et al. (2020)	
χ^{let}	Rental baseline maintenance cost	21.3	Homeownership rate	0.68
κ	Maximum loan-to-value ratio	0.8		
χ^{live}	Owner-occupied baseline maintenance cost	10.0		
Migration:				
F^m	Monetary fixed cost of migration	13.3	Share of households moving across PUMAs	0.40
τ	Utility cost of migration per km	0.0011	Share of households moving across states	0.22

All moments are either unitless or in units of decade⁻¹. Each parameter influences all moments; I merely report the most directly influenced moment for each parameter. Goods consumption is scaled in utility so that one unit of goods consumption costs \$50,000.

Calibrated Amenities

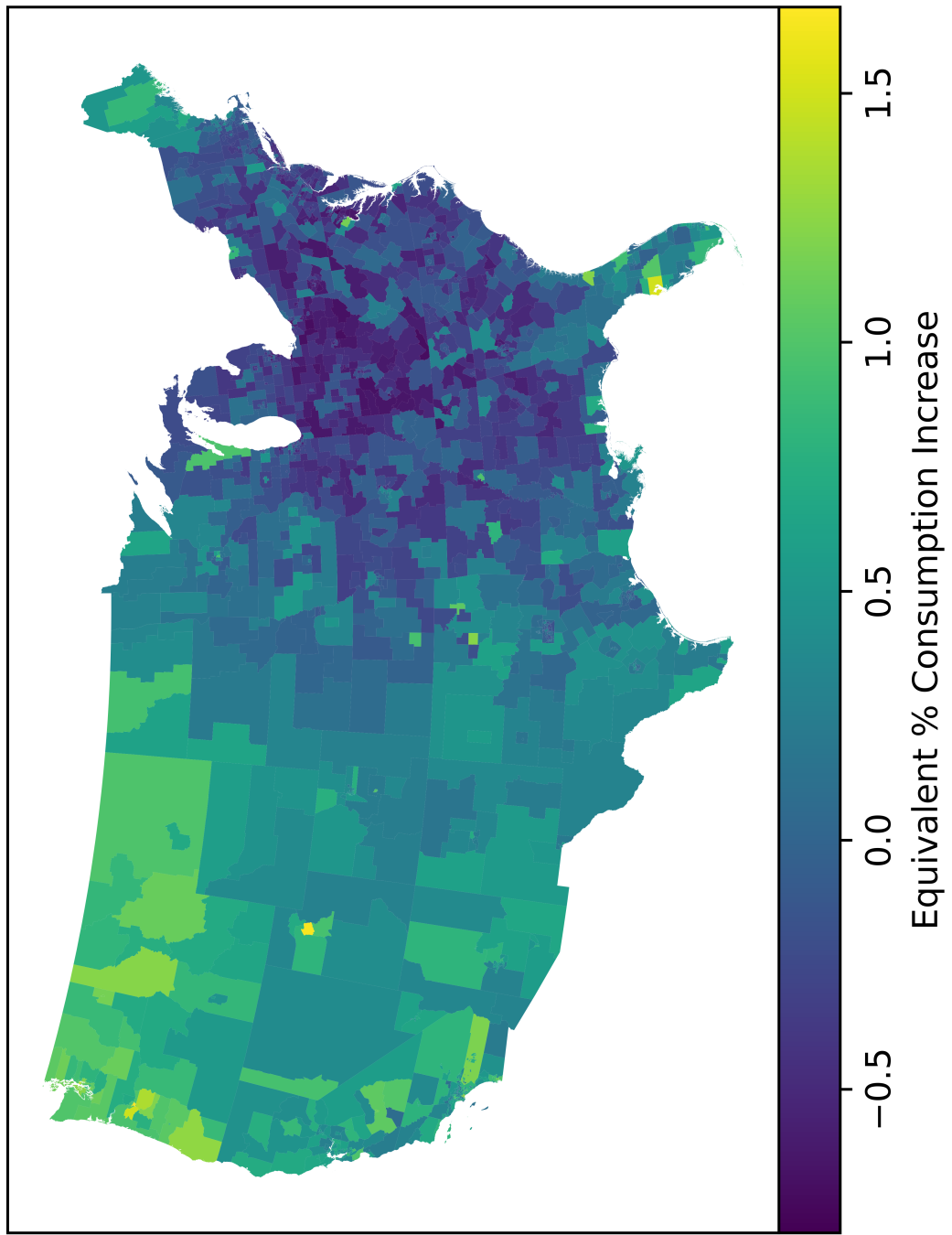


Figure 12: Estimated Amenity Values

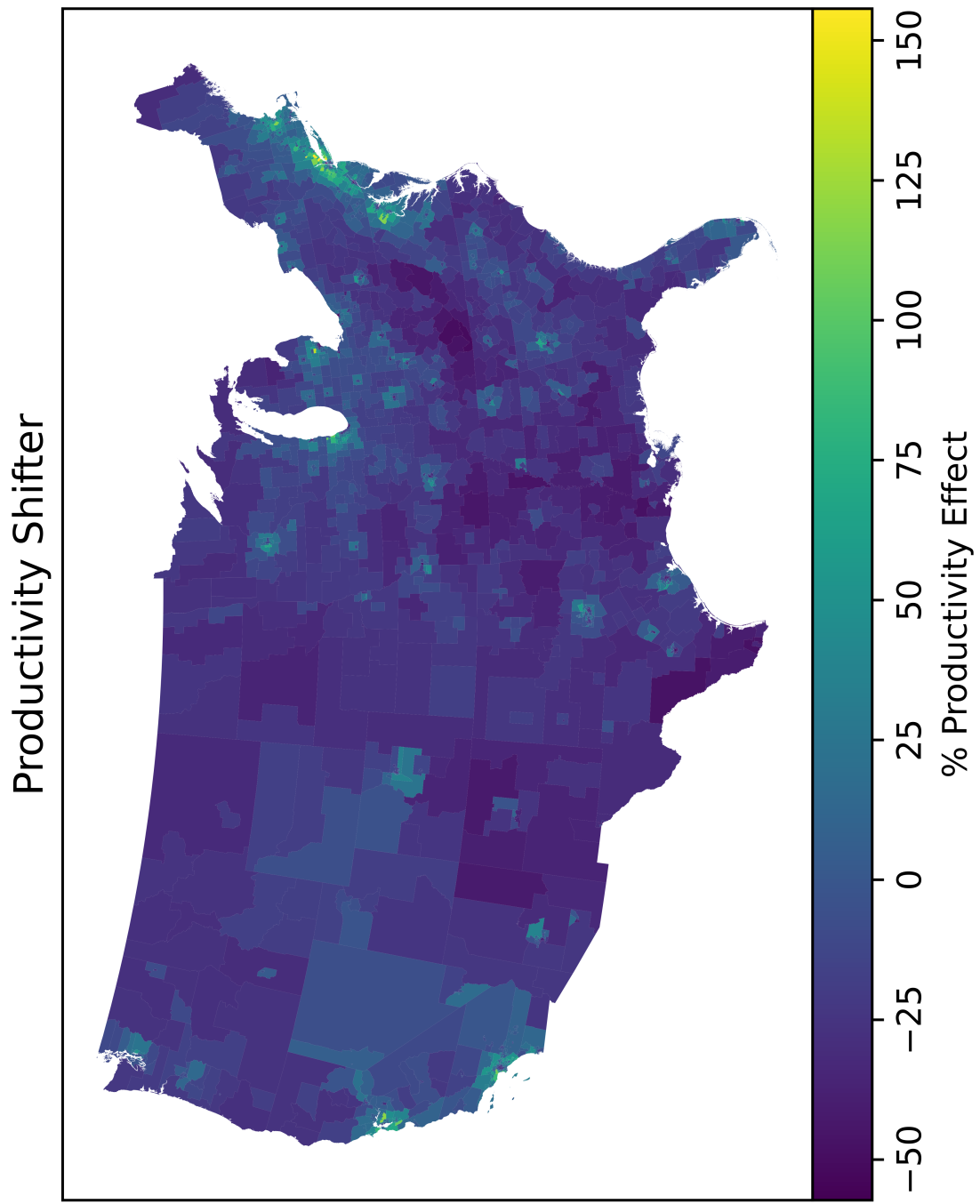


Figure 13: Estimated Productivity Shifters

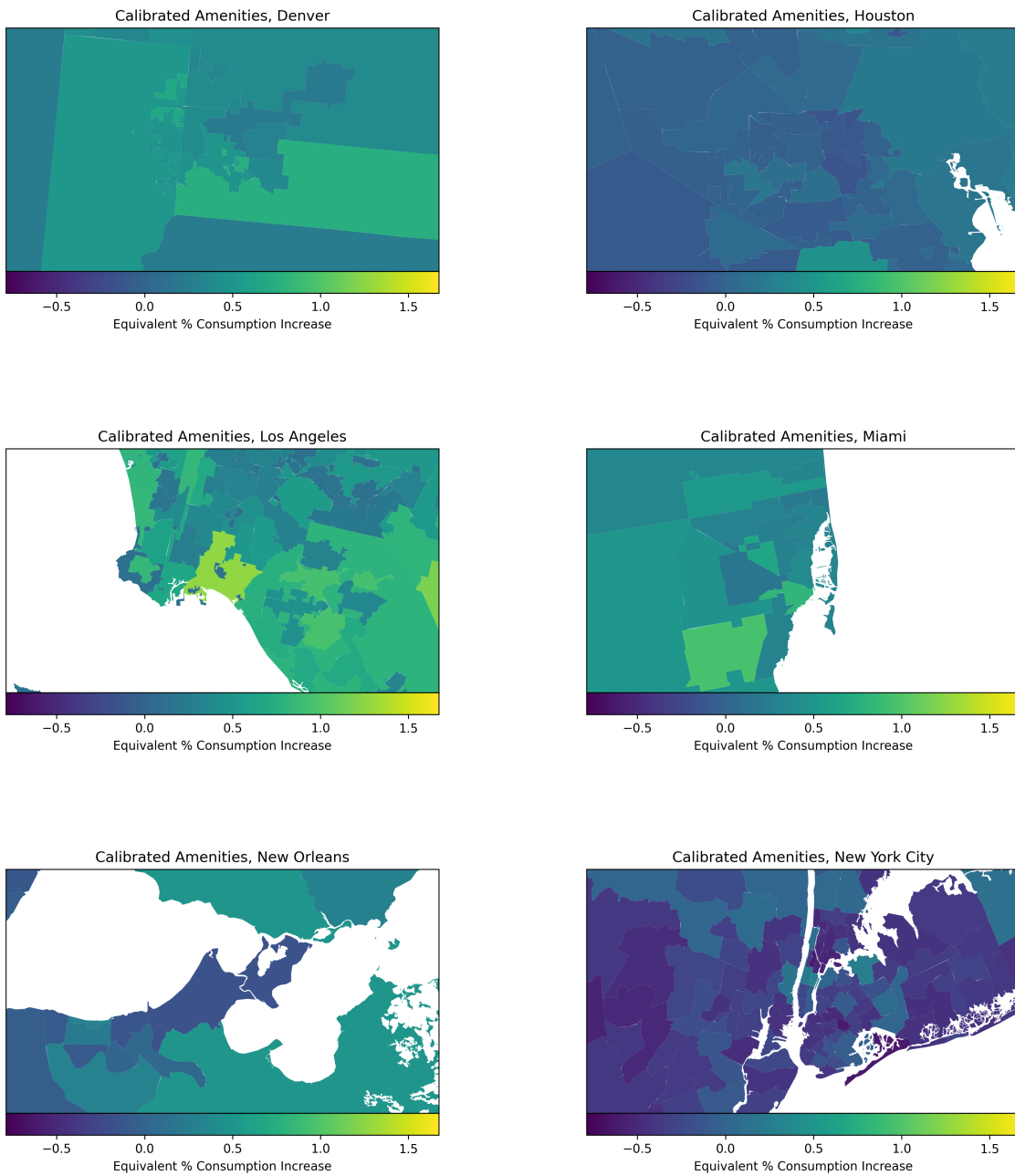


Figure 14: Calibrated Amenities by City

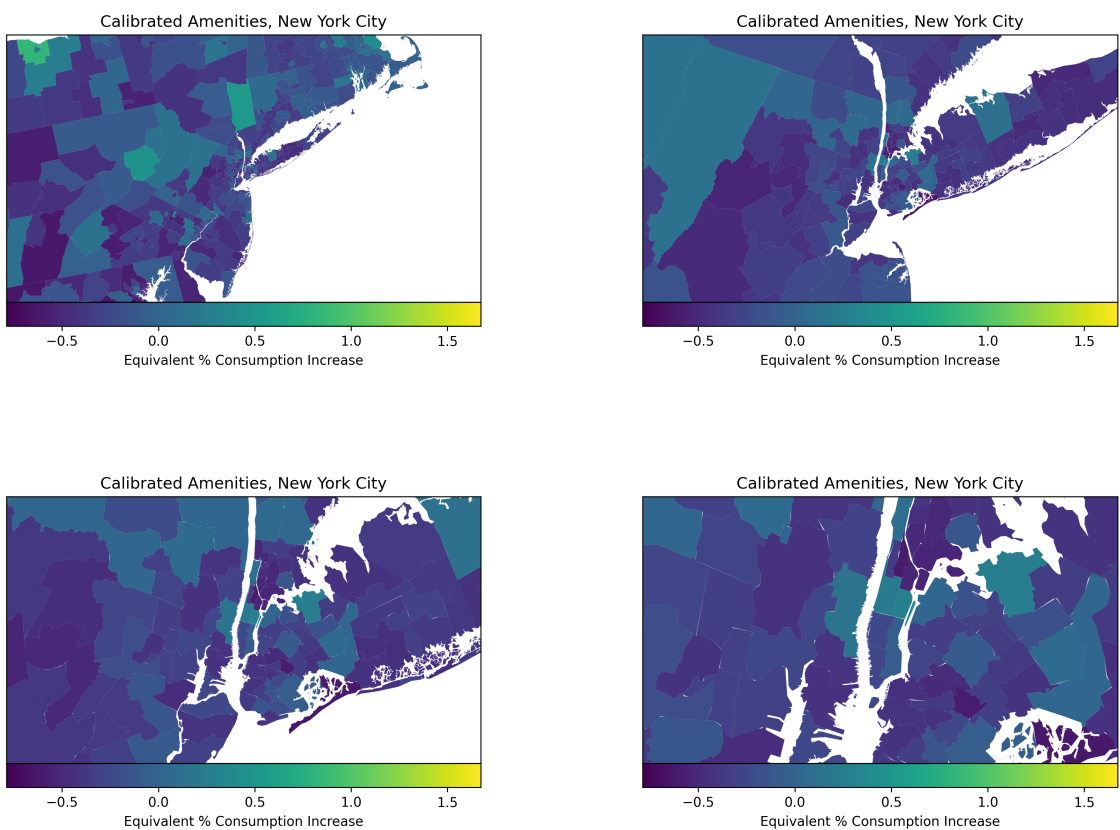


Figure 15: Calibrated Amenities Around New York City

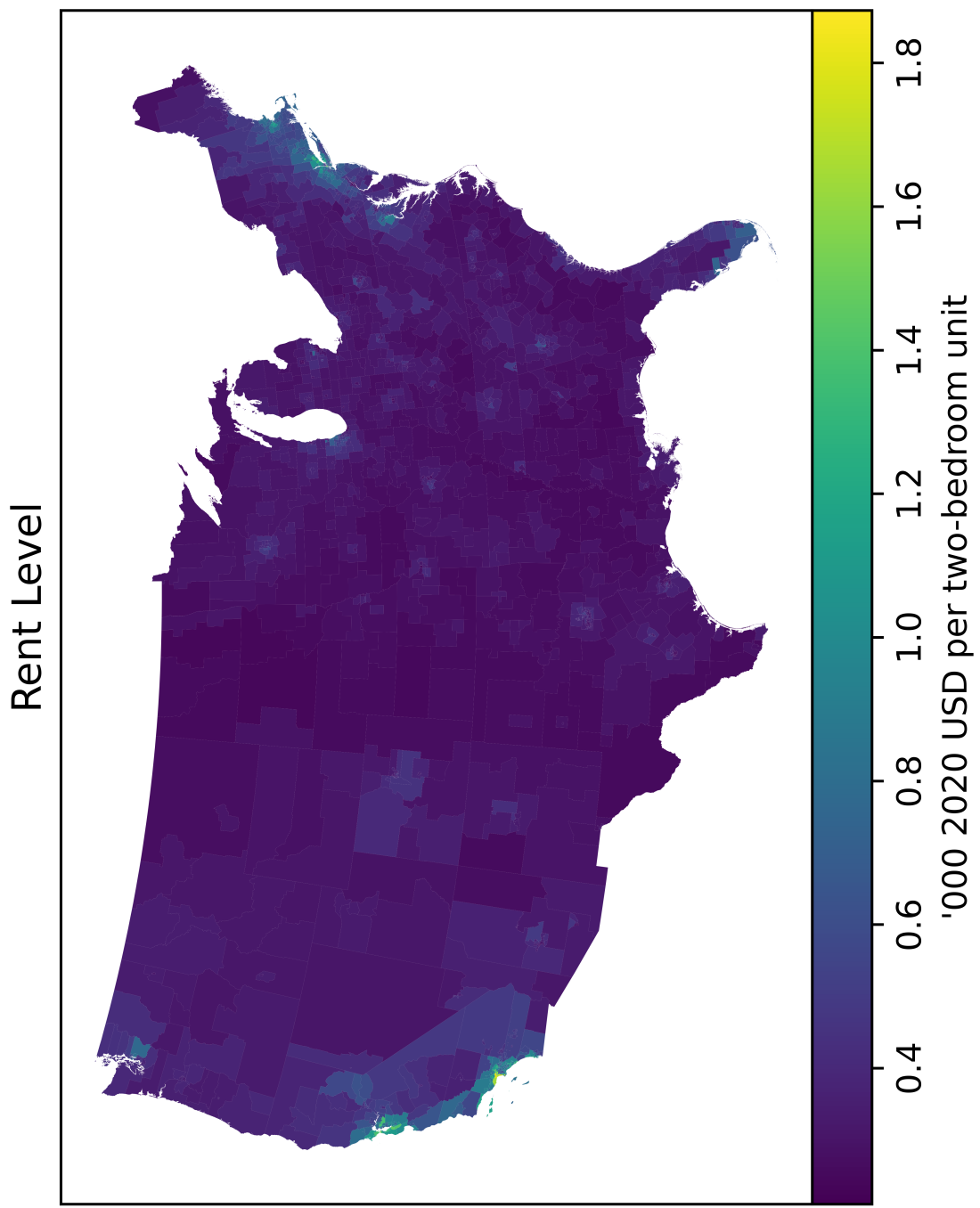


Figure 16: Equilibrium Rent Level

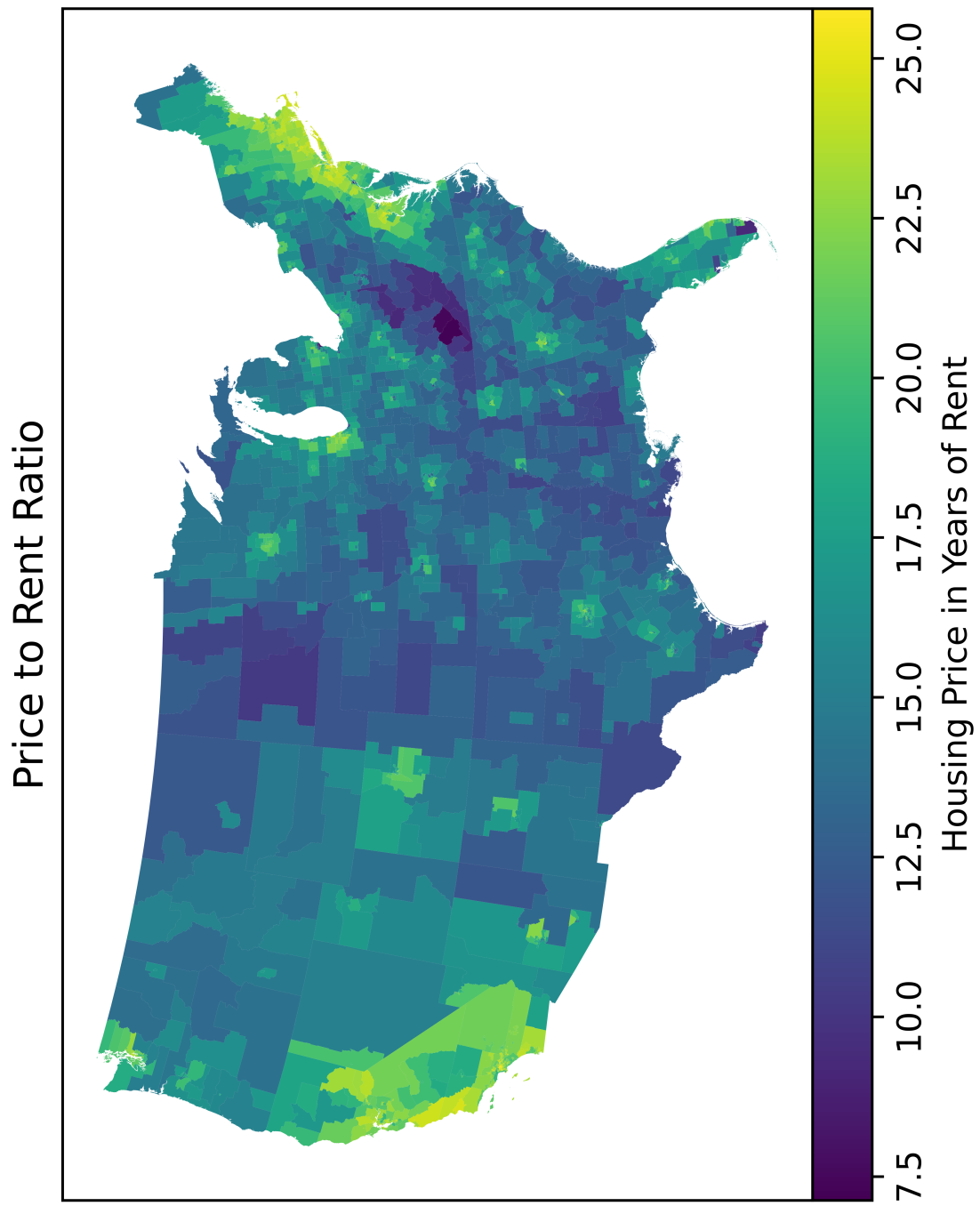


Figure 17: Equilibrium Price to Rent Ratio

6 Inequality in Welfare Losses from Climate Change

In this section, I examine inequality in the welfare losses from climate change in the U.S.—overall, within locations, and between locations. The first key contribution of this model is to incorporate housing wealth, which is determined by forward-looking equilibrium housing prices. The second key contribution is to incorporate climate uncertainty and its equilibrium impact on house prices. This requires finding the global solution of the dynamic spatial equilibrium model under aggregate uncertainty.

When household wealth depends on forward-looking housing prices, neither migration nor anticipation can greatly ameliorate the spatially-unequal impacts of climate change. Although adding migration to a version of the model without migration or homeownership does mitigate spatial inequality in climate damages, this is undone by adding homeownership. To quantify the impact of housing wealth, I compare the full model to a version of the model in which households rent housing from an absentee landlord.

Forward-looking housing prices cause news about future climate change to have immediate unequal wealth impacts at the time that the news is revealed, though these wealth impacts do reduce overall wealth inequality. However, uncertainty about future climate change causes ongoing regressive welfare impacts through increasing housing rent. Landlords effectively charge renters for the risk that landlords adopt by holding risky housing assets. Wealthier landlords profit from the reduced willingness of less wealthy landlords to invest in real estate. To quantify the effects of uncertainty, I compare the global solution to a version of the model with perfect foresight.

Finally, there is one more key way in which expectations shape the distributional consequences of climate change. With homeownership, if households systematically underestimate the severity of climate change, then this causes a progressive distributional impact to be realized during the climate transition when the news is revealed that climate change will be more severe than anticipated. This negative climate news shock causes a reduction in the value of housing assets, which are concentrated in the portfolios of wealthier households.

6.1 Inequality in Welfare Losses from Climate Change

In this section, I consider an extreme form of anticipation: a sudden switch from widespread denial to widespread acceptance of climate change. The economy begins in steady state when the stochastic climate transition described in 2.4.2 unexpectedly begins. All households immediately internalize the parameters of the climate process. In a future version, I plan to explore the implications of a more gradual transition from denial to acceptance. Nevertheless, the sudden switch should capture the full magnitude of the price changes resulting from the climate news shock, which in reality would likely unfold more slowly.

With anticipation, welfare losses from climate change manifest in two broad ways. First, when news of

climate change is revealed, households are immediately affected by the instantaneous adjustment of housing prices. Second, young households born during the climate transition are, on average, worse off than if climate change had not occurred. I consider each in turn.

6.1.1 Immediate Welfare Impacts of News Shock

Figure 18 describes welfare losses from the unexpected start of the climate transition, relative to the continuation of the steady state. For each household, I compare the value function at the beginning of the first period of the climate transition with the steady state value function.

This measure combines two effects, however. First, the effect of future climate damages; second, the wealth effect of the climate news shock, operating through housing prices. To isolate the latter, I consider, for each individual household,⁴⁴ the welfare impact of adjusting that household's liquid savings in order to exactly undo the effect of the news shock on their net worth through housing assets. That is, for each household I compute the welfare impact of a (possibly negative) news shock equal to the negated change in the value of their housing asset portfolio. Figure 19 plots the distribution of wealth impacts as a percentage of household portfolio value. Figure 20 plots the distribution of these welfare impacts.

Table 7 decomposes the variance in the immediate welfare impacts plotted in Figure 18 into within-location and between-location components. Approximately 65% of the variance is within-location.

Figure 21 maps spatial inequality in welfare losses from the unexpected start of a climate transition. Figure 22 maps the immediate house price changes resulting from the news shock. Over all areas where prices increase, the value of the housing stock increases by \$996bn. Over all areas where prices decrease, the value of the housing stock decreases by \$1.61tn. Overall, \$618bn in housing value is lost, and \$996bn in housing value is effectively transferred from negatively-affected areas to mildly- and positively-affected areas.

⁴⁴That is, I do not consider a widespread policy of compensation for housing wealth losses.

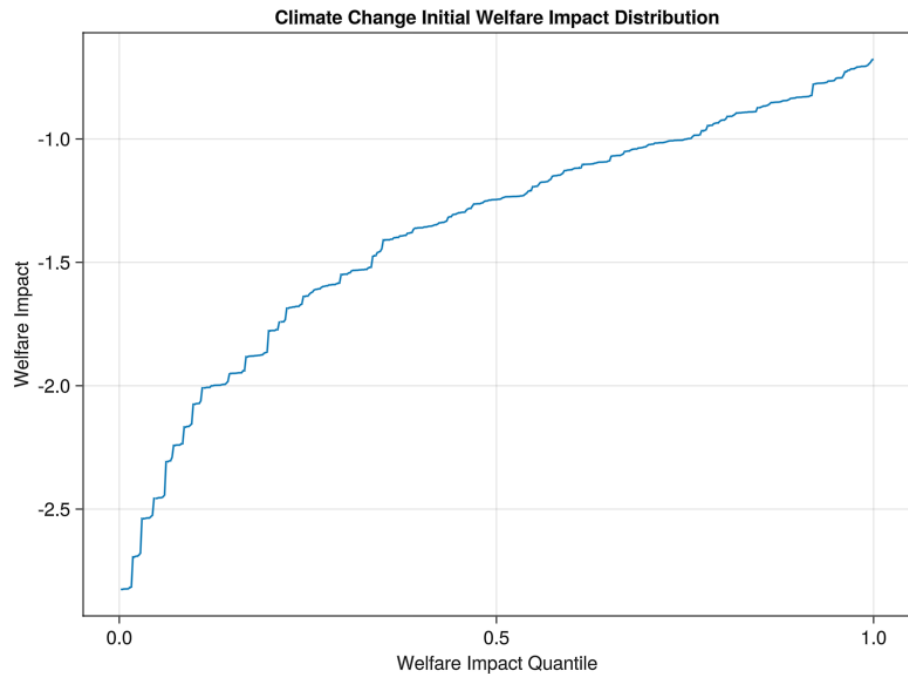


Figure 18

Initial welfare losses from the unexpected start of the climate transition, relative to steady state. Overall, welfare losses are equivalent to a \$2.8tn wealth transfer from more-harmed to less-harmed households.

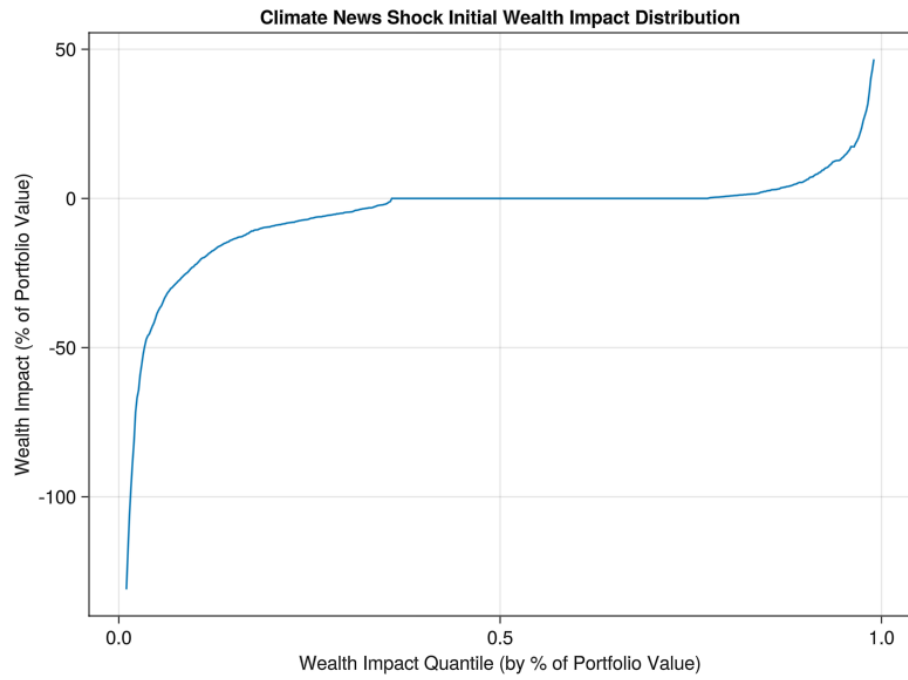


Figure 19

Initial wealth impacts due to house price adjustment from the unexpected start of the climate transition, as a percentage of household portfolio value.

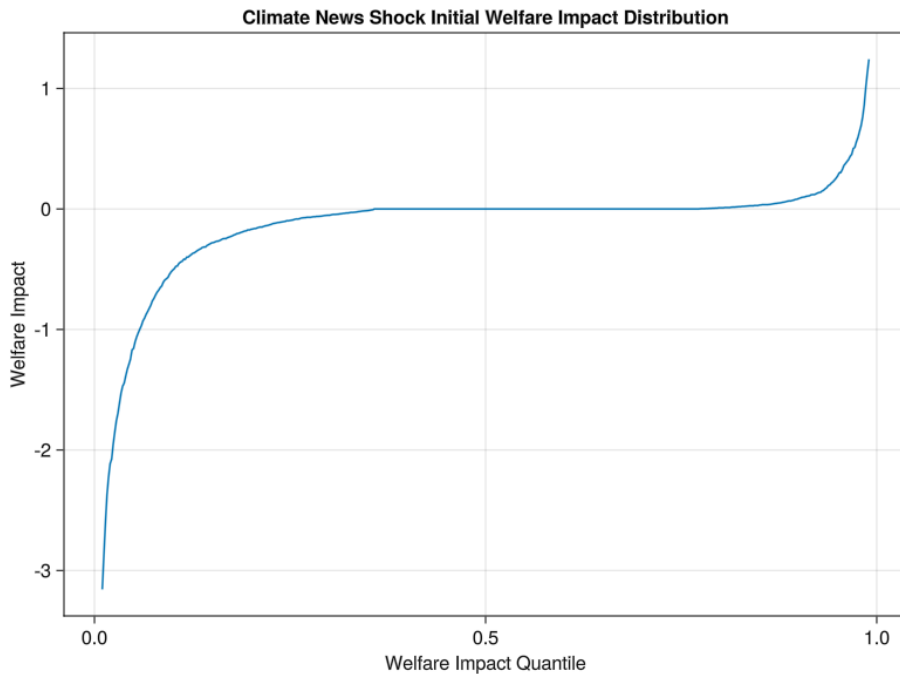


Figure 20

Initial welfare impacts due to house price adjustment from the unexpected start of the climate transition, relative to having additionally received or paid a wealth transfer exactly offsetting the wealth shock from housing assets.

Table 7: Initial Welfare Impact: Variance Decomposition

Variance Component	Value
Overall	0.018
Within-Location	0.012
Between-Location	0.006

Decomposition of variance in welfare effects of house price adjustments following the unexpected start of climate change.

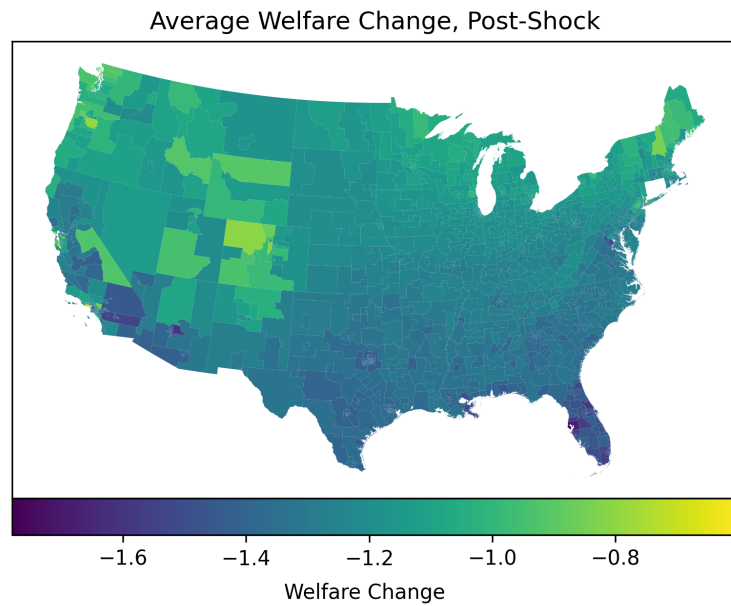


Figure 21: Average welfare reduction resulting from the unexpected start of the climate transition.

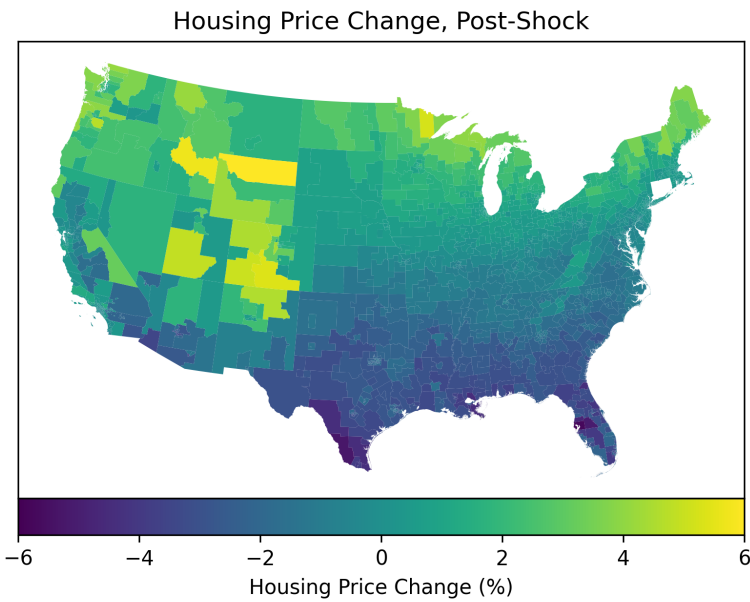


Figure 22: Immediate housing price changes resulting from a news shock, in an initial steady state, that an unexpected climate transition is beginning.

6.1.2 Welfare Impacts Along the Climate Transition

Figure 23 describes welfare losses for households born sixty years after the beginning of the climate transition, relative to the continuation of the steady state. For each household, I compare the value function at the first period of their life with the initial value function of a household born into the stationary steady state.

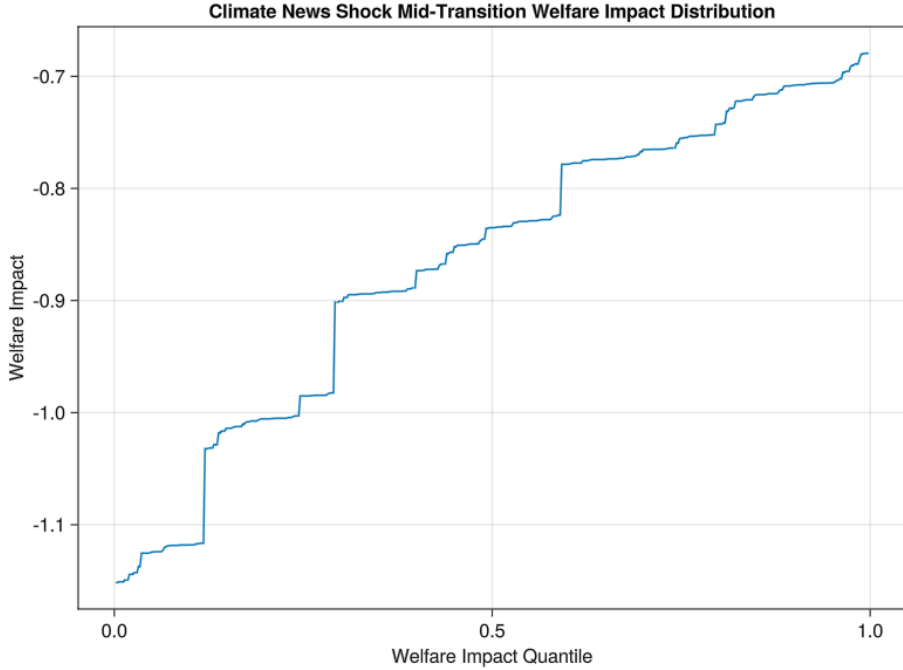


Figure 23

Welfare losses 60 years after the beginning of the climate transition. Welfare of a 20-year-old household born during the climate transition is compared with welfare of a 20-year-old household born into the steady state.

6.2 Anticipation, Forward-Looking Prices, and Uncertainty

In the calibrated model, whether climate change exacerbates or alleviates wealth inequality hinges on whether households over- or under-estimate the severity of climate change and on how uncertain they are in their assessment. That is, the sign of the distributional impact depends on both the mean and the variance of climate expectations. First, the mean: the more that households systematically underestimate the severity of climate change, the more climate change reduces wealth inequality through reducing the value of housing assets (to which wealthier households are more highly exposed). Second, the variance: the more that households are uncertain about the severity of climate change, the more climate change exacerbates wealth inequality through raising risk premia on housing assets. Higher risk premia primarily take the form of higher rent-to-price ratios on housing assets, benefiting the more risk tolerant wealthier households but harming

less wealthy households who are more risk-averse and more likely to be renters.

Note that these results depend crucially on having the global solution of the model. If we were studying a deterministic transition, there would be no uncertainty, no risk premium, and no regressive distributional impact of the risk premium.

6.3 Distributional Consequences of Under and Over-estimating Climate Change

If households underestimate the severity of future climate change, then the news that climate change will be more severe than expected will eventually arrive as a negative climate news surprise. This reduces the average value of housing assets, which are concentrated in the portfolios of wealthier households, reducing overall wealth inequality. However, because some locations experience an increase in housing values, a subset of wealthy households benefit substantially from a negative climate news surprise.

Figure 24a describes an illustrative scenario. I consider three paths from the distribution of climate paths defined by the stochastic process in Section 2.4.2. The first is the median or “no surprise” path in which the realized value of the climate shock drawn each period is equal to 0. This path approximately corresponds to the RCP4.5 scenario.

$$\varepsilon_t^{m,\text{median}} = 0 \quad \forall t.$$

The second is the “negative surprise in 2050” path, in which the realized value of the climate shock drawn each period is zero, except for the shock drawn in 2050, ε_{2050}^m , which is equal to the 95th percentile of the shock distribution (implying higher future temperatures). The third path is the “positive surprise in 2050” path, in which all shocks are zero, except that ε_{2050}^m is equal to the 5th percentile of the shock distribution (implying lower future temperatures).

The welfare of wealthier households is more sensitive to climate surprises than the welfare of less wealthy households. To understand why, I shut down one channel at a time: first, uncertainty; second, exposure of house prices to climate surprises. After shutting down exposure of house prices to climate surprises, the correlation between wealth and climate sensitivity flips: climate sensitivity is then decreasing in wealth.

To shut down uncertainty, I consider a model in which households believe that they have perfect foresight about the climate process and that the transition will effectively be deterministic along the median path. The positive or negative surprise in 2050, if it occurs, is fully unexpected. Following the surprise, households believe that the new path is deterministic. I start this model from the same initial 1990 steady state as the stochastic model, but instead of shocking this model into the full stochastic climate process, I shock it into the median path of the climate process with perfect foresight.

Figure 24b plots, in solid lines, the welfare impact of the climate surprise illustrated in Figure 24a, as a function of wealth, shutting down uncertainty. That is, until 2050, I effectively study a deterministic

transition. Until 2050, households believe that they deterministically on the median path.

For each wealth group, I plot the value at the beginning of 2050 under the positive (blue) and negative (red) surprises, relative to the no-surprise scenario. Wealthier households benefit more from the positive surprise and are more harmed by the negative surprise. The relationship between wealth and climate sensitivity is positive.

To quantify the contribution of housing wealth to this positive wealth-to-climate-sensitivity relationship, we can consider the case in which housing prices are unaffected by the surprise. That is, we ignore market clearing conditions, and simply impose exogenously that house prices along the new path are equal to what equilibrium house prices would have been along the old path. The climate surprise still affects local labor productivity, amenities, energy costs, and disaster risk. These no-price-change shock scenarios can be understood as the combination of a climate shock with a government policy maintaining house prices at the previously anticipated levels through constructing and selling homes below cost (if market prices are too high) or purchasing and demolishing homes (if market prices are too low).

The resulting welfare effects, along the wealth distribution, are plotted in Figure 24a in dashed lines. Shutting down house price exposure to the climate surprise, the wealth-to-climate-sensitivity relationship becomes negative, illustrating that the higher climate sensitivity of wealthier households is due to their exposure to housing assets.

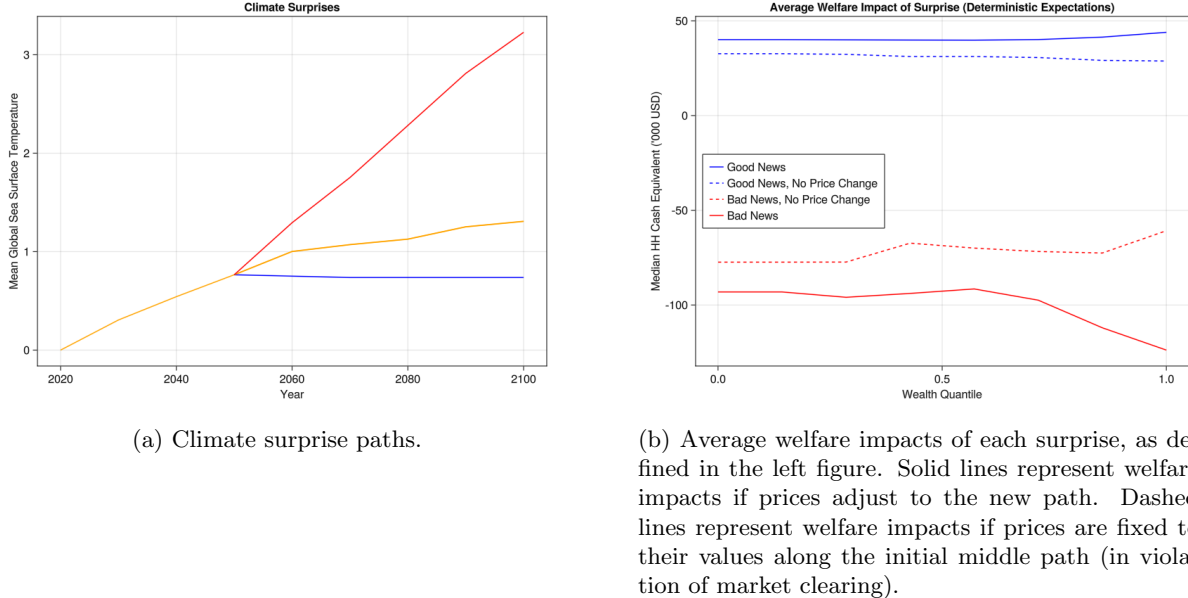


Figure 24

6.4 Distributional Consequences of Climate Uncertainty

We can understand the effect of climate uncertainty on wealth inequality by comparing the global solution of the model with aggregate climate uncertainty (the “Stochastic Model”) with a model of perfect foresight in which the transition is effectively deterministic (the “Deterministic Model”).⁴⁵ In particular, consider the median path illustrated in Figure 24a. This arises as one possible realization of the full stochastic model. Consider now a deterministic model⁴⁶ in which households expect this median path to occur with certainty.

Each model begins in a stationary steady state representing the year 1990, then is hit by the news shock that a (stochastic or deterministic) climate transition is beginning. Figure 25 illustrates how average welfare varies by wealth percentile in the stochastic and deterministic models 30 years after the beginning of the climate transition.

The difference between the two models is climate uncertainty. If we shut down uncertainty (the “Deterministic Model”), then the welfare of households in the lower half of the wealth distribution is lower than in the model with uncertainty (the “Stochastic Model”). This regressive distributional consequence of climate uncertainty is equivalent to a \$94bn wealth transfer from the bottom half of the wealth distribution to the top.⁴⁷

⁴⁵The distinction between these two models is one of household expectations, not that nature is somehow “more stochastic” in the global solution.

⁴⁶The same model generating the solid lines in Figure 24b.

⁴⁷I choose to focus on the relationship between welfare and wealth quantile as my measure of wealth inequality. The alternative would be to construct a price index for each simulated period, but this comes with the challenge that relative housing and goods prices vary across time as well as space and affect renters and homeowners differently.

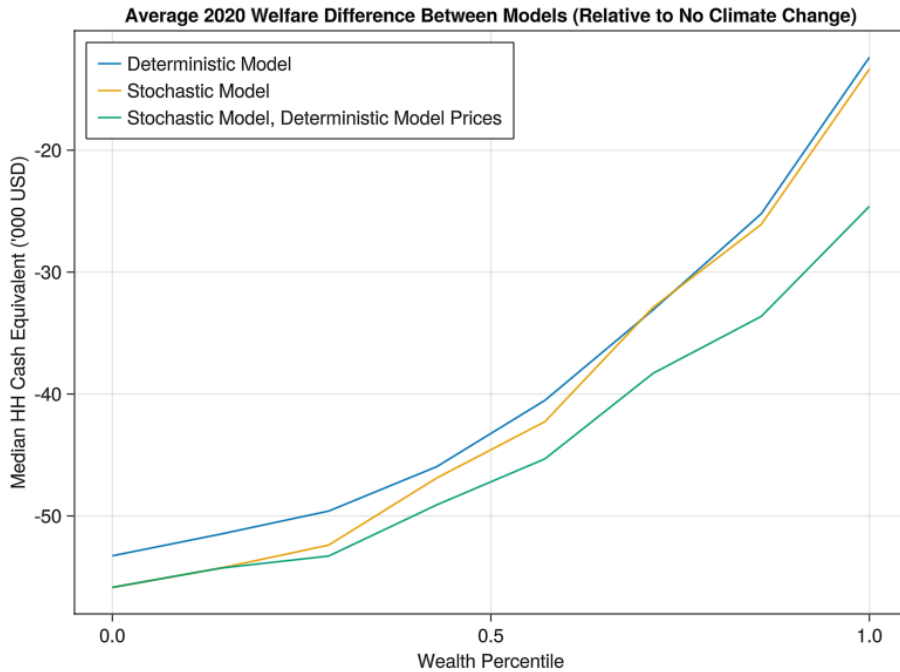


Figure 25: Welfare, relative to the no-climate-change stationary steady state, along the wealth distribution, in 2020, given the observed 1990-2020 climate realizations. The full stochastic model is shown, as well as a “deterministic model” under which the climate evolves according to the median path of the climate process with certainty, and a “stochastic model with deterministic prices” under which the climate evolves according to the full climate process, but prices are deterministically set to their path under the deterministic model (in violation of market clearing).

To understand what is driving this regressive distributional effect of climate uncertainty, I shut down the exposure of house prices to climate uncertainty. In order to do this, I define a model in which households still face uncertainty over climate impacts on productivity, amenities, energy costs, and disaster risk, but house prices are exogenously constrained, no matter the realization of climate shocks, to equal the value they would have taken in the deterministic model.⁴⁸ Figure 25 displays wealth inequality in this “Stochastic Model with Deterministic Model Prices,” compared to the Stochastic Model and the Deterministic Model. Wealthier households are worse off than they were in the stochastic model, but poorer households are unaffected on average, indicating that the uncertainty in housing prices in the Stochastic Model actually benefits richer households. This is due to an endogenous risk premium on housing assets that arises under aggregate climate uncertainty.

Figure 26 displays the paths of average house prices, across all locations, under the deterministic model and under the stochastic model. In the deterministic model, housing prices are an average of 1.16% higher in 2020. Note that the difference narrows over time, as uncertainty resolves. This also hints at the potential role

⁴⁸As before, market clearing conditions will not hold in this scenario.

of overconfidence in shaping economic climate outcomes. When markets are overconfident in their climate projections, risk premia will be smaller. Prices will be closer to the deterministic case, and the impacts of surprises will be closer to those described in Section 6.3.

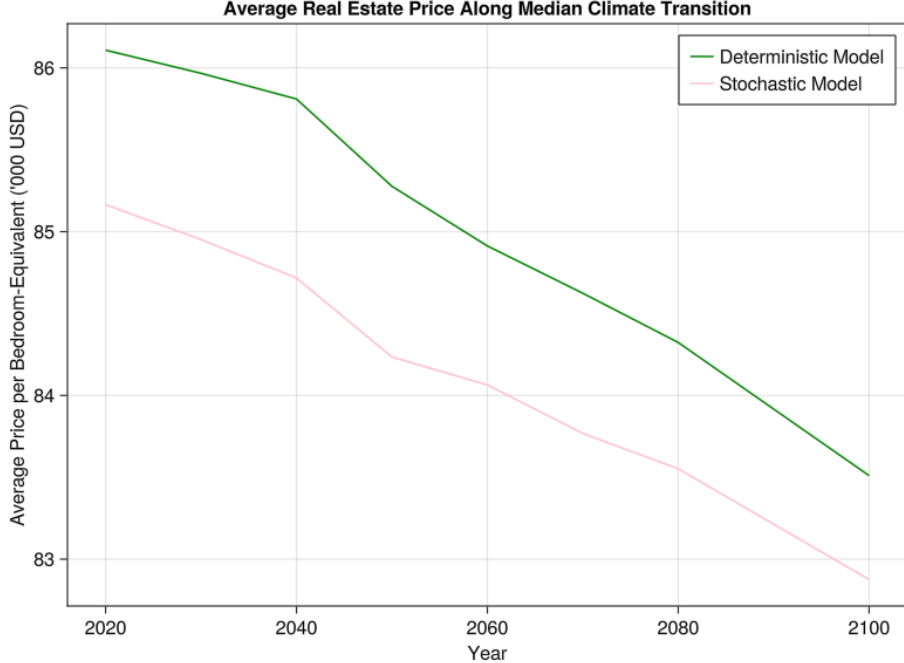


Figure 26: Prices along the median path, under both the stochastic and deterministic models. In the stochastic model, expectations are that the climate will follow the process calibrated in Section 4. In the deterministic model, expectations are that the climate will deterministically follow the median path.

7 Conclusion

How large are inequalities in the welfare effects of climate change across households? I study how homeownership shapes the answer to this question by building and quantifying a dynamic spatial equilibrium model of the contiguous U.S. with 1713 locations. In the model, heterogeneous households make forward-looking consumption-savings, migration, and real estate investment decisions which, in aggregate, determine spatially heterogeneous housing prices. Crucially, housing prices both reflect expectations about future climate change and determine an empirically realistic proportion of household wealth.

With homeownership, inequality in the welfare impacts of climate change is large. Negative climate news shocks are progressive by wealth but climate uncertainty induces ongoing regressive wealth transfers. In response to a change in expectations from widespread climate denial to widespread climate acceptance, this inequality in welfare impacts is equivalent to a \$2.8tn wealth transfer from more-harmed to less-harmed households or a \$94bn wealth transfer from less-wealthy to more-wealthy households. In contrast to a model

without individual housing asset ownership, migration adaptation does not substantially ameliorate spatial inequality in climate damages. Instead, households in severely-affected regions, whether or not they are actually displaced, suffer large climate-induced losses in housing wealth. In total, the spatially-heterogeneous adjustment of housing prices to the climate news shock is equivalent to a transfer of almost \$1tn in housing wealth from households in more-harmed to less-harmed regions.

In contrast to a model without housing wealth, anticipation does not greatly reduce spatial inequalities in climate damages. Instead, the primary effect is simply that unequal damages happen earlier, at the time that negative climate news is revealed. Furthermore, with anticipation and housing wealth, uncertainty introduces regressive wealth transfers. Climate risk causes households to be less willing to own rental housing, raising rent and expected returns on housing. Among households who do own housing, wealthier households are more willing to bear this risk, benefiting from the higher risk premia required by marginal, less-wealthy landlords. Less-wealthy renters are hurt by higher rents. Altogether, the regressive welfare impact of uncertainty is equivalent to a transfer of \$94bn from the bottom half of the wealth distribution to the top half, relative to a model with perfect foresight. The analysis of climate uncertainty depends crucially on having found the global solution of the model. This is made possible by the development of a novel deep learning method for solving recursive economic models under aggregate uncertainty.

Several factors not incorporated in this model are likely to further complicate the role of housing wealth in shaping inequalities in climate damages. Three such factors are belief heterogeneity, agglomeration, and growth. In reality, beliefs about climate change vary significantly across individuals. In a world with such belief heterogeneity, households who more accurately predict the consequences of climate change might be more likely to gain from forward-looking decisions informed by those beliefs. In reality, productivity is shaped by agglomeration forces as well as exogenous geographic advantages. If these amplify the spatial reallocation of economic activity due to climate change, they may also amplify the impacts of climate change on housing prices. Economic and population growth are also significant factors shaping housing prices. Especially because climate change occurs on the scale of centuries, the interaction of growth with climate change may have the potential to dramatically shape house price and welfare impacts.

Finally, this model develops methods with potentially interesting applications beyond the climate literature. All housing wealth depends on housing prices which reflect uncertain expectations. In reality, expectations and uncertainty over many long-term developments shape housing prices in the present. Dynamic spatial models with heterogeneous households, homeownership, and aggregate uncertainty—together with the numerical methods advances introduced here—could be used to study the impacts of expectations regarding future zoning policy, population growth, or future agglomeration forces on housing markets.

References

- Albouy, D., Graf, W., Kellogg, R., & Wolff, H. (2016). Climate Amenities, Climate Change, and American Quality of Life [Publisher: The University of Chicago Press]. *Journal of the Association of Environmental and Resource Economists*, 3(1), 205–246. <https://doi.org/10.1086/684573>
- Azinovic, M., Gaegauf, L., & Scheidegger, S. (2022). Deep Equilibrium Nets [_eprint: <https://onlinelibrary.wiley.com/doi/pdf/10.1111/iere.12575>]
- Balboni, C. (2021). In Harm's Way? Infrastructure Investments and the Persistence of Coastal Cities.
- Bates, P. D., Quinn, N., Sampson, C., Smith, A., Wing, O., Sosa, J., Savage, J., Olcese, G., Neal, J., Schumann, G., Giustarini, L., Coxon, G., Porter, J. R., Amodeo, M. F., Chu, Z., Lewis-Gruss, S., Freeman, N. B., Houser, T., Delgado, M., ... Krajewski, W. F. (2021). Combined Modeling of US Fluvial, Pluvial, and Coastal Flood Hazard Under Current and Future Climates [_eprint: <https://onlinelibrary.wiley.com/doi/pdf/10.1029/2020WR028673>]. *Water Resources Research*, 57(2), e2020WR028673. <https://doi.org/10.1029/2020WR028673>
- Bilal, A., & Rossi-Hansberg, E. (2023). Anticipating Climate Change Across the United States. <https://doi.org/10.3386/w31323>
- Borusyak, K., Dix-Carneiro, R., & Kovak, B. (2022). Understanding Migration Responses to Local Shocks.
- Caliendo, L., Dvorkin, M., & Parro, F. (2019). Trade and Labor Market Dynamics: General Equilibrium Analysis of the China Trade Shock. *Econometrica*, 87(3), 741–835. <https://doi.org/10.3982/ECTA13758>
- Crews, L. (2023). A Dynamic Spatial Knowledge Economy.
- Deryugina, T., & Hsiang, S. (2017). *The Marginal Product of Climate* (tech. rep. w24072). National Bureau of Economic Research. Cambridge, MA. <https://doi.org/10.3386/w24072>
- Desmet, K., Kopp, R. E., Kulp, S. A., Nagy, D. K., Oppenheimer, M., Rossi-Hansberg, E., & Strauss, B. H. (2021). Evaluating the Economic Cost of Coastal Flooding. *American Economic Journal: Macroeconomics*, 13(2), 444–486. <https://doi.org/10.1257/mac.20180366>
- Favilukis, J., Ludvigson, S. C., & Van Nieuwerburgh, S. (2017). The Macroeconomic Effects of Housing Wealth, Housing Finance, and Limited Risk Sharing in General Equilibrium [Publisher: The University of Chicago Press]. *Journal of Political Economy*, 125(1), 140–223. <https://doi.org/10.1086/689606>
- Fernandez-Villaverde, J., Nuno, G., Sorg-Langhans, G., & Vogler, M. (2020). Solving High-Dimensional Dynamic Programming Problems using Deep Learning, 48.
- Fried, S. (2022). Seawalls and Stilts: A Quantitative Macro Study of Climate Adaptation. *The Review of Economic Studies*, 89(6), 3303–3344. <https://doi.org/10.1093/restud/rdab099>

- Gassert, F., Cornejo, E., & Nilson, E. (2021). Making Climate Data Accessible: Methods for Producing NEX-GDDP and LOCA Downscaled Climate Indicators. *World Resources Institute*. <https://doi.org/10.46830/writn.19.00117>
- Giannone, E., Paixão, N., Pang, X., & Li, Q. (2023). A Quantitative Spatial Equilibrium Model with Wealth.
- Greaney, B. (2021). The Distributional Effects of Uneven Regional Growth, 49.
- Han, J., Yang, Y., & E, W. (2021). DeepHAM: A Global Solution Method for Heterogeneous Agent Models with Aggregate Shocks. *SSRN Electronic Journal*. <https://doi.org/10.2139/ssrn.3990409>
- Hsiang, S., Kopp, R., Jina, A., Rising, J., Delgado, M., Mohan, S., Rasmussen, D. J., Muir-Wood, R., Wilson, P., Oppenheimer, M., Larsen, K., & Houser, T. (2017). Estimating economic damage from climate change in the United States. *Science*, 356(6345), 1362–1369. <https://doi.org/10.1126/science.aal4369>
- Hsiao, A. (2023). Sea Level Rise and Urban Adaptation.
- Kaplan, G., Mitman, K., & Violante, G. L. (2020). The Housing Boom and Bust: Model Meets Evidence [Publisher: The University of Chicago Press]. *Journal of Political Economy*, 000–000. <https://doi.org/10.1086/708816>
- Kleinman, B., Liu, E., & Redding, S. J. (2023). Dynamic Spatial General Equilibrium, 46.
- Knutson, T., Camargo, S. J., Chan, J. C. L., Emanuel, K., Ho, C.-H., Kossin, J., Mohapatra, M., Satoh, M., Sugi, M., Walsh, K., & Wu, L. (2020). Tropical Cyclones and Climate Change Assessment: Part II: Projected Response to Anthropogenic Warming [Publisher: American Meteorological Society Section: Bulletin of the American Meteorological Society]. *Bulletin of the American Meteorological Society*, 101(3), E303–E322. <https://doi.org/10.1175/BAMS-D-18-0194.1>
- Komissarova, K. (2022). Location Choices over the Life Cycle: The Role of Relocation for Retirement.
- Krusell, P., & Smith, A. A., Jr. (1998). Income and Wealth Heterogeneity in the Macroeconomy. *Journal of Political Economy*, 106(5), 867–896. <https://doi.org/10.1086/250034>
- Krusell, P., & Smith, A. A., Jr. (2022). Climate Change Around the World.
- Maliar, L., Maliar, S., & Winant, P. (2021). Deep learning for solving dynamic economic models. *Journal of Monetary Economics*, 122, 76–101. <https://doi.org/10.1016/j.jmoneco.2021.07.004>
- Pang, X., & Sun, P. (2023). MOVING INTO RISKY FLOODPLAINS:
- Rasmussen, D., & Kopp, R. E. (2017). Probability-Weighted Ensembles Of U.S. County-Level Climate Projections For Climate Impact Modeling [Publisher: Zenodo]. <https://doi.org/10.5281/ZENODO.582327>
- Rode, A., Carleton, T., Delgado, M., Greenstone, M., Houser, T., Hsiang, S., Hultgren, A., Jina, A., Kopp, R. E., McCusker, K. E., Nath, I., Rising, J., & Yuan, J. (2021). Estimating a social cost of carbon for global energy consumption [Number: 7880 Publisher: Nature Publishing Group]. *Nature*, 598(7880), 308–314. <https://doi.org/10.1038/s41586-021-03883-8>

- Saiz, A. (2010). The Geographic Determinants of Housing Supply [Publisher: Oxford Academic]. *The Quarterly Journal of Economics*, 125(3), 1253–1296. <https://doi.org/10.1162/qjec.2010.125.3.1253>
- Sinai, T., & Souleles, N. S. (2005). Owner-Occupied Housing as a Hedge Against Rent Risk*. *The Quarterly Journal of Economics*, 120(2), 763–789. <https://doi.org/10.1093/qje/120.2.763>
- Wing, O. E. J., Lehman, W., Bates, P. D., Sampson, C. C., Quinn, N., Smith, A. M., Neal, J. C., Porter, J. R., & Kousky, C. (2022). Inequitable patterns of US flood risk in the Anthropocene [Number: 2 Publisher: Nature Publishing Group]. *Nature Climate Change*, 12(2), 156–162. <https://doi.org/10.1038/s41558-021-01265-6>
- Yao, R., & Zhang, H. H. (2005). Optimal Consumption and Portfolio Choices with Risky Housing and Borrowing Constraints. *Review of Financial Studies*, 18(1), 197–239. <https://doi.org/10.1093/rfs/hhh007>

A Harmonization of Climate Damage Estimates

A.1 Labor Productivity

I take estimates of the effect of temperature on wages from Deryugina and Hsiang, 2017. They use a panel of U.S. counties from 1969 to 2014 to estimate the effect of temperature on wages, using idiosyncratic weather variation. Although they do not study the effect of long-term adaptation, they argue that, in equilibrium, the marginal response of income to short-term weather realizations is equal to the marginal effect of income to long-term climate variation. They use an envelope-theorem argument: in the neighborhood of equilibrium temperatures, the benefit of long-term climate adaptations must be zero.

They thus estimate the effect of daily temperatures on log annual total income per capita. Their Figure 4a (my Figure 27) shows their estimates. They choose 55°F as the reference temperature, because it is the temperature with the greatest positive effect on productivity in their estimation. I recenter at 65°F. Upon recentering, the marginal effect of temperatures above 65°F remains fairly constant. The overall effect of temperatures below 65°F is negative but small, with an average effect of 6.6×10^{-6} per °C-day between 15°F and 65°F, an order of magnitude smaller than the average effect of -4.5×10^{-5} per °C-day between 65°F and 85°F. It is true, however, that the marginal effect of temperatures below 65°F is not constant, and it would be ideal to use projections of HDD and CDD centered at 55°F. Table 1 shows these extracted estimates.

Using climate projections on HDD and CDD changes per °C global warming, as in Section 3.3.2, I compute income damages for each county per °C global warming. Figure 2 displays the resulting projections of income reductions for each PUMA.

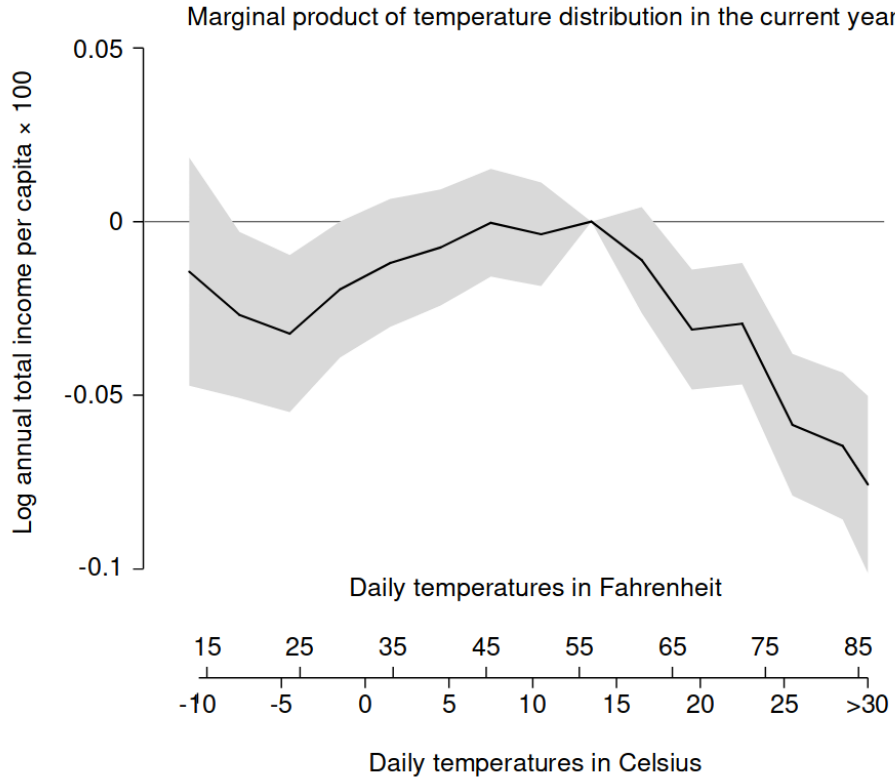


Figure 27: Impact of a single day at a certain temperature on log annual total income.
Reproduced from Deryugina and Hsiang, 2017.

A.2 Disaster Projections

I use projections of climate impacts on total combined damages from flooding from Bates et al. (2021), as reported in Wing et al. (2022).

I argue that their projections, together with the estimates I use on heat and cold amenities, capture the great majority of climate impacts on natural disasters. Of the 18 FEMA hazard categories, “Earthquake” and “Volcano” are likely not climate-sensitive. “Wildfire,” “Heat Wave,” “Cold Wave,” “Winter Weather,” “Ice Storm,” “Drought,” “Avalanche,” and “Hail” are not separately identified from the estimates on heat and cold climate amenities which I take from the literature (Section 3.3.2). This leaves primarily flooding and wind-related hazards and wind-related hazards—“Coastal Flooding,” “Landslide,” “Riverine Flooding,” “Tsunami,” “Hurricane,” “Tornado,” “Strong Wind,” “Lightning.”

The projections I use are likely to capture the great majority of our current best understanding of the climate-sensitivities of flooding and wind-related disasters. These projections include all forms of flooding, including those which happen in conjunction with storms, leaving primarily wind-related damages. Current projections of the impact of climate change on wind-related damages *per se* are highly uncertain, with

confidence intervals centered near zero.

A recent meta-analysis of projections of tropical cyclone activity under climate change (Knutson et al., 2020), find confident projections of increasing tropical cyclone precipitation, but small and highly uncertain changes in terms of wind speeds. Among the models they survey, median projections for a 2° warming scenario predict a 16% *decrease* in tropical cyclone frequencies in the North Atlantic basin, but a 3% increase in average intensity. the net result is a 10% increase in the annual number of category 4-5 cyclones, with an interquartile range of [-21%, 28%]. Cyclone intensity refers to wind speed only, and this uncertainty does not extend to precipitation and flooding. The median projected increase in precipitation under the 2°C warming scenario is 16% with interquartile range [8%, 21%]. Flooding due to storm surges is also projected to increase, due to rising sea levels (Little et al. 2015). Indeed, the greatest impact of climate change on property damages are expected to take the form of these “compound events,” (AghaKouchak et al., 2020) and compound events which include flooding are encompassed by the projections I use.

As a test of this coverage, I compare the mean annual residential flooding damages, or Average Annual Losses (AAL), from all contiguous U.S. flooding, under 2020 climate conditions, predicted by the model of Bates et al. (2021). Their prediction is \$30bn, which actually exceeds the mean annual damages in SHELDUS between 2011 and 2020 in the “Coastal Flooding,” “Hurricane,” “Riverine Flooding,” “Severe Storm,” and “Tsunami” categories. These realized damages are \$21.39bn (2021 USD) and account for 71% of all realized property damage from disasters in that period.

Due to data limitations, I have only two variables per county from the analysis of Bates et al. (2021). The first is Average Annual Losses (AAL), per county, given 2020 climate conditions. The second is the percentage change in AAL per county between 2020 and 2050 under RCP 4.5. In order to harmonize this with the other estimates, I divide the AAL change by 0.63°C, the median global warming under RCP 4.5 in that time period (Rasmussen and Kopp, 2017). This gives me a linearized measure of the projected increase in AAL per °C global warming:

$$\frac{d}{dT} \widehat{\text{AAL}}_\ell(T) = \frac{\text{AAL}_{\ell,2050} - \text{AAL}_{\ell,2020}}{0.63 \text{ } ^\circ\text{C}}$$

A.3 Heat and Cold Amenities

I take estimates of heat and cold amenities from Albouy et al., 2016, who use a Rosen-Roback style model and the IPUMS 5% sample of the 2000 Census to impute amenities for each U.S. PUMA as the residual of real wage differentials. Thus, I am not double-counting the impact of temperatures on wages. They factor energy costs into real wages, so that I am not double-counting the impact of energy costs. They estimate a range of specifications.

I pick the richest model that is consistent with my model, reported in their Figure 5F (my Figure

28b). The dependent variable is willingness-to-pay (WTP) to avoid a single day at a certain temperature, and experience a day at 65°F instead. They fit WTP to a four-piece linear spline with geographic, non-temperature weather, and demographic controls, and state fixed effects. All other specifications use fewer controls, except for their Figure 5E (my Figure 28a), which fits WTP to a 7th-degree cubic spline.

The cubic spline specification is very close to linear for temperatures less than 65°F, and close to linear between 65°F and 85°F, but constant above 85°F, possibly due to lack of data. The linear specification separately estimates slopes below 45°F, between 45°F and 65°F, between 65°F and 80°F, and above 80°F. They find similar slopes for both segments below 65°F and both segments above 65°F. I therefore believe that it is not unreasonable to assume constant, but different, marginal effects for days below and above 65°F, respectively. I take their estimates for WTP at each extreme, 0°F and 110°F, and assume constant marginal value of each degree-day below and above 65°F.⁴⁹

Assuming constant marginal effects of each degree-day below and above 65°F allows me to impute cold disamenities as a function of annual heating-degree-days (HDD), the sum over each day t of the year

$$\sum_t \max(65^\circ\text{F} - T_t, 0)$$

of the number of degrees by which that day's temperature T_t falls below 65°F. I similarly impute heat disamenities as a function of annual 65°F-baseline cooling-degree-days (CDD). I report these WTP per degree-day estimates in Table 2.

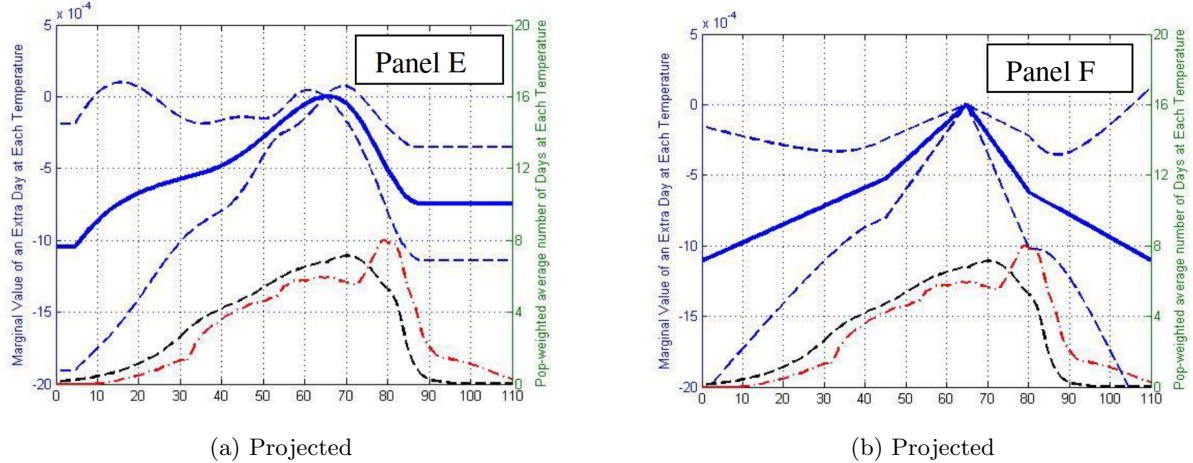


Figure 28: Marginal value of a day at a given temperature, relative to a day at 65°F, as a percentage of annual income. From: Albouy et al., 2016, Figure 9

⁴⁹Equivalently, I take the arithmetic mean of each pair of segments, weighted by segment length.

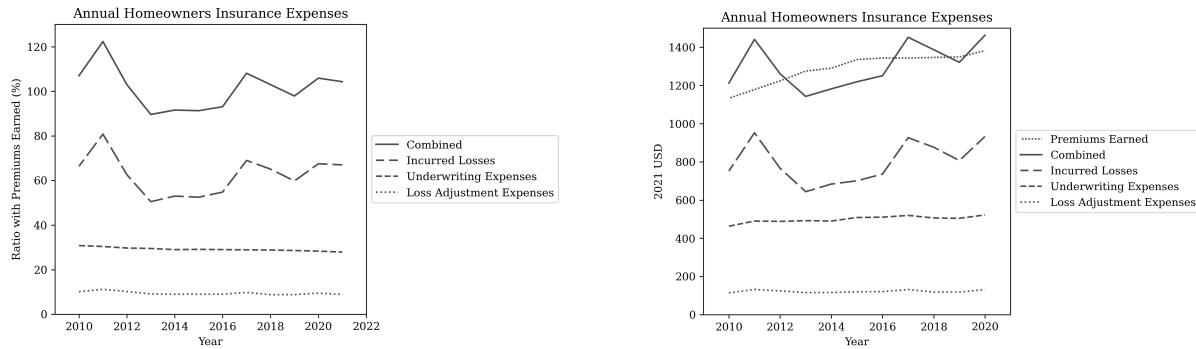
B State Space Model for Insurance Estimation

B.1 Data Sources

I use annual data for the U.S. between 2003 and 2020, compiled by the Insurance Information Institute (III), on average homeowners insurance premiums, average losses per policy-year, sources of losses, and sources of expenses. Expenses are divided first into incurred losses (i.e. payouts to policyholders), adjustment expenses, and underwriting and other expenses. Incurred losses are categorized by hazard (e.g. water damage, theft, etc.). These data are originally reported by the National Association of Insurance Commissioners and by Insurance Services Office, Inc. I use data on global annual greenhouse gas emissions from the World Resources Institute.

B.2 Estimating Anticipated Losses

Accounting variables such as insurance losses and expenses are reported as the ratio between that variable and total earned premiums. “Incurred losses” are total claims paid to policyholders for a year, and “loss adjustment expenses” are additional expenses related to investigating and settling claims. I group all other expenses into “underwriting expenses,” or expenses related to originating or maintaining insurance policies rather than handling claims.



(a) Breakdown of expenses experienced by insurers from homeowners insurance business (ratio with premiums earned%). The combined ratio is the sum of the loss ratio (incurred losses divided by premiums earned) and the expense ratio (expenses divided by premiums earned). When the combined ratio is greater than 100, the insurer is losing money. Data are from the Insurance Information Institute (III).

(b) Breakdown of expenses experienced by insurers from homeowners insurance business (2021 dollars). Data are the same as the left figure, but values are given in dollar terms instead of as a ratio with premiums earned.

Figure 29

Figures 29a and 29b show the breakdown of expenses experienced by homeowners insurance companies. The majority of expenses are incurred losses, with loss adjustment expenses and underwriting expenses each

accounting for about a quarter of total expenses.

The solid line indicates the “combined ratio,” a common metric used to assess the profitability of an insurance company. I assume that insurers are zero-profit, so that the anticipated combined ratio is equal to 100. I use this assumption to back out the expected level of incurred losses that insurers anticipate paying each year.⁵⁰

Figure 30 shows the average homeowners insurance premium and estimated anticipated losses, 2003-2020, in 2021 USD. The estimated anticipated losses appear to track the mean of realized losses well.

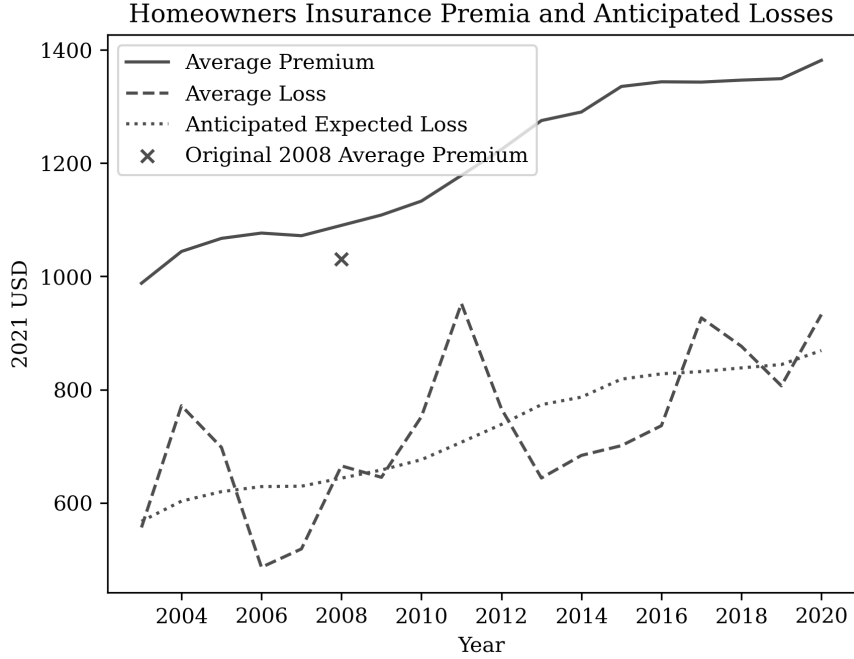


Figure 30: Average homeowners insurance premium and estimated anticipated losses, 2003-2020, in 2021 USD. The only significant decrease in average premium, in the original data, occurs in 2008, and is immediately reversed in 2009. I drop this observation on the grounds that it is likely a transient change due to the financial crisis rather than a persistent change in climate beliefs. Dollar losses (expenses) are imputed by multiplying the loss (expense) ratio by the average premium. Prior to 2010, dollar losses are imputed by multiplying claim frequencies (claims per 100 policy-years) by claim severity (average amount paid per claim). Nominal values are deflated by CPI.

B.2.1 Linear Regression

I show here that reduced-form evidence suggests that homeowners insurance premiums are responsive to disaster realizations in such a way that suggests that insurers are uncertain about the true distribution from which these realizations are drawn. I use this to inform a Bayesian estimation of the insurer’s uncertainty over the contribution of emissions to disaster risk in Appendix B.

⁵⁰Additional details of this imputation procedure are in Appendix C. Expenses consist of both fixed and variable expenses that depend on realized losses, which I must invert.

I begin by defining the simple estimating equation,

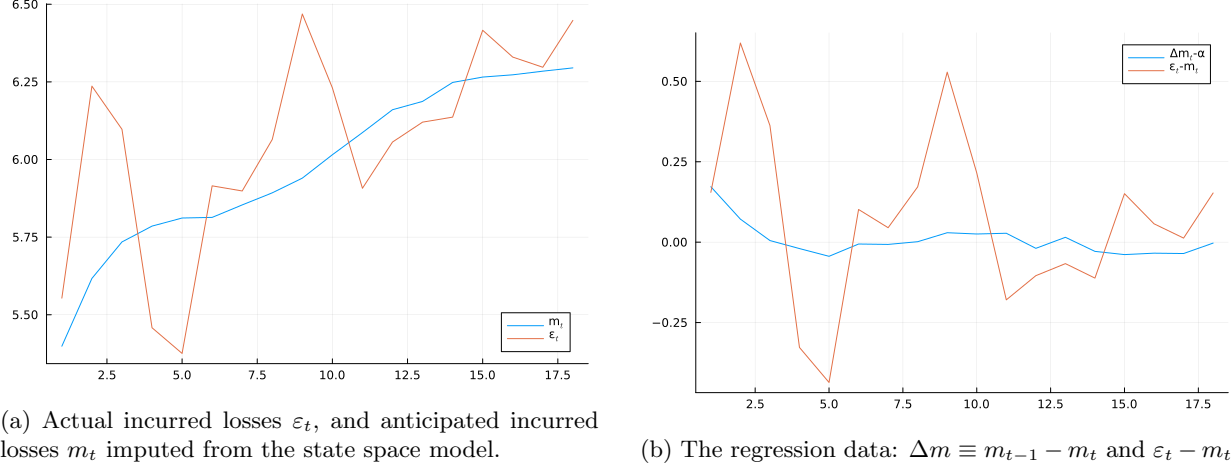
$$m_{t+1} - m_t = \alpha + \frac{\tilde{\sigma}^2}{\sigma_\varepsilon^2}(\varepsilon_t - m_t) + \frac{\tilde{\sigma}^2}{\sigma_\eta^2}(\eta_t - m_t). \quad (8)$$

where m_t is the insurer's prior mean of losses in year t , which I impute from the insurance premium (with details in Appendix C). ε_t is the insurer's realized losses in year t , and η_t is a news shock which explains residual variation in premiums.

That is, I simply regress changes in imputed prior means on observed (log) loss surprises ε_t , and use the model to interpret the reduced-form coefficient on ε_t . Although $m_t = L_t - (\sigma^2 + \sigma_\varepsilon^2)/2$ depends on parameters, the effect of these parameters is small, and can be solved for by fixed point. More seriously, unless $\mu_t = m_t$, the error term $\frac{\tau_\eta}{\tau}(\eta_t - m_t)$ will be biased and correlated with the regressor through the insurer's prior bias $\mu_t - m_t$,

$$\begin{aligned} \mathbb{E}[\eta_t - m_t] &= \mu_t - m_t \\ \text{Cov}(\varepsilon_t - m_t, \eta_t - m_t) &= (\mu_t - m_t)^2 - 2(\mu_t - m_t), \end{aligned}$$

so this should be considered a descriptive exercise. Figure 31b shows the data used in this regression.



(a) Actual incurred losses ε_t , and anticipated incurred losses m_t imputed from the state space model.

(b) The regression data: $\Delta m \equiv m_{t-1} - m_t$ and $\varepsilon_t - m_t$.

I estimate Equation 8 by OLS, and report the results in Table 8. In columns 5-8, I fix the intercept α at 0.77% to match the forecast of Wing et al. (2022) of a 26% increase in flooding damages over 30 years. In columns 1,2,5, and 6, I estimate the slightly modified Equation 9 in which the error is reduced-form and not modeled as a signal. In columns 2,4,6, and 8, I drop the first observation because it is by far the largest value of the regressor. In all specifications there is a significant effect of loss surprises on premiums, although the significance is lower when the first observation is included.

Table 8: Parameter estimates.

	(1)	(2)	(3)	(4)	(5)	(6)	(7)	(8)
α	0.046*** (0.012)	0.054*** (0.010)	0.046*** (0.012)	0.054*** (0.010)				
$\varepsilon - m_t$	0.083* (0.043)	0.076*** (0.022)	0.083* (0.043)	0.076*** (0.022)	0.166** (0.058)	0.095*** (0.024)	0.163** (0.059)	0.095*** (0.025)
N	18	17	18	17	18	17	18	17
R^2	0.190	0.453	0.190	0.453	0.326	0.485	0.313	0.483

$$m_{t+1} - m_t = \alpha + \frac{1}{1 + \sigma_\varepsilon^2 / \sigma^2} (\varepsilon_t - m_t) + \zeta_t. \quad (9)$$

B.3 Model

I attribute to a representative home insurer the same climate model as in the main model. Insurer storm losses $\exp(d_t)$ are generated by a persistent-transitory process. Log-losses d_t are drawn from a Normal distribution with unobserved mean μ_t , which follows a Gaussian random walk that is affected by emissions e_t . Each year, the insurer also observes a news shock n_t , unobserved to the econometrician, whose mean is a linear function of μ_t . Without loss of generality, η_t has mean μ_t . Formally,

$$\begin{aligned} \mu_{t+1} &= \rho\mu_t + \beta e_t \\ n_t &\sim \mathcal{N}(\mu_t, \sigma_n^2) \\ d_t &\sim \mathcal{N}(\mu_t, \sigma_d^2) \end{aligned}$$

The parameters $\{\sigma_n^2, \sigma_d^2, \rho\}$ are known to the insurer. The values $\{n_t, d_t, e_t\}$ are observed each period. The parameters β and μ_t are unobserved and learned about over time.

The timing of the model is as follows. Each period:

1. The insurer sets a premium π_t .
2. The shocks n_t and d_t are realized and observed.
3. The insurer updates their prior over μ_t and β .
4. The true mean μ_t is updated according to the AR(1) process.

If the insurer has an initial multivariate normal prior over μ_0 and β , then, if fully rational Bayesian learners, they update their beliefs according to the Kalman filter. Rewriting the model in terms of matrices:

$$\begin{aligned}\underbrace{\begin{bmatrix} d_t \\ n_t \end{bmatrix}}_{\mathbf{z}_t} &= \underbrace{\begin{bmatrix} 1 & 0 \\ 1 & 0 \end{bmatrix}}_{\mathbf{H}_t} \underbrace{\begin{bmatrix} \mu_t \\ \beta \end{bmatrix}}_{\mathbf{x}_t} + \mathbf{v}_t, \quad \mathbf{v}_t \sim \mathcal{N}(0, \Sigma_v) \\ \underbrace{\begin{bmatrix} \mu_{t+1} \\ \beta \end{bmatrix}}_{\mathbf{x}_{t+1}} &= \underbrace{\begin{bmatrix} \rho & e_t \\ 0 & 1 \end{bmatrix}}_{\mathbf{F}_t} \underbrace{\begin{bmatrix} \mu_t \\ \beta \end{bmatrix}}_{\mathbf{x}_t}\end{aligned}$$

If the insurer's prior for \mathbf{x}_t at the end of period $t - 1$ is

$$\mathbf{x}_t | \mathcal{I}_t \sim \mathcal{N} \left(\hat{\mathbf{x}}_t \equiv \begin{bmatrix} \hat{\mu}_t \\ \hat{\beta}_t \end{bmatrix}, \hat{\mathbf{P}}_t \right),$$

then their prior for \mathbf{x}_{t+1} at the end of period t is

$$\begin{aligned}\hat{\mathbf{x}}_{t+1} &= \mathbf{F}_t(\mathbf{I} - \mathbf{K}_t \mathbf{H}_t) \hat{\mathbf{x}}_t + \mathbf{F}_t \mathbf{K}_t \mathbf{z}_t \\ \hat{\mathbf{P}}_{t+1} &= \mathbf{F}_t(\mathbf{I} - \mathbf{K}_t \mathbf{H}_t) \hat{\mathbf{P}}_t \mathbf{F}_t' \\ \mathbf{K}_t &= \hat{\mathbf{P}}_t \mathbf{H}_t' (\mathbf{H}_t \hat{\mathbf{P}}_t \mathbf{H}_t' + \Sigma_v)^{-1}\end{aligned}$$

where \mathbf{K}_t is the optimal Kalman gain.

B.3.1 Nesting Step

I observe $\{d_t, e_t, \hat{x}_t\}$ and wish to estimate $\{\sigma_n, \sigma_d, \rho, \hat{\beta}_0\}$. First, I simply rewrite the above equations in terms of block matrices:

$$\begin{aligned} \begin{bmatrix} \mathbf{x}_{t+1} \\ \mathbf{z}_{t+1} \\ \hat{\mathbf{x}}_{t+1} \end{bmatrix} &= \begin{bmatrix} \mathbf{F}_{t+1} & 0 & 0 \\ \mathbf{H}_{t+1} & 0 & 0 \\ 0 & \mathbf{F}_t \mathbf{K}_t & \mathbf{F}_t (\mathbf{I} - \mathbf{K}_t \mathbf{H}_t) \end{bmatrix} \begin{bmatrix} \mathbf{x}_t \\ \mathbf{z}_t \\ \hat{\mathbf{x}}_t \end{bmatrix} + \begin{bmatrix} 0 \\ \mathbf{v}_t \\ 0 \end{bmatrix} \\ \begin{bmatrix} 0 \\ \mathbf{v}_t \\ 0 \end{bmatrix} &\sim \mathcal{N} \left(0, \begin{bmatrix} 0 & 0 & 0 \\ 0 & \mathbf{R}_t & 0 \\ 0 & 0 & 0 \end{bmatrix} \right) \\ \begin{bmatrix} d_t \\ \hat{\mu}_t \end{bmatrix} &= \begin{bmatrix} 0 & 0 & 0 & 1 & 0 & 0 \\ 0 & 0 & 0 & 0 & 1 & 0 \end{bmatrix} \begin{bmatrix} \mathbf{x}_{t+1} \\ \mathbf{z}_{t+1} \\ \hat{\mathbf{x}}_{t+1} \end{bmatrix} = \begin{bmatrix} 0 & 0 & 0 & 1 & 0 & 0 \\ 0 & 0 & 0 & 0 & 1 & 0 \end{bmatrix} \begin{bmatrix} \mu_t \\ \beta \\ n_t \\ d_t \\ \hat{\mu}_t \\ \hat{\beta}_t \end{bmatrix} \end{aligned}$$

Observe that, for any guess of the parameters $\{\sigma_n, \sigma_d, \rho, \hat{\beta}_0\}$, all of the matrices in this system are known to us. That is, we can treat the above as a linear Gaussian state space model and apply the Kalman filter to it. This is the nesting step.

B.3.2 State Space Model Estimation

For any prior and given set of parameters, the Kalman filter yields a likelihood of the observed data, in our case $\{d_t, \hat{\mu}_t\}$. I thus estimate the parameters by maximum likelihood. Table 9 displays the result.

After estimating parameters, the Kalman smoother provides estimates of the unobserved state. Figure 32 shows the results. Given the parameter estimates, variation in $\hat{\mu}_t$ is almost entirely due to variation in beliefs $\hat{\beta}_t$ about β , as opposed to being driven by beliefs that the unobserved mean μ_t has changed over time.

Variable	Estimate
σ_n^{err}	0.21306
σ_d^{err}	0.28874
ρ	0.98
T_0	1965.87

Table 9: Results of state space estimation. Point estimates are by maximum likelihood.

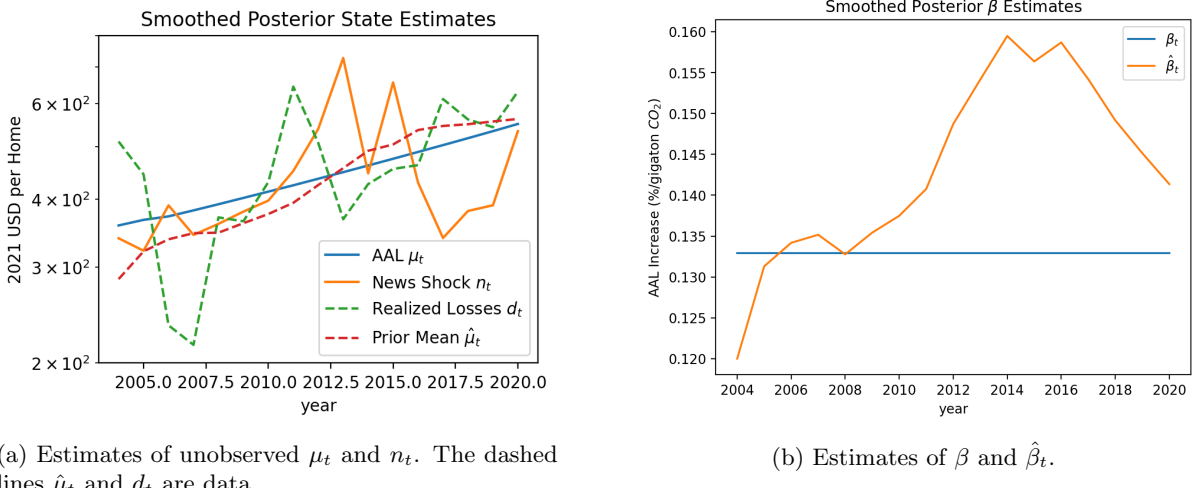


Figure 32

C Homeowners Insurance Anticipated Incurred Losses

In order to account for the fact that expenses other than the incurred expenses (henceforth “non-incurred expenses”) have a time trend and covary with incurred expenses, I regress non-incurred expenses on incurred losses and a time trend. That is, I decompose it into fixed and variable costs, where I allow for a time trend in fixed costs. Though the number of observations is small, the fit is very good. I regress non-incurred expenses on incurred losses and a time trend, and find a small time trend and . That is, I decompose it into fixed and variable costs, where I allow for a time trend in fixed costs.

$$\text{Expenses}_t = \alpha + \beta(\text{Incurred Losses})_t + \gamma\text{Year}_t + \varepsilon_t$$

Table 10: Expenses on incurred losses.

	Expense Ratio
Intercept	731.743*** (42.405)
Incurred Loss Ratio	0.079*** (0.009)
Year	-0.346*** (0.021)
R-squared	0.976
R-squared Adj.	0.970
N	12

I then assume risk-neutrality of insurers and apply the zero-profit condition that insurers are targeting a constant combined ratio of 100. I can thus estimate anticipated expected annual losses by setting anticipated expected combined losses equal premiums earned. By “anticipated expected” (henceforth simply “anticipated”) losses, I mean

$$\mathbb{E} [\text{Losses} \mid \mathcal{I}_t],$$

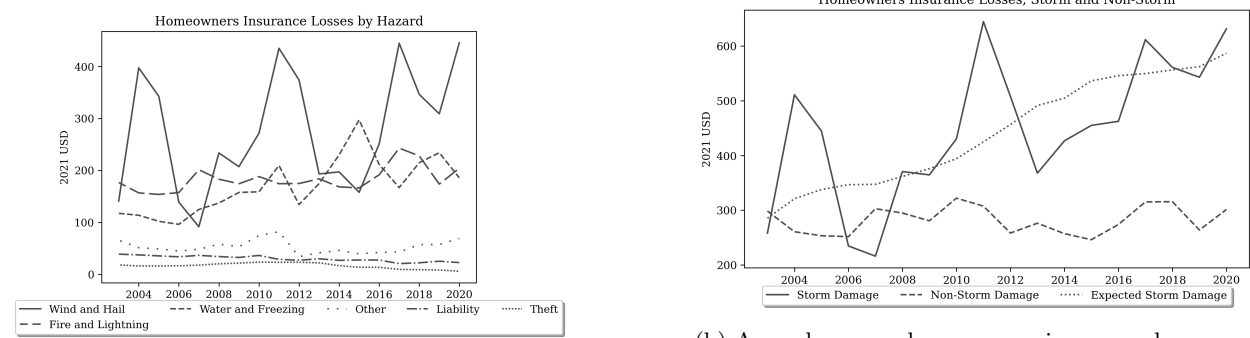
the expected value of anticipated losses given the insurer’s information set at time t . The mean combined ratio over the sample period was 101.425, suggesting that it is reasonable to assume that a value of 100 is targeted. Note that we would expect the combined ratio to be greater than 100 if insurers experience greater-than-expected losses over the sample period.

Let $\mathbb{E}[x \mid \mathcal{I}_t]$ denote the anticipated value of x conditional on the insurer’s information set at time t . For each year t , let L_t denote realized incurred loss ratio, N_t denote non-incurred expense ratio, and C_t denote the combined ratio. Then,

$$\begin{aligned}\mathbb{E}[C_t \mid \mathcal{I}] &= 100 \\ &= \mathbb{E}[L_t \mid \mathcal{I}] + \mathbb{E}[N_t \mid \mathcal{I}] \\ &= \mathbb{E}[L_t \mid \mathcal{I}] + \alpha + \beta \mathbb{E}[L_t \mid \mathcal{I}] + \gamma \text{Year}_t \\ \mathbb{E}[L_t \mid \mathcal{I}] &= (\mathbb{E}[C_t \mid \mathcal{I}] - \alpha - \gamma \text{Year}_t) / (1 + \beta)\end{aligned}$$

C.1 Storm Component of Losses

Figure 33a shows the breakdown of losses by hazard. Note that there is no clear trend in any category except “Wind and Hail” and “Water and Freezing.” In Figure, I group “Wind and Hail” and “Water and Freezing” losses into “Storm Losses” and all other incurred losses into “Non-Storm Losses.” The time trend of non-storm losses is vanishingly small, \$0.72/year. I thus assume that the time trend in anticipated non-storm losses is zero, and that all variation in anticipated losses is due to variation in anticipated storm losses. For each year, I simply subtract the sample mean of non-storm losses from total anticipated incurred losses to obtain my estimate of anticipated storm losses.



(a) Annual average homeowners insurance losses per policy-year, by hazard. Losses are reported in data as shares of total incurred losses, and are here imputed by multiplying by imputed total incurred losses.

(b) Annual average homeowners insurance losses per policy-year, by storm category. Losses are reported in data as shares of total incurred losses, and are here imputed by multiplying by imputed total incurred losses.

D Full Household’s Problem

In sum, the household’s problem is given by

$$\begin{aligned}
& V_t(b, z, h_0^{\text{live}}, h_0^{\text{let}}, \ell_0, a, \{\varepsilon_l\}_l) \\
&= \max_{h^{\text{live}}, h^{\text{let}}, \ell, g, h} \varepsilon_l - \tau d(\ell, \ell_0) + u(g, h, \alpha_{\ell t}) + \beta \mathbb{E} V_{t+1}(b', z', h^{\text{live}'}, h^{\text{let}'}, \ell, a+1, \{\varepsilon'_l\}_l) \\
\text{s.t. } & u(g, h, \alpha_{\ell t}) = \alpha_\ell \frac{(g^{1-\sigma} + \gamma h^{1-\sigma})^{\frac{1-\eta}{1-\sigma}} - 1}{1-\eta} \\
& b' = R(\tilde{b}) + A_{\ell t} e^z + \rho_{\ell t} h^{\text{let}} - g - \rho_{\ell t} h^{\text{rent}} - \chi_{\ell t}^{\text{live}} h^{\text{live}} - \chi_{\ell t}^{\text{let}} h^{\text{let}} \\
& \tilde{b} = b - F^m D^{\text{move}} + \sum_{s \in \{\text{live, let}\}} D^{\text{sell}, s} [(1-\phi) q_{\ell_0 t} h_0^s - q_{\ell t} h^s] \\
& R(\tilde{b}) = \begin{cases} (1+r^f) \tilde{b} & \tilde{b} \geq 0 \\ (1+r^m) \tilde{b} & \tilde{b} < 0 \end{cases} \\
& b' \geq -\kappa q_{\ell t} (h^{\text{live}} + h^{\text{let}}) \\
& h = \begin{cases} h^{\text{live}} & h^{\text{live}} > 0 \\ h^{\text{rent}} & \text{otherwise} \end{cases} \\
& D^{\text{move}} = \mathbb{1}[\ell \neq \ell_0] \\
& D^{\text{sell}, s} = D^{\text{move}} \vee \mathbb{1}[h_0^s \neq h^s] \quad \forall s \in \{\text{live, let}\}
\end{aligned} \tag{10}$$

Expected continuation utility is defined as

$$\mathbb{E} V_{t+1}(b', z', h^{\text{live}'}, h^{\text{let}'}, \ell, a+1) \equiv \mathbb{E}_{z', h^{\text{live}'}, h^{\text{let}'}, \{\varepsilon'_l\}_l} [V_{t+1}(b', z', h^{\text{live}'}, h^{\text{let}'}, \ell, a+1, \{\varepsilon'_l\}_l) \mid z, h^{\text{live}}, h^{\text{let}}]$$

with stochastic transitions,

$$\begin{aligned}
\text{s.t. } & z_{it+1} = p z_{it} + \zeta_{ait} + \nu_{it} \\
& \nu \sim \mathcal{N}(0, \sigma_\nu) \\
& \varepsilon_{\ell it} \sim \text{Gumbel}(0, 1)
\end{aligned} \tag{11}$$

The properties of the Gumbel distribution imply that households choose locations in proportion to the (exponentiated) value of living in that location (see Appendix E).

D.0.1 Household Distribution Transition Function

The individual policy function solving (10) maps beginning-of-period state $x \in \mathbf{X}$ to chosen end-of-period (pre-shock) state $x^{\text{choice}} \in \mathbf{X}^{\text{choice}}$,

$$\begin{aligned}\text{Policy}_t(x, \{\varepsilon_\ell\}_\ell) &= x^{\text{choice}} \in \mathbf{X}^{\text{choice}} \\ x^{\text{choice}} &= (b', z, h^{\text{live}}, h^{\text{let}}, \ell, a).\end{aligned}$$

For $\mathbf{X}_0^{\text{choice}} \subseteq \mathbf{X}^{\text{choice}}$, taking $\{\varepsilon_\ell\}_\ell$ as unknown, the structure of the Gumbel distribution gives,

$$\Pr_\varepsilon(\ell | b, z, h^{\text{live}}, h^{\text{let}}, \ell_0, a + 1; \Gamma_t) = \frac{\exp\left(\psi \tilde{V}_\ell(b, z, h_0^{\text{live}}, h_0^{\text{let}}, \ell_0, a)\right)}{\sum_l \exp\left(\psi \tilde{V}_l(b, z, h_0^{\text{live}}, h_0^{\text{let}}, \ell_0, a)\right)}$$

where

$$\tilde{V}(b, z, h_0^{\text{live}}, h_0^{\text{let}}, \ell_0, a) = \max_{h^{\text{live}}, h^{\text{let}}, g, h} \tau d(l, \ell_0) + u(g, h, \alpha_{\ell t}) + \beta \mathbb{E} V_{t+1}(b', z', h^{\text{live}'}, h^{\text{let}'}, l, a + 1, \{\varepsilon'_l\}_l),$$

subject to the same constraints as in (10). This naturally defines idiosyncratic and distributional transition functions from \mathbf{X} to $\mathbf{X}^{\text{choice}}$. For $\mathbf{X}_0^{\text{choice}} \subseteq \mathbf{X}^{\text{choice}}$,

$$\begin{aligned}P_t(\mathbf{X}_0^{\text{choice}} | x) &= \Pr_\varepsilon(\text{Policy}_t(x, \{\varepsilon_\ell\}_\ell) \in \mathbf{X}_0^{\text{choice}}) \\ \lambda_t^{\text{choice}}(\mathbf{X}_0^{\text{choice}}) &= \int_{x \in \mathbf{X}} P_t(\mathbf{X}_0^{\text{choice}} | x) d\lambda_t(x).\end{aligned}$$

The idiosyncratic transition function (11) defines idiosyncratic and distributional transition functions from $\mathbf{X}^{\text{choice}}$ to \mathbf{X} . For $\mathbf{X}'_0 \subseteq \mathbf{X}$,

$$\begin{aligned}T_t(\mathbf{X}'_0 | x^{\text{choice}}) &= \Pr(x' \in \mathbf{X}'_0 | x^{\text{choice}}) \\ \lambda_{t+1}(\mathbf{X}'_0) &= \int_{x \in \mathbf{X}} T_t(\mathbf{X}'_0 | x^{\text{choice}}) d\lambda_t^{\text{choice}}(x).\end{aligned}$$

E Extreme-Value Location Preference Shocks

Integrating over the location preference shocks $\{\varepsilon'_l\}_l$ gives

$$\mathbb{E} V_{t+1}(b', z', h^{\text{live}'}, h^{\text{let}'}, \ell, a + 1) = \psi^{-1} \log \left(\sum_\ell \exp\left(\psi \tilde{V}_\ell(b, z, h_0^{\text{live}}, h_0^{\text{let}}, \ell_0, a)\right) \right)$$

where

$$\tilde{V}_\ell(b, z, h_0^{\text{live}}, h_0^{\text{let}}, \ell_0, a) = \max_{h^{\text{live}}, h^{\text{let}}, g, h} \tau d(\ell, \ell_0) + u(g, h, \alpha_{\ell t}) + \beta \mathbb{E} V_{t+1}(b', z', h^{\text{live}'}, h^{\text{let}'}, \ell, a+1, \{\varepsilon'_l\}_l).$$

F Imputation Procedures